

Heterogeneously Catalysed Amination and Isomerisation of Isohexides

Von der Fakultät für Mathematik, Informatik und Naturwissenschaften der RWTH Aachen University zur Erlangung des akademischen Grades einer Doktorin der Naturwissenschaften genehmigte Dissertation

vorgelegt von

Master of Science

Rebecca Veronika Engel, geb. Pfützenreuter

aus Leinefelde

Berichter: Universitätsprofessorin Dr. Regina Palkovits
 Universitätsprofessor Dr. Carsten Bolm

Tag der mündlichen Prüfung: 20. Juni 2016

Diese Dissertation ist auf den Internetseiten der Universitätsbibliothek online verfügbar.

The work, presented in this thesis, was carried out from October 2012 until January 2016 at the Chair for Heterogeneous Catalysis and Chemical Technology at the RWTH Aachen University under the supervision of Prof. Dr. Regina Palkovits and Dr. Marcus Rose.

Life is not easy for any of us. But what of that?

We must have perseverance and above all confidence in ourselves.

We must believe that we are gifted for something, and that this thing, at whatever cost, must be attained.

Marie Skłodowska Curie

Acknowledgement

At this point I would like to thank everyone who supported me in the last years during my doctoral studies and in general. In the first place, I want to thank my family, especially my parents, Sybille and Thomas, as well as my grandparents, Oma Lotti, Oma Petra, and Opa Klaus. They encourage me in whatever I am doing and help wherever they can. Without their support I would hardly have achieved as much. Furthermore, I am deeply grateful for my husband, Julien Engel, who is constantly encouraging and supporting me in my studies and career goals. I couldn't wish for a better partner.

I thank my doctoral advisor, Prof. Dr Regina Palkovits, for welcoming me in her working group. Our discussions not only on my research but also on other matters within the academic world are highly appreciated. Additionally, I am grateful for the numerous opportunities to present my work on national and international conferences.

A huge "thank you" to my supervisor, Dr. Marcus Rose, for choosing me as his first doctoral student and providing these exciting and challenging topics. I am grateful for our fruitful discussions. They improved my work and helped me to develop myself further as a researcher.

I want to thank Prof. Dr. Carsten Bolm for refereeing my thesis.

Thanks to Dr. Stefan Palkovits for introducing me to Python and the numerous discussions on reaction kinetics and kinetic modelling.

I am thankful to our collaborators in industry, Dr. Alireza Haji Begli, Dr. Christine Kröner, and Prof. Dr. Markwart Kunz from *Südzucker AG*, for their valuable suggestions concerning the isohexide amination. Additionally, I would like to thank the analytical staff of the Central Department Research, Development and Services of the company *Südzucker AG* for their support concerning analytical issues and for measuring samples.

I want to thank Prof. Dr. Pascal Dietzel and his co-workers for hosting me three month in his working group at Bergen University, Norway. The discussions on MOF synthesis and characterisation are much appreciated.

Furthermore, I want to thank my mentor Prof. Dr. Katharina Landfester for our discussions about my career as well as the whole TANDEM group of 2015. It was a great year with you.

My thanks to ACalNet, a thematic network of the DAAD, for the travel grant to the NAM24 in Pittsburgh/PA, USA in 2015.

I am grateful for the thorough annotations from Henry Vandelinde, Ph.D. that improved my thesis significantly. Further thanks concerning their input and corrections on this thesis go to Julien Engel, Lennart Sandbrink, Andrea Willms, and Swaantje Maaz.

Thanks to the colleagues of the electrical and mechanical workshops as well as the analytical departments. Especially I want to thank Elke Biener, Hannelore Eschmann, and Heike Fickers-Boltz for their helpful remarks on GC and Noah Avraham on HPLC analysis. Thank you all for measuring so many samples. Additionally, my thanks go to Heike Fickers-Boltz and Wolfgang Falter for their support regarding GC-MS. I am thankful to Heike Bergstein for ICP-OES and to Karl-Josef Vaeßen for the TG and XRD measurements.

I want to thank my research and bachelor students as well as research assistant, by name Anja Fink, Katharina Schmitz, Khai-Nghi Truong, Lucas Mertens, Marta Helmin and Thomas Diehl, for the good collaboration.

I want to thank all members of the Palkovits Group and the whole institute for the great working atmosphere and cooperation. I want to highlight only a few. My time with the *Nanocats* would have not been the same without my amazing lab colleagues: Andrea Willms, Andrea Stomps, Ghith Al Shaal, Lennart Sandbrink, Sven Müller, and Carsten Stobbe. Thanks for the scientific discussions but also the fun times. Sven and Lennart, thank you for the many laughs and the lab playlist!

TABLE OF CONTENTS

1	INTRODUCTION AND MOTIVATION	1
2	STATE OF THE ART	5
2.1	ISOHEXIDES	6
2.1.1	ISOHEXIDE PRODUCTION	7
2.1.2	ISOHEXIDE APPLICATION	13
2.2	ISOHEXIDE-DERIVED BIOPOLYMERS	15
2.2.1	BIOPOLYMERS SYNTHESISED DIRECTLY FROM ISOHEXIDES	15
2.2.2	BIOPOLYMERS SYNTHESISED FROM ISOHEXIDE DERIVATIVES	18
2.3	CATALYTIC AMINATION OF ALCOHOLS	20
2.3.1	SYNTHESIS OF PRIMARY AMINES	22
2.3.2	SYNTHESIS OF ISOHEXIDE AMINE DERIVATIVES	24
3	RESULTS AND DISCUSSION	29
3.1	CATALYTIC AMINATION OF ISOHEXIDES	30
3.1.1	INFLUENCE OF THE SUBSTRATE ON THE PRODUCT DISTRIBUTION	31
3.1.2	CATALYST SCREENING	33
3.1.3	INVESTIGATION OF THE HYDROGEN AUTOTRANSFER MECHANISM	40
3.1.4	INVESTIGATION OF REACTION PARAMETERS	46
3.1.5	STABILITY AND DEACTIVATION OF THE COMMERCIAL RU/C CATALYST	52
3.2	CATALYTIC ISOMERISATION OF ISOHEXIDES	56
3.2.1	INVESTIGATION OF THE REACTION MECHANISM	59
3.2.2	INVESTIGATION OF AN UNKNOWN COMPOUND	66
3.3	KINETIC MODELLING OF THE CATALYTIC ISOHEXIDES ISOMERISATION	71
3.3.1	MASS TRANSPORT LIMITATIONS	71
3.3.2	DETAILS OF THE REACTION NETWORK AND KINETIC MODEL	75
3.3.3	DATA MODELLING AND DETERMINATION OF THE RATE CONSTANTS	79
3.3.4	DETERMINATION OF THE ARRHENIUS PARAMETERS	90
4	CONCLUSION	93
5	EXPERIMENTAL	97
5.1	GENERAL INFORMATION	98
5.2	CATALYST PREPARATION	100
5.3	CATALYSIS PROCEDURES	101

5.3.1	ISOHEXIDE AMINATION	101
5.3.2	ISOHEXIDE ISOMERISATION AND MECHANISTIC INVESTIGATIONS	102
5.3.3	ISOHEXIDE ISOMERISATION KINETIC EXPERIMENTS	102
5.3.4	ISOHEXIDE ADSORPTION EXPERIMENT	103
5.4	KINETIC MODELLING	103
5.5	ANALYTICS	104
5.5.1	GAS CHROMATOGRAPHY	104
5.5.2	GAS CHROMATOGRAPHY – MASS SPECTROMETRY	105
5.5.3	HIGH-PRESSURE LIQUID CHROMATOGRAPHY	108
5.5.4	NUCLEAR MAGNETIC RESONANCE SPECTROSCOPY	109
5.5.5	CATALYST CHARACTERISATION	110
6	REFERENCES	111
7	ABBREVIATIONS AND FORMULA SYMBOLS	121
7.1	LIST OF ABBREVIATIONS	122
7.2	LIST OF FORMULA SYMBOLS	124
8	CURRICULUM VITAE	125
9	APPENDIX	129

1 Introduction and Motivation

From today's point of view, it may seem like coal, crude oil, and natural gas have always been mankind's major sources for energy and materials. However, in the 18th century the sole source was biomass, e.g. wood for fire or dyes extracted from plants. The transition to use fossil resources, especially coal, started slowly in the second half of the 18th century with the beginning of the industrial revolution. Over the years, crude oil and natural gas were also employed as resources not only for the production of energy but also for chemicals and materials. These resources were cheap and readily available. Thus, in industrial production, the use of biomass was mostly limited to the gum, fibre, and timber industries as well as to the production of drugs or flavours and fragrances by extraction from plants.^[1] Nowadays, merely 200 years after the industrial revolution, the fossil resources of the world are depleting, but the demand for energy, chemicals, and oil-derived products is steadily increasing. Hence, in order to sustain the supply, a change to renewable alternatives is inevitable.

In the context of alternative energies, wind, water, and solar power are already established technologies. However, for the production of most chemicals and materials a carbon-based feedstock is needed.^[2] For this purpose, biomass is a suitable substitute in the chemical industry. Thus, the concept of biorefineries in which chemicals and transportation fuels are produced from biomass instead of fossil fuels was developed.^[3-4] Within these biorefineries, the conversion of sugars is one of the most important transformations. The easiest way to obtain sugars directly from biomass is by using sugar beet or cane as feedstock, extracting the sugars directly from the raw material.^[5] Also the hydrolysis of starch, e.g. from corn, is a direct way to obtain glucose as one of the main sugar compounds for further transformation.^[4] However, these are food plants and when using these approaches a competition with the food supply cannot be excluded. This competition gives rise to an ethical issue: people in developing countries suffered from malnourishment after food prices increased due to biofuel production.^[2] Therefore, nowadays the focus of the research lies on uneatable lignocellulosic feedstock like wood, grass, crop residues, or straw.^[2, 4] A prominent example using lignocellulosic material to produce platform chemicals is the Biofine process with levulinic acid as the main product.^[6] In fact, the production of levulinic acid directly from biomass is by now a commercial process, and the company *GFBiochemicals* is planning to scale up its levulinic acid production in Italy to 10,000 t a⁻¹.^[7]

Considering the fact that the transportation sector is the most important consumer of fossil fuels besides the energy industry, it is comprehensible that the production of biofuels is more popular than the production of chemicals based on renewables.^[2, 8] Thus, it is an intensely investigated field of research.^[9-12] However, the availability of biomass is not as unlimited as it seems. By 2050 only 30 to 75 % of the predicted energy demand can be covered by biogenic feedstock.^[13] In these numbers, solely the energy production is considered. For the

fabrication of transportation fuels and chemicals, the percentages are estimated to be even lower due to loss of energy content during transformations. Moreover, in order to be economically viable the prices for bio-based transportation fuels have to be competitive. So far, using biogenic feedstock is more expensive than using fossil fuels. Since the revenues generated by chemicals and products based on these are much higher than by transportation fuels contemplating the production volume, it is more feasible to use biomass as feed in the chemical industry.^[14] Therefore, research in the field of bulk and fine chemicals based on platform molecules obtained from biomass is increasing. Prominent examples are 5-hydroxymethylfurfural (5-HMF), levulinic acid, and isosorbide.^[15-17] They can be directly converted into products or are transformed into suitable derivatives first. For example the mono- and dinitrate derivatives of isosorbide are established drugs used to treat angina pectoris.^[18] Additionally, in the field of polymer research an increasing amount of biogenic monomers are under investigation; e.g. furandicarboxylic acid, a derivative of 5-HMF, is a potential substitute for terephthalic acid in polymers.^[19] Furthermore, isosorbide is applied as monomer in the synthesis of polyethers amongst others. Poly(isosorbide terephthalate) (PIT) is an alternative for poly(ethylene terephthalate) (PET).^[20] By substituting ethylene glycol with isosorbide not only the amount of oil-derived compounds in the polymer is decreased but also the thermal properties are enhanced enabling the fabrication of improved products. In contrast to conventional PET bottles, bottles made from PIT can tolerate hot fillings. This property can increase the value of the product justifying higher production costs.

Generally, the interest in polymers based on isohexide monomers, i.e. also isomannide and isoidide, is enhanced. The reason is not only their biogenic nature but also their rigid structure potentially increasing the stability of the polymers as shown in PIT. It was found that isoidide compared to its isomers yielded higher molecular weights, most likely due to having a more linear structure than isomannide and isosorbide.^[19-20] Therefore, it is often the preferred isohexide monomer. Unfortunately, isoidide cannot be directly obtained from biomass. Thus, suitable alternative synthesis pathways like the isomerisation of isosorbide or isomannide have to be investigated. Additionally, isohexide derivatives, such as amines, are studied in polymerisation reactions leading to interesting polymers.^[19-20] However, the synthesis of the isohexide amine derivatives is so far only possible by multi-step organic synthesis or by using homogeneous catalysis. Both approaches have several drawbacks, including the extensive work-ups and stoichiometric amounts of reagents for the organic synthesis routes as well as costly ligands, working in organic solvents under inert gas atmosphere, and complex catalyst separation for the homogeneous catalysis.

In this work, the catalytic amination of isosorbide and isomannide is investigated using solid catalysts in aqueous medium for an improved production of isohexide amine derivatives. Because of the good performances of homogeneous ruthenium catalysts in the amination of

isohexides,^[21-22] ruthenium supported on activated carbon (Ru/C) is examined as suitable heterogeneous catalyst but also other supported metal catalysts are screened. Additionally, the stability of a commercial Ru/C catalyst is studied. Furthermore, the impact of the different substrates, isomannide or isosorbide, on the amination reaction is investigated along with the influence of different reaction conditions. The possibility of a hydrogen autotransfer mechanism as in the experiments with molecular catalysts, in which no external hydrogen is necessary, is explored.

Additionally, the research in this work focuses on the isomerisation of isohexides as potential production route of isoidide. Herein, the aim is a deeper understanding of this reaction. Thus, the reaction mechanism is investigated by means of deuterium labelling experiments. Further insights are gained through first kinetic investigations and determination of rate constants and Arrhenius parameters. Hence, within this work first steps towards the catalytic production of promising isohexide-derived monomers are to be undertaken.

2 State of the Art

2.1 Isohexides

Isohexides are 1,4:3,6-dianhydrohexitols consisting of two tetrahydrofuran rings, which are *cis*-connected in a 120° angle.^[23-27] Thus, the molecules are “V”-shaped. They have two secondary alcohol groups in 2- and 5-position. There are three isohexide isomers 1,4:3,6-dianhydro-D-mannitol, 1,4:3,6-dianhydro-D-sorbitol, and 1,4:3,6-dianhydro-L-iditol, more commonly known as isomannide, isosorbide, and isoidide, respectively (Figure 1). The isomers differ only in the configuration of their hydroxy groups. In isomannide both hydroxy groups have *endo*- and in isoidide both possess *exo*-configuration.^[25] In isosorbide the hydroxy groups have two differently configured hydroxy groups. The one in 2-position shows *exo*-configuration whereas the one in 5-position is *endo*-configured.^[26] The dashed lines in Figure 1 represent hydrogen bonds, which are formed between the hydrogen of the *endo*-configured hydroxy group and the oxygen of the adjacent ring. The presence of those hydrogen bonds was confirmed by infrared spectroscopy.^[28]

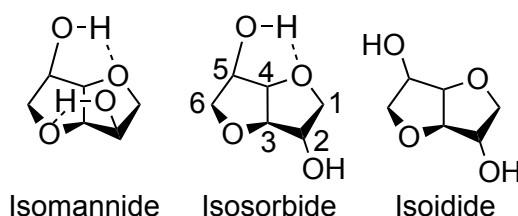


Figure 1. The structures of the isohexide isomers.

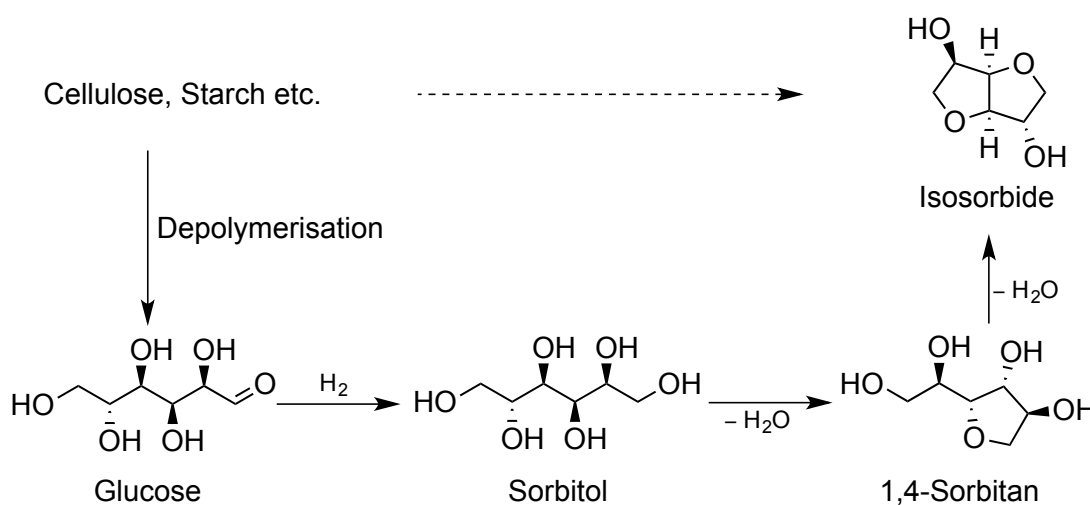
The different orientations of the hydroxy groups lead to differences in properties and reactivity of the isomers. For example, the melting temperature of isomannide is with 86-90 °C much higher than for isoidide and isosorbide with 64-65 °C and 61-64 °C, respectively.^[24, 26, 29] As for the reactivity of the hydroxy groups, the *endo*-configured one in isosorbide has a higher reactivity. This circumstance is probably due to the enhanced nucleophilicity because of the molecular hydrogen bond.^[26] However, if a sterically demanding substituent is involved, the hydroxy group in *exo*-position can preferably be substituted.^[26, 30-31] Strikingly, when the reactivity of the isomers is compared, e.g. in polymerisation reactions, isomannide shows the lowest activity whereas isoidide shows the highest despite the configuration of their hydroxy groups.^[20]

The investigation of isohexides, their structure, properties, and synthesis started already in the middle of the last century by individual working groups.^[23-25, 27, 29, 32] Nowadays, the interest in these molecules is renewed because they are interesting biogenic platform chemicals for versatile transformations and applications.^[17] The focus of the attention lies especially on polymers with isohexide moieties as renewable alternatives to state of the art compounds.^[19-20]

2.1.1 Isohexide Production

2.1.1.1 Isosorbide

The only isohexide produced on a large scale is isosorbide. Therefore, it is so far the isomer gaining the most attention in terms of application and research. In general, it can be produced in a multi-step process starting from biomass as displayed in Scheme 1.^[17] First the polysaccharides like cellulose and starch are depolymerised to glucose. Subsequently, glucose is hydrogenated to sorbitol, which in turn is then dehydrated to 1,4-sorbitan and further to isosorbide.



Scheme 1. Reaction route to isosorbide starting from polysaccharides.

Currently, isosorbide is commercially produced from starch.^[17] However, cellulose as major component of uneatable lignocellulose with more than 40 % of the total biomass composition would be the preferred starting material since it is not in competition with food production.^[14] Thus, wood and straw or even biowaste can be used as conceivable feedstock. Unfortunately, in comparison to starch the hydrolytic conversion of cellulose is significantly more challenging due to its high crystallinity and an increased amount of inter- and intramolecular hydrogen bonds.^[9, 33]

Generally, enzymes or acids are suitable catalysts for cellulose hydrolysis. It is reported that cellulase enzymes can catalyse the saccharification at 50 °C with close to 100 % yield.^[9] Although high selectivity can be provided, the space-time yield is low.^[17] Other drawbacks of the use of enzymes are for example their high costs and the use of buffer systems adjusting the pH-value to enable good working conditions. Additionally, substrate properties (crystallinity, degree of polymerisation, accessible area etc.) and concentration have an impact on the cellulase enzyme systems' activity.^[34] In traditional wood saccharification processes like the Bergius-Rheinau or the Scholler-Tornesch process, mineral acids like

hydrochloric or sulphuric acid are used, respectively.^[4, 35-36] The need of large amounts of highly corrosive mineral acids, the expensive construction of corrosion-resistant plants as well as the recovery of the acids are drawbacks of this technology.^[4] Therefore, research focuses on the identification of more sustainable processes applying solid acid catalysts.^[8, 14, 37]

The second step from polysaccharides towards isosorbide is the conversion of glucose to sorbitol, which is mainly done using nickel catalysts. In 2011 the overall capacity of sorbitol was 1.7 Mt.^[38] The glucose hydrogenation using solid nickel catalysts was patented already in 1942.^[39] More detailed investigations were conducted especially with Raney-nickel.^[40-41] Also supported nickel catalysts were investigated in the production of sorbitol from glucose.^[42-44] However, the nickel catalysts were not very stable due to leaching of the active species. Supported ruthenium catalysts are promising alternatives not only because of their superior activity but also better stability.^[40, 45-46]

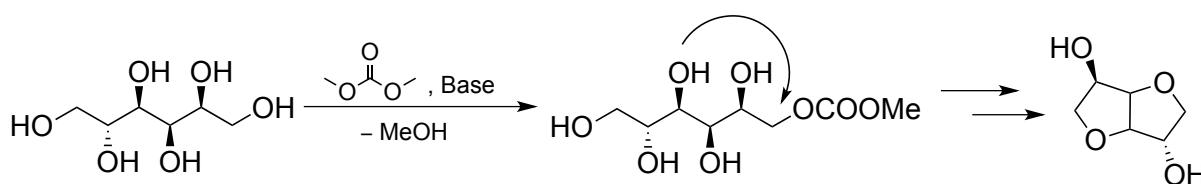
The conversion of sorbitol to isosorbide, a twofold dehydration reaction with sorbitan as intermediate, is an intensely studied reaction.^[26, 47-51] Generally, this conversion can be done using homogeneous or heterogeneous acid catalysts. In 1986 FLÈCHE *et al.* investigated the influence of the kind of acid on the dehydration of sorbitol.^[26] Mineral acids seem very suitable yielding isosorbide with over 70 % after 20 h at 135 °C in case of hydrochloric and sulphuric acid. However, phosphoric acid leads mainly to sorbitan with 68 % under the applied conditions. Reasonable yields of over 50 % can also be obtained using ion exchange resins. Lewis acids like tin or aluminium chloride are not efficient for isosorbide production because similar to phosphoric acid mainly sorbitan is formed. Processes using mineral acids and ion exchange resins for the production of anhydrosugar alcohols, especially isosorbide from sorbitol, in a solvent as well as under solvent-free conditions were patented in the early 2000s.^[52-53]

Many different solid acid catalysts beyond ion exchange resins were investigated as potential catalysts in the conversion of sorbitol to isosorbide because of the aforementioned reasons.^[40] Recently, H-beta zeolites^[47] and sulfonic acid-functionalised micro-bead silica were identified as suitable catalysts.^[54] Also sulfated materials like copper oxide^[48], titania^[49] or zirconia^[55] were found to be active in the dehydration of sorbitol to isosorbide. For example sulfated copper oxide catalysts, when calcined at temperatures not higher than 650 °C, lead to full conversion with high isosorbide selectivity of up to 68 % in 4 h time on stream at 200 °C reaction temperature.^[48] Using sulphated titania at 210 °C, the isosorbide selectivity could even be enhanced up to 75 % again at full conversion after 2 h reaction time.^[49] Another suitable catalyst is niobium oxide with very high conversion of over 80% but low selectivity of maximum 30%. However, through a modification with phosphoric acid this

phosphated niobium oxide leads to an increased isosorbide selectivity of over 60 % at full conversion in the same time and at lower temperatures than its unmodified equivalent.^[56]

KAMIMURA *et al.* were able to decrease the reaction time significantly to 10 min and also the temperature to 180 °C using microwave irradiation.^[50] This was accomplished with 5 mol-% *p*-toluenesulfonic acid as catalyst and expensive ionic liquids as solvents. However, the applied ionic liquids have a good recyclability with up to 98 % enhancing the economical viability.

The synthesis of isosorbide from sorbitol by dimethyl carbonate chemistry is a different approach followed by ARICÒ *et al.*^[51, 57] Besides an excess of dimethyl carbonate (DMC) a base is needed to form the methoxycarbonyl intermediate facilitating the ring closure. In contrast to other examples of DMC chemistry the reaction of sorbitol needs to be conducted in a solvent because of the high reactivity of isosorbide with DMC to its methoxycarbonyl and methyl derivatives. With sodium methoxide as base and methanol as solvent at reflux conditions isolated isosorbide yields of up to 76 % can be obtained.^[51] Through the use of nitrogen bicyclic bases like DABCO or DBU these yields can even be enhanced up to 98 %.^[57]



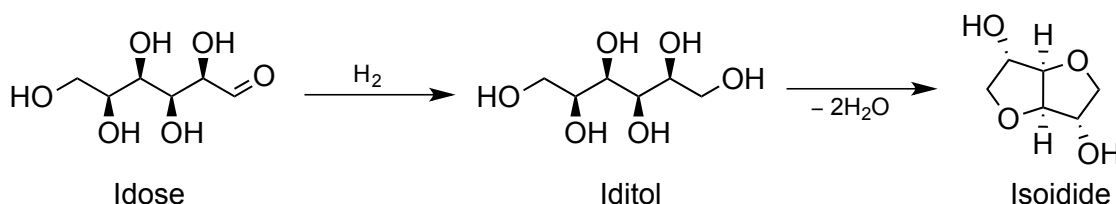
Scheme 2. Production of isosorbide by DMC chemistry.^[51]

YAMAGUCHI *et al.* reported a catalyst-free approach towards isosorbide.^[58] The dehydration in water at temperatures between 250 and 300 °C leads to isosorbide in good yields. The reason for this is the increased amount of hydronium and hydroxide ions under these conditions because of the autoprotolysis of water.

Up to now, the single reaction steps for the production of isosorbide based on biogenic polysaccharides have been described. Yet, stepwise syntheses usually cause high E-factors because of the intermediate separation and purification steps. Thus, a direct conversion of cellulose into isosorbide would be preferred. In fact, the direct hydrogenolysis of cellulose into sugar alcohols is already under investigation.^[33, 59-64] In most cases sorbitol and sorbitan are the main products. However, also isosorbide can be obtained that way. Usually, the nature of the catalysts for this transformation is bifunctional. The acid function is needed for the dehydration while a transition metal catalyses the hydrogenation. The appropriate balance between both catalytic functions is essential.^[33]

2.1.1.3 Isoidide

Isoidide is favoured in some applications in comparison to its isomers, e.g. in polymerisation reactions, because of its stereochemistry with two *exo*-configured hydroxy groups.^[19-20] Regardless, it is not yet an established platform chemical because the corresponding precursor L-idose (cf. Scheme 4) cannot be directly extracted from plant biomass and generally it exists scarcely in nature.^[20, 73] Therefore, an alternative reaction route is discussed: the isomerisation starting from its isomers.



Scheme 4. Potential production route of isoidide starting from Idose.

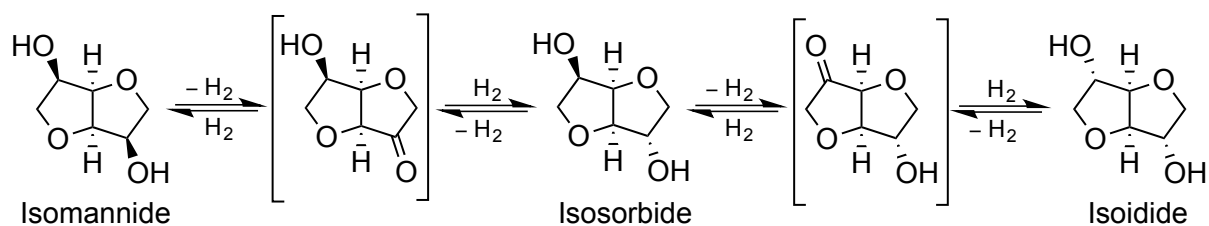
The isomerisation of isomannide and isosorbide was reported already in 1945 by FLETCHER *et al.*^[29] and picked up by WRIGHT and BRANDNER in the 1960s who also filed a patent for this reaction.^[32, 74] In both cases, heterogeneous nickel catalysts were applied at elevated temperatures of ≥ 200 °C, pressures of 100 to 250 bar, and in water as solvent. After 2 to 4 h the equilibrium is reached. The normalised ratio of the isomers in the equilibrium is approximately 55:40:5 for isoidide, isosorbide, and isomannide, respectively.

More recently, LE NÔTRE *et al.* described the isomerisation of isohexides using ruthenium supported on activated carbon as catalyst in water.^[73, 75] Starting from isosorbide the equilibrium was reached after 2 to 4 h at 220 °C and 40 bar hydrogen pressure applied at room temperature. The authors reported significant mass loss up to 30 % and attributed this to the formation of side products produced through hydrodeoxygenation of the substrate. Yet, they could decrease the amount of mass loss to 6 % by adjusting the pH-value of the solution to 10. They gave suppressed acid-catalysed hydrodeoxygenation side reactions as reason for this improvement. The mass loss increased with reaction time nonetheless.

So far, there are three different mechanisms mentioned in the literature for the isohexide isomerisation:

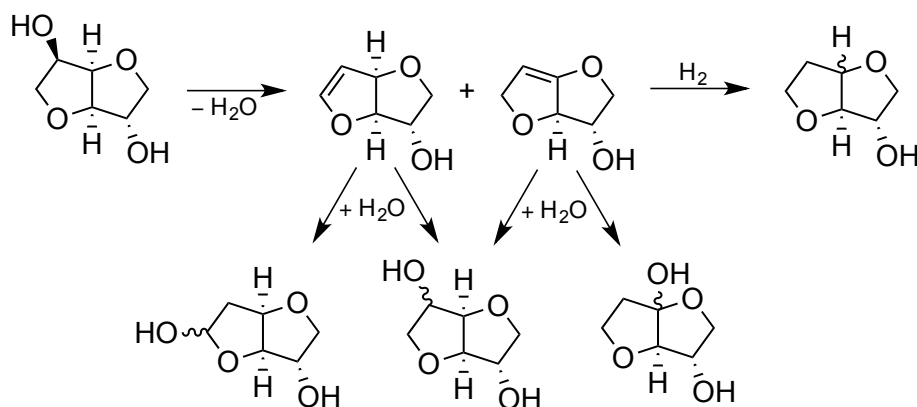
1. Dehydrogenation/re-hydrogenation (via a ketone intermediate).^[29, 32, 73]
2. Dehydration/re-hydration.^[73]
3. Direct hydride abstraction and re-addition.^[32]

The most discussed of the above-mentioned mechanisms is thus far the first option. Yet, the ketones were never observed as intermediates. The reaction is displayed in Scheme 5.



Scheme 5. Dehydrogenation/re-hydrogenation mechanism for the isohexide isomerisation.

LE NÔTRE *et al.* discussed the second possibility, the dehydration/re-hydration mechanism (Scheme 6).^[73] However, corresponding by-products such as unsaturated isohexide derivatives, derivatives with the hydroxy group in 1- or 6-position, or without one or even both hydroxy groups were absent in the product mixture. Thus, the authors dismissed this pathway. The direct hydride abstraction as third alternative was mentioned only once since the authors could not rule it out completely.^[32]



Scheme 6. Potential dehydration/re-hydration mechanism for the isomerisation of isohexides.

Furthermore, there is only one homogeneously catalysed example of the isomerisation of isohexides to yield isoidide.^[22] In this case, a molecular, pincer-type catalyst is used in *tert*-amyl alcohol as the solvent and no external hydrogen was applied to the system. Yet, the isomerisation occurs, and starting from isomannide after 21 h reaction time a product distribution of 23 %, 43 %, and 33 % of isomannide, isosorbide, and isoidide was observed, respectively. In this case the most probable mechanism would be the dehydrogenation/re-hydrogenation because under these conditions and with the molecular catalyst the authors propose a hydrogen autotransfer (HAT) mechanism. Thereby the hydrogen abstracted in the dehydrogenation step is bound to the catalyst and used for the re-hydrogenation.

2.1.2 Isohexide Application

Dianhydrohexitols are known for a long time, e.g. isosorbide was first mentioned in 1927.^[76] Ever since they are interesting molecules for applications in different fields and for further transformations. Nowadays, isosorbide and isomannide are commercially available and so are some of the isohexides derivatives (Figure 2).

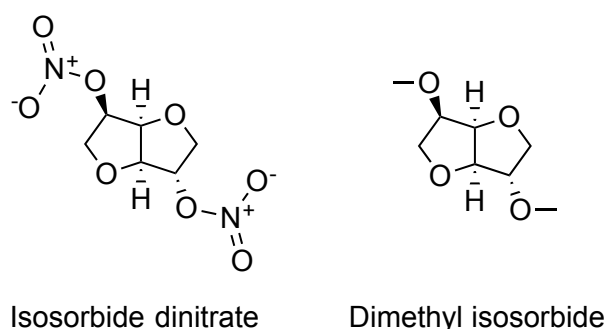


Figure 2. Commercially available isosorbide derivatives: dimethyl isosorbide (left) and isosorbide dinitrate (right).

Very important is the application of both mono- and dinitrate derivatives of the isohexides in medicine.^[18, 77-78] They are vasodilating drugs enhancing the oxygen supply of the cardiac muscle and, therefore, are used to treat angina pectoris and heart failure. Another commercial isosorbide derivative used in pharmaceutical applications is dimethyl isosorbide (DMI). It is discussed as pharmaceutical cosolvent especially for steroids and also as a stabiliser for acetylsalicylic acid in aspirin or for antibiotics.^[26, 79-80] Also other ether derivatives of isosorbide are considered as green solvents with high boiling points.^[30, 81]

Furthermore, DMI as well as isosorbide monoalkylethers have hydrotropic and solubilising properties.^[82] Long alkyl ether derivatives of isosorbide like sodium dodecyl isosorbide sulphates are conceivable surfactants.^[83-84] They are bio-based alternatives for petroleum-derived alkyl ether sulphates, e.g. lauryl ether sulphate, which is produced from ethylene oxide. Moreover, isosorbide glyceryl ether derivatives are in general applicable as additives in cleansers, detergents or personal care applications.^[85]

Biogenic ether compounds as well as lactones and furanes are amongst others discussed as parts in biofuel compositions.^[10] Therefore, also isosorbide derivatives are potential fuel additives. Through aliphatic substituents their relative energy content can be increased and, thus, specific combustion requirements can be met.^[17] The notion of isohexide derivatives as fuels and fuel blends is approached already in patents. For example isosorbide hydroxy ethers are reported as detergents in gasoline-type fuels^[86] and alkyl, aryl, and nitric ether derivatives of isosorbide as additives in diesel cycle fuel compositions.^[87]

Dianhydrohexitols contain steric information. Therefore, they can be used as biomass-derived chiral auxiliaries or catalysts. In fact, already in 1979 isosorbide was applied as chiral auxiliary in the asymmetric reduction of ketones using NaBH_4 .^[88] Since then, many applications using the isohexide scaffold in asymmetric catalysis were reported as recently reviewed by KADRAOUI *et al.*^[89] Some examples are the use of isohexide derivatives as chiral auxiliaries,^[90-91] ligands,^[92-95] phase-transfer^[96] or organocatalysts.^[97] Additionally, isohexide derived ionic liquids have been used in asymmetric synthesis.^[98-99] Moreover, chiral dopants with an isohexide scaffold for cholesteric liquid crystal materials are discussed.^[100]

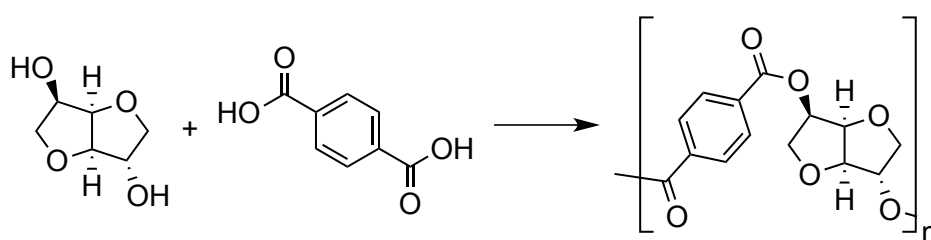
A very broad field of application for isohexides and their derivatives is their use as monomers in polymer production. Therefore, this topic is covered in the following chapter.

2.2 Isohexide-Derived Biopolymers

First works towards isohexide-derived polymers were reported in the 1980s^[101-103] and already in the 1990s first review articles on dianhydrohexitols as building blocks for polymers were published.^[104-105] Up to now the interest of renewable alternatives for oil-derived monomers is increasing and thus, also the interest in isohexides as biogenic monomers.^[19-20] Moreover, derivatives of isohexides are important building blocks in polymer production. Examples are the isohexide amines^[106-107] and their dicarboxylic acid derivatives amongst others.^[108]

2.2.1 Biopolymers Synthesised Directly from Isohexides

The most common application of isohexides in polymer production is as diol monomer in the synthesis of polyesters. In 1984 THIEM and LÜDERS described the synthesis of polyterephthalates based on isohexides and the interest in these polymer increases ever since.^[101-102] The most prominent example of isohexide-based polyterephthalates is poly(isosorbide terephthalate) (PIT) as displayed in Scheme 7.



Scheme 7. Synthesis of poly(isosorbide terephthalate) (PIT).

It has outstanding thermal properties, which are significantly enhanced in comparison to its conventional analogue poly(ethylene terephthalate) (PET) made from ethylene glycol. PET exhibits a glass transition temperature of 70 °C whereas the T_g of PIT is in the range of 150 to 200 °C, depending on the synthesis.^[20] Therefore, in contrast to commercial PET bottles, bottles made from PIT can endure hot fillings. Unfortunately, the amount of unreacted terephthalic acid in PIT is much larger than in PET and the molecular weights are lower. For this reason copolymers with different isosorbide ratios are investigated. For example poly(ethylene-co-isosorbide terephthalate) (PEIT) is a promising copolymer since its glass transition temperature increases linearly with increasing amount of isosorbide (Figure 3).^[109] Therefore, the thermal properties can be tailor-made. BERSOT *et al.* reported an efficient PEIT synthesis in 2011 using a bimetallic catalyst.^[110] Thus, the reaction temperature could be decreased leading to a product, which is less yellow in colour than obtained before.

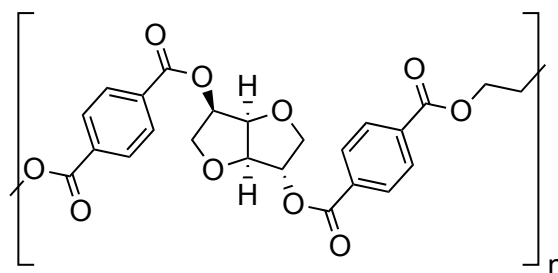
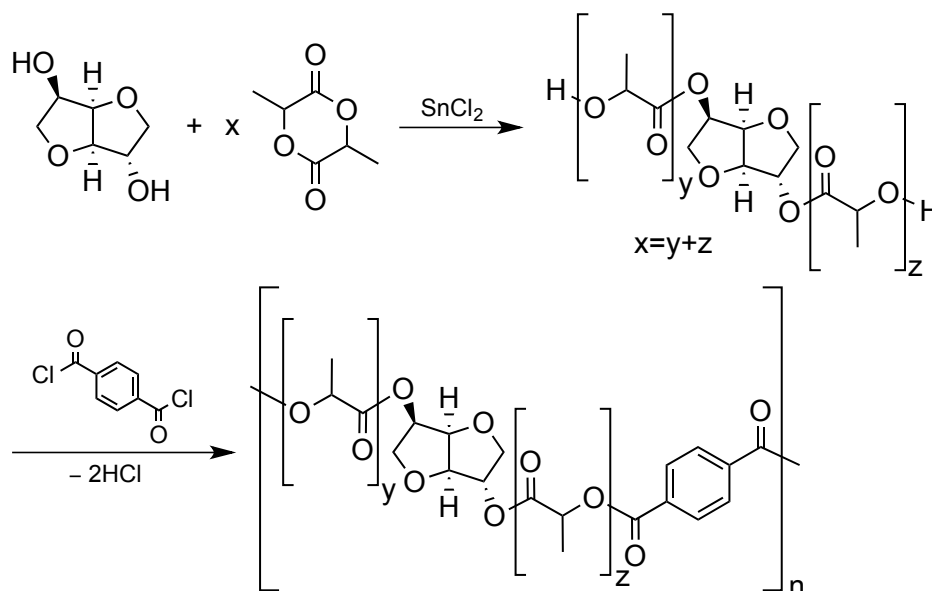


Figure 3. Structure of poly(ethylene-co-isosorbide terephthalate) (PEIT).

Furthermore, KRICHENDORF and WEIDNER published the one-pot synthesis of copolyesters based on isosorbide, L-lactide, and terephthalic acid (Scheme 8).^[111] Again the glass transition temperatures correlate almost linearly with the isosorbide content and are as high as 181 °C.

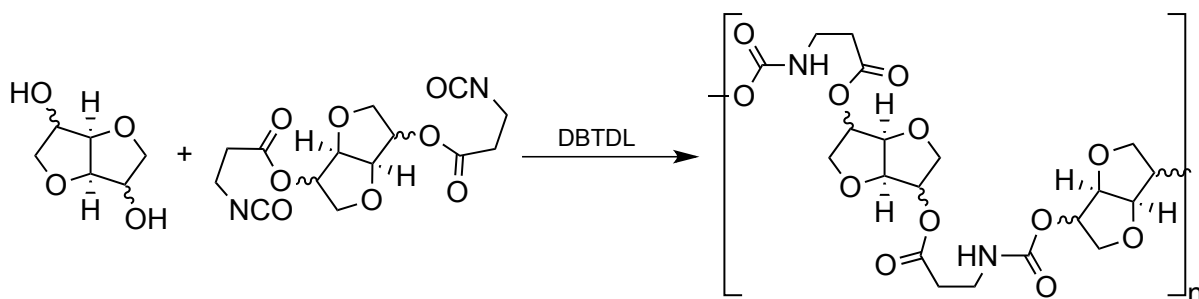


Scheme 8. Synthesis of a copolyester containing isosorbide.^[111]

In 2010 the first enzymatic catalysed synthesis of isosorbide-derived polyesters was described.^[112] CATALANI and co-workers used an immobilised lipase B from *Candida antarctica* (Novozym 435) as a catalyst. They investigated the bulk and azeotropic polymerisation of isosorbide mainly with various diethyl esters. In a more recent work, the same group described the synthesis of homo- and copolyester based on isosorbide and isomannide and unsaturated acids like diethyl fumarate using the same enzyme as in their previous work.^[113]

Moreover, isohexides can serve as the diol monomer in the production of polyurethanes.^[114-118] ZENNER *et al.* published a synthesis of polyurethanes where isohexides are not only used as diol monomer but also the isocyanate has an isohexide backbone.^[119] Usually, polymers made from isosorbide or isoidide have higher molecular weights than their isomannide

analogues. Remarkably, this is one example in which the polymers based on isomannide have higher molecular weights when compared to its isosorbide equivalents. Additionally, they have higher glass transition and decomposition temperatures as well as a higher crystallinity.



Scheme 9. Synthesis of polyurethanes based on isohexides using dibutyltin dilaurate (DBTDL) as catalyst.^[119]

2.2.2 Biopolymers Synthesised from Isohexide Derivatives

Isohexide amines are very promising monomers and their synthesis is already well investigated, as described in chapter 2.3.2. They can be used as starting material for the synthesis of polyurethanes as described already in 1986.^[103] However, more common is their use in the production of polyamides. First works were published by THIEM *et al.*^[106]

Recently, VAN VELTHOVEN *et al.* reported the synthesis of polyamides using diaminoisoidide and pimelic acid as well as the synthesis of copolyamides with diaminobutane.^[107] Again, the glass transition temperature increases with increasing amount of diaminoisoidide and is as high as 103 °C for the homopolymer. Yet, also the crystallinity of the polymer decreases with higher isohexide content. Unfortunately, only low number-average molecular weights of 1,000-2,000 g mol⁻¹ could be obtained.

Semicrystalline polyamides based on isosorbide and isoidide diamine derivatives were described by JASINSKA *et al.*^[120-122] The authors investigated melt polycondensation of the isohexides compounds with sebacic or brassylic acid (Figure 4) and also copolyamides with diaminobutane were described. To increase the molecular weights the obtained polyamides were subjected to solid state polymerisation yielding number-average molecular weights of over 18,000 g mol⁻¹. A detailed study on the structure of the (co)polyamides revealed an influence of the diaminoisohexides units on the chain conformation and hydrogen bond density.^[121-122]

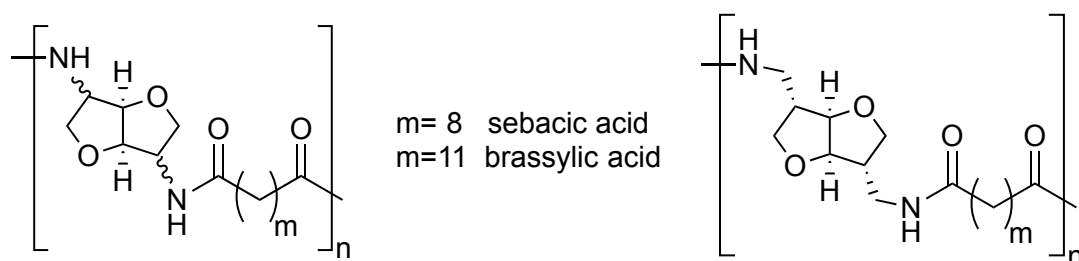


Figure 4. Structures of polyamides based on isohexides (left) or isoidide-2,5-dimethyleneamine (right) adapted from DELIDOVICH *et al.*^[19]

WU *et al.* published an analogous study on polyamides, as described above, but with an 1C-extended isoidide monomer: isoidide-2,5-dimethyleneamine (Figure 4). They investigated homopolymers with sebacic and brassylic acid as well as copolyamides with 1,6-hexamethylene diamine. The reaction conditions are also similar to the ones described above. Solid state polycondensation of the prepolymer leads to high number-average molecular weights of 49,000 g mol⁻¹. The rigidity of the polymer increases with an increasing amount of isohexide-derived monomer.

Furthermore, there are also hydroxy group modified isohexide monomers like isohexide-diacetals, which can be polymerised to polyacetals (Figure 5) in an acid-catalysed acetal metathesis polymerisation.^[123]

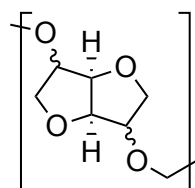


Figure 5. Structure of isohexide-based polyacetals.

GALLAGHAR *et al.* reported polymethacrylates using acetylated methacrylic isosorbide (AMI) as monomer (Figure 6).^[124] The polymer poly(AMI) was synthesised in a free radical polymerisation reaction. A high number-average molecular weight of 88900 g mol^{-1} and a high T_g of 130°C could be obtained. Additionally, block copolymers with *n*-butyl acrylate (nBA) were synthesised by reversible addition-fragmentation chain transfer (RAFT) polymerisation (Figure 6). With approximately -45 and $+120^\circ\text{C}$, their glass transition temperatures are well separated. Therefore, it is assumed that the two domains of poly(AMI) and poly(nBA) are microphase separated.

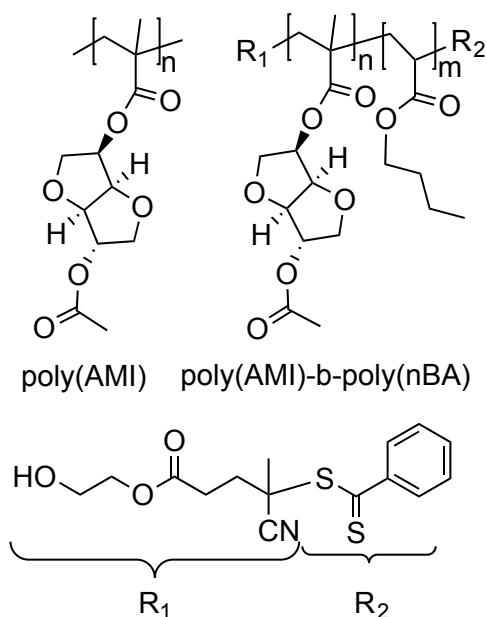
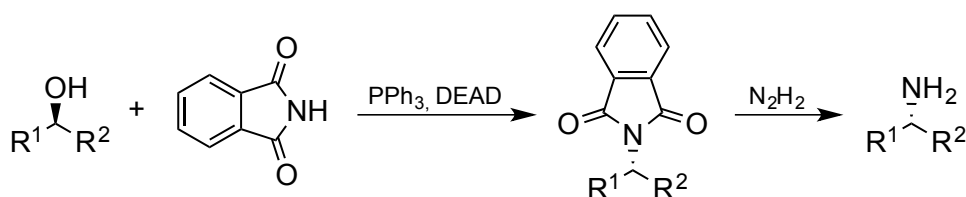


Figure 6. Structures of polymethacrylates based on isosorbide: poly(AMI) (left) and poly(AMI)-b-poly(nBA) (right).^[124]

2.3 Catalytic Amination of Alcohols

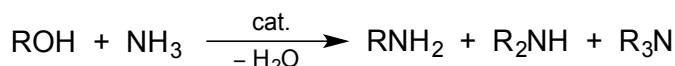
Amines are important intermediates in the chemical industry not only for the production of fine but also for bulk chemicals. Furthermore, they are used in a broad field of applications varying from bioactive compounds and pharmaceuticals to dyes, agrochemicals, as well as polymers.^[125] Especially the polymer synthesis is a very attractive application. Lately, the worldwide production of polyamides is at six million tons per year and the demand is increasing.^[126] The importance of amines can additionally be underlined considering the huge amount of ammonia of over 100 million tons produced annually.^[125, 127] Although a large portion of this goes into the fabrication of fertilisers, still 5 to 7 million tons per year are used in the production of amines excluding caprolactam and hexamethylene diamine.^[125]

There are many organic syntheses towards amines. A prominent example for the synthesis of amines starting from alcohols is the Mitsunobu reaction.^[128] Thereby, the alcohol reacts with phthalimide under the presence of triphenyl phosphine and diethyl azodicarboxylate (DEAD). A subsequent hydrazinolysis leads to the corresponding amine (Scheme 10). This reaction proceeds under the inversion of the stereocentre. Yet, the need of equimolar amounts of those reagents and the costly work up are the drawbacks of this method. Therefore, catalytic routes are favourable for industrial application.



Scheme 10. General Mitsunobu reaction for the synthesis of primary amines.^[128]

Since the beginning of the 20th century and the development of the Haber-Bosch process, ammonia is available on large scale.^[129] Thus, the most important method to produce amines and especially lower alkyl amines is the direct conversion of alcohols with ammonia (Scheme 11).^[125] Furthermore, the availability of various alcohols on industrial scale as well as the formation of water as the sole by-product are benefits of this process.^[127]



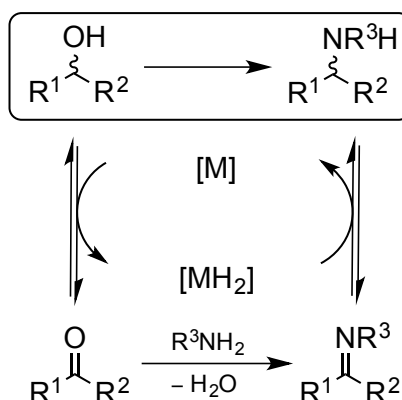
Scheme 11. Catalytic production of amines from alcohols with ammonia.

This is usually a gas phase reaction at elevated temperatures of 350 to 500 °C in the presence of catalysts like Al₂O₃, W₂O₅, Cr₂O₅, mixed oxides, or zeolites.^[125, 130] For longer chain alkyl amines transition metal catalysts based on nickel, copper, cobalt, and iron are used together with an excess of ammonia with two to eight equivalents. Typical reaction

conditions are 100 to 250 °C and 5 to 200 bar hydrogen pressure applied in a fixed bed reactor. The hydrogen is often introduced into the reaction mixture in order to maintain the catalytic activity of the metal catalyst.^[125, 130]

Nowadays, bio-based alcohols are considered as starting material for renewable amine alternatives. Furthermore, they can expand the portfolio of amine-functionalised intermediates.^[131] However, these harsh conditions described above are not suitable for most of the highly polar biogenic substrates because they have usually a low thermal stability. Additionally, gas phase reactions are not feasible due to the low vapour pressures of most of those compounds. Currently, new pathways using milder conditions in the liquid phase are investigated.^[132-137] These methods are better suitable for biogenic substrates. Although there are plenty of different catalytic systems, homogeneous as well as heterogeneous ones, they have one similarity: they all are based on the principle of hydrogen autotransfer (HAT), also called borrowing hydrogen.^[138]

The hydrogen autotransfer mechanism is often observed in the activation of alcohols and, therefore, has to be considered in the catalytic route towards *N*-alkylated amines using alcohols.^[138] The basic HAT concept is displayed in Scheme 12.



Scheme 12. Hydrogen autotransfer (HAT) mechanism.

First the alcohol is dehydrogenated to the ketone, which subsequently reacts with the amine in a condensation reaction to form the imine. In the final step, the imine is re-hydrogenated to yield the corresponding amine. Since the hydrogen bound to the catalyst is used for the re-hydrogenation step, no external hydrogen is needed. This makes such reactions very attractive. For the synthesis of primary amines, ammonia is applied as corresponding amine.

Many homogeneous catalysts react corresponding to this mechanism. Yet, there are also examples dealing with solid catalysts.^[139] However, concerning amination reactions, all examples concentrate on quite simple molecules, leading in many cases to multiple alkylation of the applied amine.

2.3.1 Synthesis of Primary Amines

In 2008 GUNANATHAN and MILSTEIN published the homogeneously catalysed conversion of alcohols to amines.^[132] The applied catalyst was a ruthenium-Pincer-complex (Figure 7, 1). The alcohols were reacted with ammonia in organic or aqueous media in 12 to 30 h depending on the substrate. However, only primary alcohols were investigated. Additionally, using primary alcohols as substrates also Ru(II)-triphos catalyst systems (Figure 7, 2) are possible for the production of primary amines.^[140]

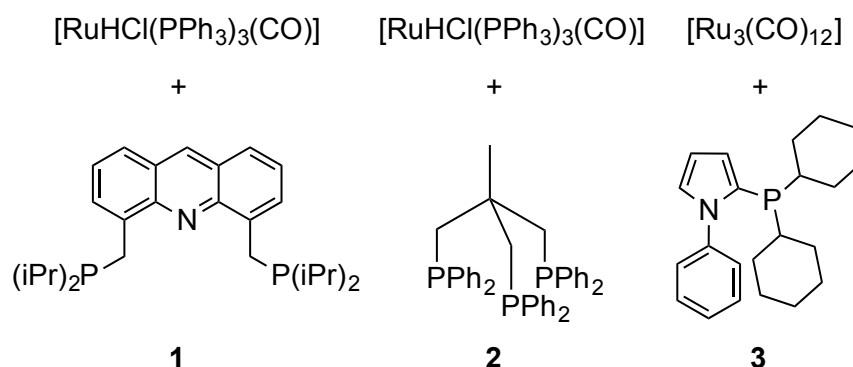


Figure 7. Homogeneous ruthenium-based catalyst systems in the synthesis of primary amines as published by GUNANATHAN *et al.*^[132] (1), DERRAH *et al.*^[140] (2), and IMM *et al.*^[133] as well as PINGEN *et al.*^[134] (3).

Only two years later the production of primary amines starting from secondary alcohols was described by IMM *et al.*^[133] as well as PINGEN *et al.*^[134] Again molecular ruthenium catalysts with various phosphine ligands were used for the direct conversion of alcohols with ammonia. The primary amine yields strongly depend on the substrate, solvent, and the applied ligand systems and range from 30 to 93 %.^[133] The best results were obtained with a ligand derived from a pyrrole phosphine (Figure 7, 3). Additionally, the company *Evonik* filed a patent for the use of Xantphos ligands in homogeneous ruthenium catalyst systems for the amination of primary alcohols.^[141] Furthermore, phosphine complexes with platinum as the active metal centre were published for the amination of secondary allyl alcohols.^[135] Different substrates could be successfully converted into their corresponding amines using degassed aqueous ammonia solution as the ammonia source. However, organic solvents were still necessary. For secondary alcohols only the multiple alkylation of aqueous ammonia was reported as an example of the application of homogenous catalysts in pure aqueous media.^[142-143] The described catalysts were a Cp^*Ir -catalyst^[142] and a bimetallic polymer catalyst with iridium as well as boron as active centres.^[143]

Furthermore, biocatalytic approaches in the synthesis of primary amines are published. In 2015 both MUTTI *et al.*^[144] as well as CHEN *et al.*^[145] described dual enzyme cascades for the asymmetric amination of alcohols. As usual in enzyme catalysis, mild reactions were applied

to achieve close to full conversion and up to >99 % ee. Moreover, even whole cell biocatalysts are reported for the synthesis of primary amines.^[146]

However, enzymes and homogeneous catalysts have certain drawbacks. Some of the disadvantages of enzymes have been addressed in chapter 2.1.1. As for molecular catalysts the complex synthesis of these compounds makes them rather expensive. They are for the most part air and moisture sensitive. Therefore, the need to work under inert gas atmosphere complicates their application in catalysis. Additionally, the separation of the catalyst and the product is expensive.^[14] Usually, most of these issues can be avoided through the application of solid catalysts. Processes for the heterogeneously catalysed gas phase amination of compounds with an appropriate thermal stability, low boiling point, and high vapour pressure are known for a long time as stated above.

Recently, the research interest concerning heterogeneously catalysed amination reactions in the liquid phase under milder conditions is increasing. This approach would be an attractive pathway for the conversion of biogenic alcohols. Lately, the desirability especially of supported nanoparticles as catalysts for the catalytic amination of biomass-based alcohols was highlighted by PERA-TITUS and SHI.^[131]

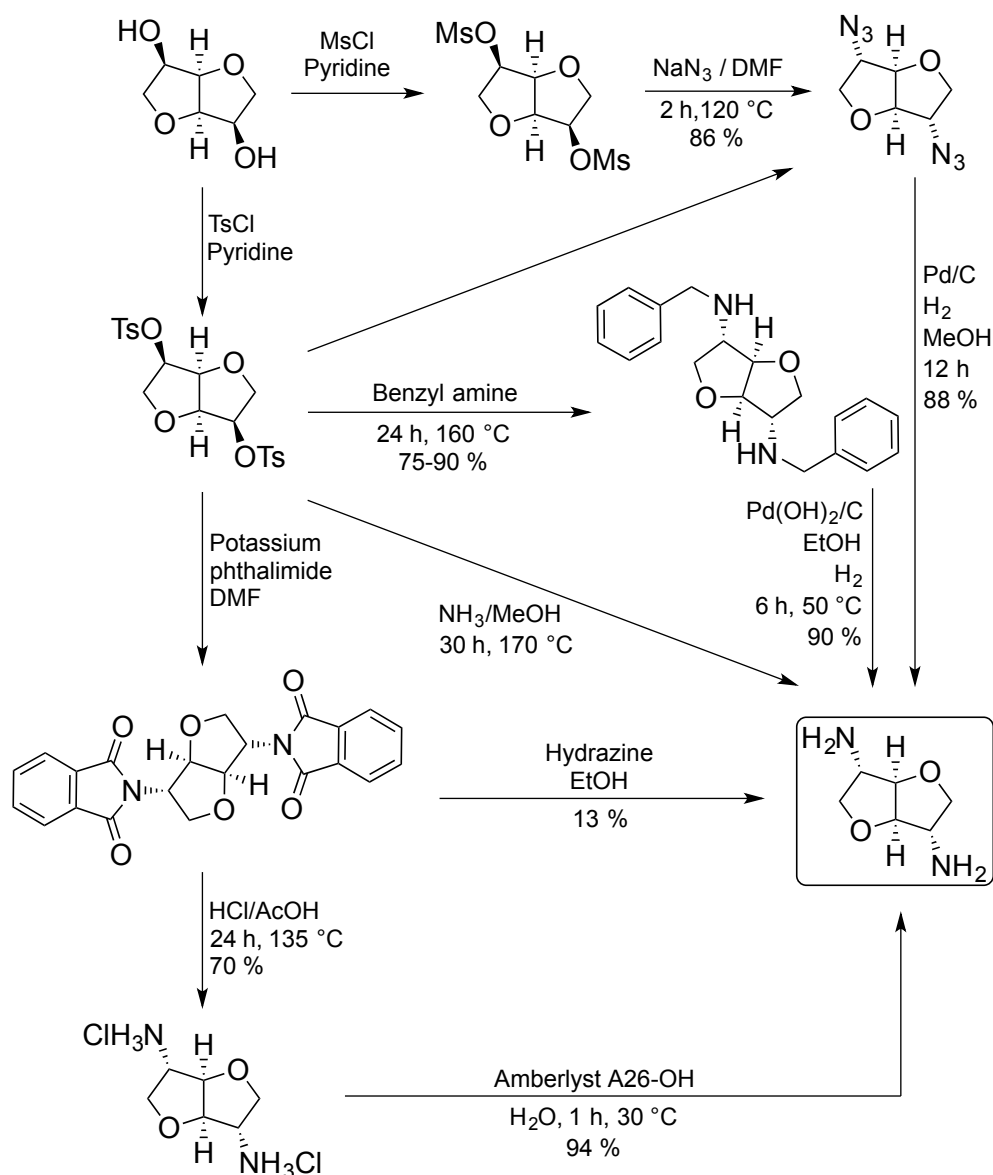
SHIMIZU *et al.* reported the synthesis of primary amines from secondary alcohols using supported nickel catalysts^[137, 147] At 160 °C, in organic solvent, and after reaction times of 20 to 72 h good to excellent yields of the primary amines could be obtained. The conversions were generally high with up to 100 %. The drawback of this catalyst lies in its handling. Although it is a solid catalyst it has to be handled under inert gas atmosphere constantly because of its fast passivation.

Another heterogeneous NiCuFeO_x-catalyst for the amination of secondary alcohols was published by CUI *et al.*, which is non-sensitive to air and moisture.^[136] However, the amination reactions were performed in organic solvent and led in most cases to the secondary amine derivatives. In order to yield the primary amines a large excess of ammonia with approximately 40 eq. is needed.

In 2014 the amination of C₃-alcohols in water was reported using solid rhodium catalysts.^[148] The application of a Rh-In-catalyst yielded the best results. Yet, the conversion after 24 h was low with maximum 11 %. Even an increase in reaction time to 160 h led to a medium conversion and low amine yield of 25 %.

2.3.2 Synthesis of Isohexide Amine Derivatives

As described in chapter 2.2.2, isohexide amine derivatives are suitable monomers for polyamide production based on renewables.^[106-107] Synthetic pathways towards primary amines derived from isohexides are known since the 1940s.^[149] Scheme 13 gives an overview over those synthesis strategies.



Scheme 13. Overview of synthetic strategies towards isohexide diamines adapted from DELIDOVICH *et al.*^[19]

MONTGOMERY *et al.* described a two-step synthesis of the isohexides to their diamine derivatives.^[149] First, the isohexide is tosylated followed by transformation to the diamine in an autoclave reaction in 30 h at 170 °C in a methanolic ammonia solution leading to 60 to 80 % of crude isohexide diamine.

In another route towards the isohexide diamine mesitylated or tosylated isomannide reacts with sodium azide in a nucleophilic substitution under inversion of the stereocentres.^[150] The

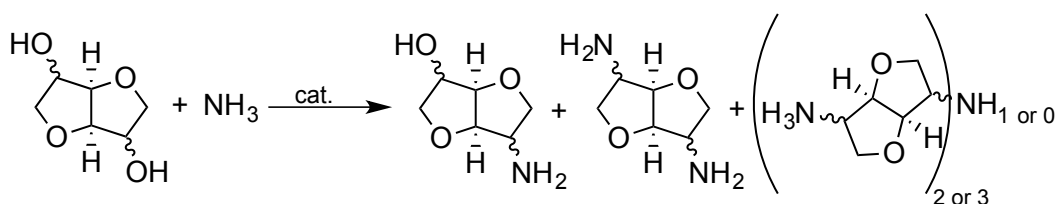
isoidide diazide can then be hydrogenated yielding the diamine with up to 88 %.^[151] However, this route is not feasible for industrial applications due to the explosive diazide intermediate.

1956 COPE *et al.* published a three-step synthesis in which the isoidide diamine was produced starting from isomannide.^[25] Again the tosylated isomannide derivative reacts with potassium phthalimide in a nucleophilic substitution under inversion of the stereocentre. The last step is a deprotection using hydrazine (analogue to the Mitsunobu reaction). One major drawback of this pathway is the low yield, especially of the diamine in the last step. THIYAGARAJAN *et al.* could overcome this in 2011 using a different deprotection method of the isoidide phthalimide derivative.^[152] Yet, adding a fourth reaction step was necessary. The phthalimide derivative is first hydrolysed and the so formed ammonium chloride salt of the isoidide diamine is then converted to the final product in 94 % yield using Amberlyst A26-OH as basic catalyst under mild reaction conditions.

Only a short while later the same group published a novel three-step synthesis route towards isoidide and isosorbide diamines.^[153] Through tosylation followed by a substitution with benzylamine under inversion of the stereocentre and finally a hydrogenation under mild conditions the amine derivatives are obtained with up to 90 % yield. However, this pathway is not applicable for isoidide as substrate. In this case a tricyclic amine compound instead of the isomannide diamine is found.

Yet, all of the above described methods are not suitable for a potential large-scale application of the isohexide diamines e.g. as monomers for the production of bio-based polymers. Even when a scale-up of the reactions is possible, costly work-up procedures between the single steps are necessary and increase the operating expense (OPEX) of the process. Additionally, in most of the described reaction steps equimolar amounts of unwanted by-products are produced increasing the E-factor of the routes. Therefore, a direct catalytic conversion of the dianhydrohexitols is preferred analogously to the above-mentioned general production of primary amines.

The direct conversion of isohexides to their amine derivatives can generally lead to amino alcohols and diamines as well as secondary and tertiary amine products (Scheme 14). Yet, due to their quite complex structure the secondary and tertiary amine products are not very likely to occur. Since the first step is the dehydrogenation of the alcohol to the prochiral ketone intermediate, regardless of following the HAT mechanism or not, the stereo information is lost during the reaction course. Thus, the amine products can have different configurations.



Scheme 14. General reaction scheme of the catalytic amination of isohexides.

In 2010 the company *Evonik* filed a patent for the catalytic synthesis of isohexide diamines. However, they are not starting from the isohexides directly but their ketone derivatives.^[154] In this case, the synthesis of the amine derivatives is a two-step process. First the ketone reacts with ammonia to yield the imine, which is subsequently hydrogenated in a fixed-bed reactor to the corresponding amine. Unfortunately, the ketone starting materials in turn have to be synthesised in stoichiometric oxidation reactions using oxidising agents like nitroxyl radicals based on (2,2,6,6-tetramethylpiperidin-1-yl)oxyl (TEMPO) from the corresponding dianhydrohexitol.^[155] More recently also a biocatalytic pathway was published wherein the ketone is produced using laccase as catalyst and TEMPO as the oxidising agent.^[156]

IMM *et al.* in cooperation with the company *Evonik* were the first to describe the direct catalytic conversion of isosorbide to its amine derivatives in 2011 using a homogeneous catalyst system.^[21, 157] More precisely, the authors tested different ruthenium complexes with various phosphine ligands, for which amino alcohols and diamines could be observed. However, the best result of 96 % diamines at full conversion was obtained with the catalyst system $[\text{RuHCl}(\text{PPh}_3)_3(\text{CO})]/\text{Xantphos}$ (Figure 8, **4**) in 2-methyl-2-butanol as solvent, at 170 °C and after 20 h reaction time.^[21]

2013 PINGEN *et al.* published the amination of isomannide as well as other biogenic alcohols using molecular catalysts.^[22] The same reaction conditions as reported by IMM *et al.* were applied in the reaction of isomannide with ammonia and the outcome was identical: 96 % diamines at full conversion, although a different catalyst system was applied. In this case a PNP-pincer-type ruthenium complex (Figure 8, **5**) was used analogously to the works by MILSTEIN and co-worker. Recently, the company *BASF* filed a patent on the catalytic amination of isohexides in organic solvents using different PNP-pincer-type catalysts at 200 °C.^[158]

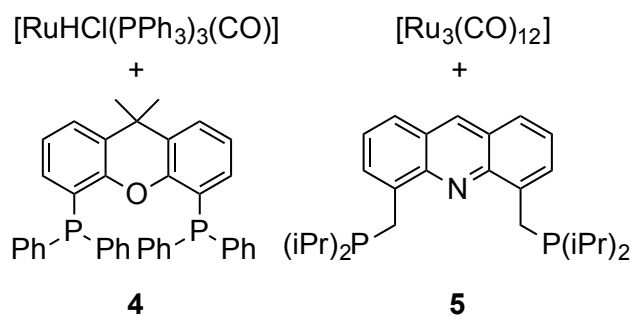


Figure 8. Homogeneous catalyst systems for the amination of isohexides as published by Imm^[21] and Pingen *et al.*^[22]

Additionally, the biocatalytic production of dianhydrohexitol amine derivatives was described recently.^[159] LERCHNER *et al.* used engineered dehydrogenases and transaminases as catalysts. Thus, in the first step the alcohol is oxidised to the ketone, which is subsequently converted to the amine.

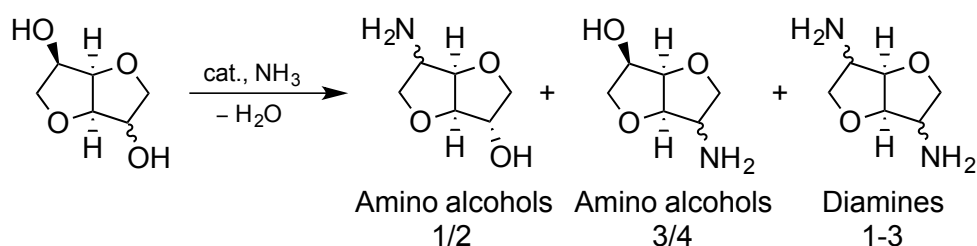
However, due to the aforementioned drawbacks of enzymes and molecular catalysts (cf. chapter 2.3.1) solid catalysts would be preferred. So far, the only heterogeneously catalysed method for the amination of isohexides is reported in this work (chapter 3.1).^[160]

3 Results and Discussion

3.1 Catalytic Amination of Isohexides

This chapter was partially published in R. Pfützenreuter, M. Rose, "Aqueous-Phase Amination of Biogenic Isohexides by using Ru/C as a Solid Catalyst", *ChemCatChem* **2016**, 8, 251-255.

The direct catalytic amination of isohexides leads to different amination products. The reaction starting from isosorbide or isomannide is shown in Scheme 15. Additionally, isomerisation products can be observed when hydrogen is applied.



Scheme 15. Reaction scheme of the catalytic amination of isosorbide or isomannide.

The amination products are distinguished in amino alcohols and diamines and numbered serially in the order in which they appear in the gas chromatogram. The exact assignment of the configuration of the functional groups was thus far not achieved since the amines could not yet be separated preparatively. If not stated otherwise, the ammonia source for the reactions is aqueous (aq.) ammonia solution (25 wt.-%) and the catalyst is a commercial supported Ru/C catalyst with 5 wt.-% metal loading by the supplier *Sigma Aldrich*. Detailed information about the experimental procedures and analytics can be found in chapters 5.3.1 and 5.5.1, respectively. It shall be noted at this point that two different sets of autoclaves were used for the amination of isohexides, leading to different results under otherwise equal conditions. This influence will be addressed in the interpretation of the results in the following chapters.

3.1.1 Influence of the Substrate on the Product Distribution

In this work the direct catalytic amination was investigated with isosorbide and isomannide as substrates because isoidide is currently not commercially available. Strikingly, the observed product distribution varies strongly with the substrate (Figure 9).^[160] The variance in conversion and total yield can be attributed to the use of different autoclaves (cf. 5.3.1.1). However, it has no effect on the line of argument.

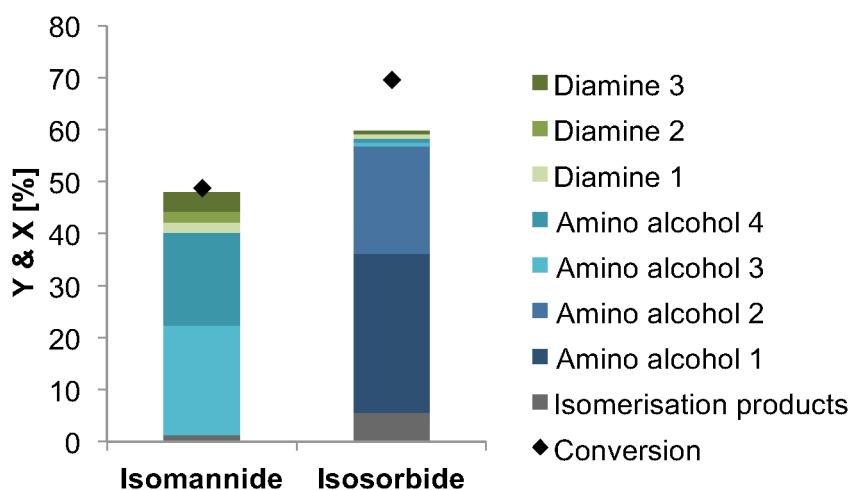


Figure 9. Product distribution depending on the substrate. Reaction conditions: 170 °C, 2 mol-% Ru/C, 5 g aq. ammonia solution, 10 bar H₂ (at RT), 500 rpm, and 24 h reaction time. The difference in conversion and total yield can be ascribed to the use of different autoclaves. For detailed information see chapter 5.3.1.

When isosorbide is applied as substrate the major products are the amino alcohols 1 and 2; whereas, when isomannide is the starting material mainly the amino alcohols 3 and 4 are formed. Additionally, significant amounts of diamines can be observed as products only for the isomannide experiments. From this fact and that the exact two opposite amino alcohols are produced in the experiments starting from isomannide in comparison to isosorbide, it can be concluded that the remaining hydroxy groups have the same configuration in the amino alcohols 1/2 and 3/4, respectively. Therefore, the residual hydroxy group in the amino alcohols 1 and 2 is *exo*-configured and *endo*-configured in amino alcohol 3 and 4.

Furthermore, a conclusion about the reactivity of the hydroxy groups can be drawn as the diamines are merely formed in significant amounts starting from isomannide. The *endo*-configured hydroxy groups show an increased reactivity for the amination in relation to the *exo*-configured ones when heterogeneous catalysts are applied. Using molecular catalysts the product spectrum consists only of diamines regardless of the applied substrate.^[21-22] Thus, in homogeneous catalysis the stereochemistry of the hydroxy groups has no influence on the outcome of the amination. Therefore, the dehydrogenation is most likely not the rate-determining step when molecular catalysts are applied. However, this reactivity variation of

the differently configured hydroxy groups is observed when heterogeneous catalysts are applied so it can be reasoned that in this case the dehydrogenation is rate-determining.

Also in the isomerisation of the isohexides the transformation of the *endo*-configured hydroxy group is preferred using solid catalysts (cf. chapter 2.1.1.3). Once more, the proposed reaction mechanism for the isomerisation proceeds through a dehydrogenation/rehydrogenation under inversion of the stereocentre. Thus, the dehydrogenation seems to be the rate-determining reaction step in both the amination and isomerisation reaction. Overall, on the surface of a solid catalyst, the *endo*-configured hydroxy groups appear to have a lower activation barrier for the dehydrogenation than the *exo*-configured ones. This circumstance might be explained by an increased nucleophilicity of the hydroxy groups in *endo*-position as a result of their intramolecular hydrogen bond (cf. Figure 1 in chapter 2.1). Additionally, on the surface of a solid catalyst the hydroxy groups show a different accessibility depending on their configuration, with the *endo*-configured one having the lower sterical hindrance. Taking all this into consideration, it can be reasoned that preferably the *endo*-configured hydroxy groups undergo the dehydrogenation and following amination. Thus, the formation of the diamines occurs mainly starting from isomannide.

3.1.2 Catalyst Screening

3.1.2.1 Commercial Hydrogenation Catalysts

Since the dehydrogenation of the secondary alcohol and the re-hydrogenation of the imine are major reaction steps for the amination of isohexides, different commercial hydrogenation catalysts were screened.^[160] An overview of the results is displayed in Figure 10. Aside from different Ru/C catalysts from different suppliers, reduced ruthenium powder, Pd/C from different suppliers, Pt/C, and Raney-Ni were tested.

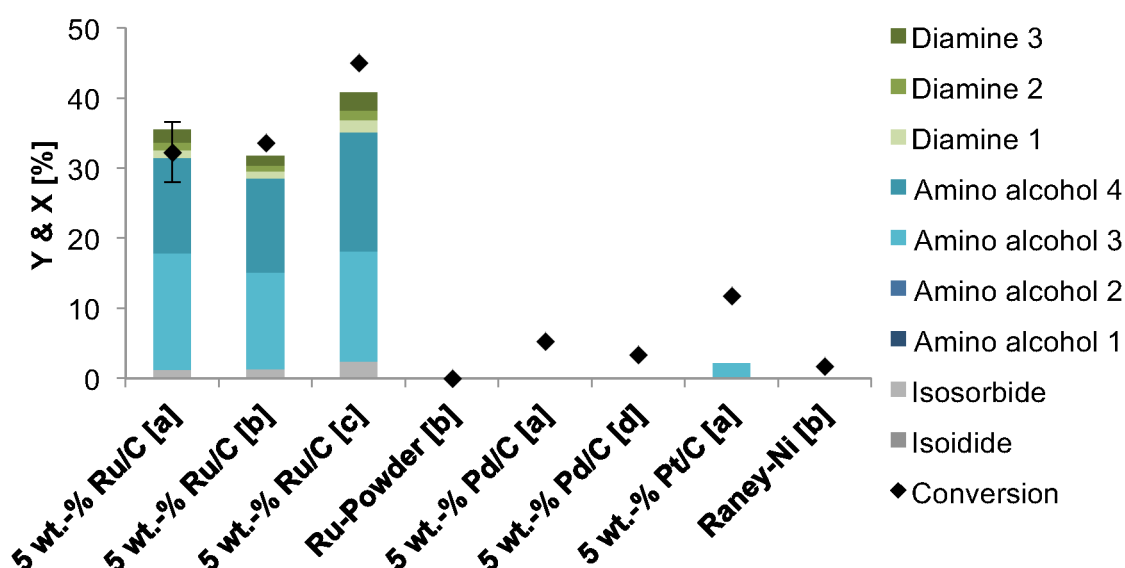


Figure 10. Screening of different commercial hydrogenation catalysts. Reaction conditions: 160 °C, 1 g isomannide, 5 g aq. ammonia solution, 10 bar H₂ (at RT), 500 rpm, and 24 h reaction time. The amount of metal referred to the substrate was 2 mol-% except for Raney-Ni with 20 mol-%; [a] *Sigma Aldrich* [b] *abcr* [c] *Escat 4401*; *abcr* [d] *Johnson Matthey*.

It is easy to see, that from the screened catalysts only ruthenium supported on activated carbon catalysts (Ru/C) are active in the amination of isomannide in aq. ammonia solution. Only minor amounts of amino alcohol 3 are formed with Pt/C as catalyst. Raney-Ni is not active, although the tenfold amount of the active compound was used in this experiment. Interestingly, also reduced ruthenium does not catalyse the amination reaction. Thus, not only is the active metal ruthenium important to the direct catalytic amination, but also the specific surface area of the support and/or the size of the ruthenium nanoparticles (NP).

The experiment with the Ru/C catalyst from *Sigma Aldrich* was repeated three times in order to determine the experimental error. Thus, the displayed values for the conversion and yield obtained with the mentioned catalyst in Figure 10 are mean values. Additionally, the standard deviation (± 4 %) for the conversion is displayed. The standard deviation for the total yield is ± 3 % but was omitted in the figure for clarity. This quite large deviation is not unusual when working with biomass and biogenic platform chemicals. In addition, there is almost no

difference between the conversion and total yield when catalysts with low surface areas were applied, i.e. ruthenium powder and Raney-Ni, but larger variances occur using supported catalysts. Hence, the deviation can also be due to adsorption of the substrate as well as the products on the large specific surface areas of the activated carbons used as support material. Moreover, the error of the gas chromatography (GC) itself influences the standard deviations.

Ruthenium catalysts are also the most active catalysts in hydrogenation reactions of various biogenic platform chemicals like glucose,^[46] levulinic acid,^[161] or lactic acid.^[162] In the past and, therefore, mainly in petrochemistry mostly platinum, rhodium, palladium, or nickel catalysts were used for hydrogenations.^[163] Additionally, those reactions were usually conducted in the gas phase or in organic solvents. As already mentioned above for the conversion of biomass-based compounds liquid phase processes, especially in aqueous medium, are necessary. The most efficient catalysts in aqueous-phase hydrogenation reactions of platform chemicals are supported ruthenium nanoparticles.^[164] They facilitate a rapid and selective conversion. Since two main steps of the amination are the dehydrogenation of the alcohol and the re-hydrogenation of the imine intermediate to the amine product it is not surprising that Ru/C catalysts are most suitable for the aqueous-phase amination of isohexides.

Until now, there is not a clear answer on why ruthenium-based catalysts are superior in the aqueous-phase hydrogenation of carbonyl groups. However, several theories have been proposed.^[163] They include the oxophilic character of ruthenium and the formation of hydrogen bonds between the adsorbed ketone and coadsorbed water molecule. It is suggested that the latter leads to a decrease in activation energy for the hydrogenation. Another hypothesis is that the dissociation of water molecules on the ruthenium surface enhance the surface concentration of hydrogen atoms; therefore, facilitating the hydrogenation.

3.1.2.2 Synthesised Ru/C Catalysts

In order to investigate the influence of the support material as well as different synthesis parameters, several Ru/C catalysts were synthesised by the wet impregnation method. The details of the synthetic procedure can be found in chapter 5.2.

In Figure 11 an overview of the results using activated carbons with different specific surface areas as support materials is shown. The results are displayed with increasing value of the specific surface areas ($S_{\text{BET, Aldrich}} < S_{\text{BET, SX 1G}} < S_{\text{BET, ROX 0.8}} < S_{\text{BET, RX3 Extra}} < S_{\text{BET, A Supra EUR}}$). The exact values for the specific surface areas can be found in the appendix (Table A 1).

Leftmost the mean value of the results obtained with the commercial Ru/C catalyst at 170 °C and 6 h is shown as comparison. The values of the standard deviation are $\pm 2\%$ for the conversion and $\pm 3\%$ for the total yield, but only the first is displayed for clarity. In comparison to the standard deviation of the conversion mentioned in chapter 3.1.2.1 ($\pm 4\%$) the value is smaller in this case. An explanation could be the reduced reaction time from 24 to 6 h. Yet, the standard deviation for the freshly synthesised catalysts can vary.

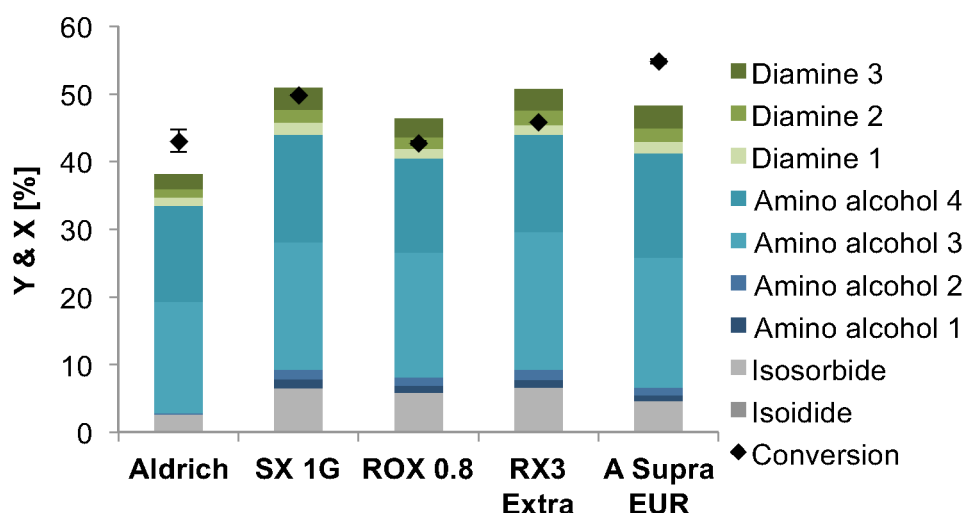


Figure 11. Screening of different activated carbons as support material for Ru/C catalysts in comparison to the commercial Ru/C by *Sigma Aldrich*. Reaction conditions: 170 °C, 2 mol-% Ru/C, 1 g isomannide, 5 g aq. ammonia solution, 10 bar H₂ (at RT), 500 rpm, and 6 h reaction time.

Figure 11 shows no correlation of the conversion and total yield with the specific surface area of the catalyst. Yet, the metal loading, as determined by inductive coupled plasma optical emission spectroscopy (ICP-OES), varies in between the tested catalyst. Considering this fact, and comparing normalised values, a correlation of lower specific surface areas leading to higher total yields might be made (Table A 1). However, the variance is negligible contemplating the error of the GC analysis as well as the ICP-OES measurements. Thus, the specific surface area has no distinct influence on the catalyst's performance.

Nevertheless, the total yield obtained with the freshly synthesised catalyst is higher than when using the commercial catalyst in all cases. The active metal on supported catalysts can be passivated through oxidation. Therefore, the metal needs to be reduced once more under reaction conditions. The commercial ruthenium catalyst used in this work was stored under argon atmosphere but it was not handled under inert gas atmosphere while working with it. Hence, due to the long period of storage and frequent use, surface passivation cannot be excluded. Thus, the surface passivation of the ruthenium of the freshly synthesised Ru/C catalysts is most likely less severe than for the commercial one, leading to better results. Additionally, the size of the ruthenium nanoparticles can have an influence on the catalyst's

performance. It is possible that the nanoparticles of the commercial catalyst are larger than the ones of the freshly synthesised catalysts, therefore, potentially less active.

Remarkably, when using the freshly synthesised catalysts also amino alcohols 1 and 2 are obtained in noticeable amounts from isomannide. These are the amino alcohols with the residual hydroxy group in *exo*-position favourably produced starting from isosorbide (cf. 3.1.1). The higher activity of the catalyst also increases the isomerisation activity. Thus, not only a larger amount of isosorbide is detected in the product spectrum but also more isosorbide is available for the amination reaction.

Furthermore, the influences of parameters of the catalyst synthesis like the heating rate of the reduction and the reduction temperature have been investigated. Figure 12 shows the obtained conversion and yield with freshly synthesised catalysts having the same support material and reduction temperature of 350 °C but with different heating rates through the reduction process. Additionally, the result with the commercial catalysts is shown for comparison.

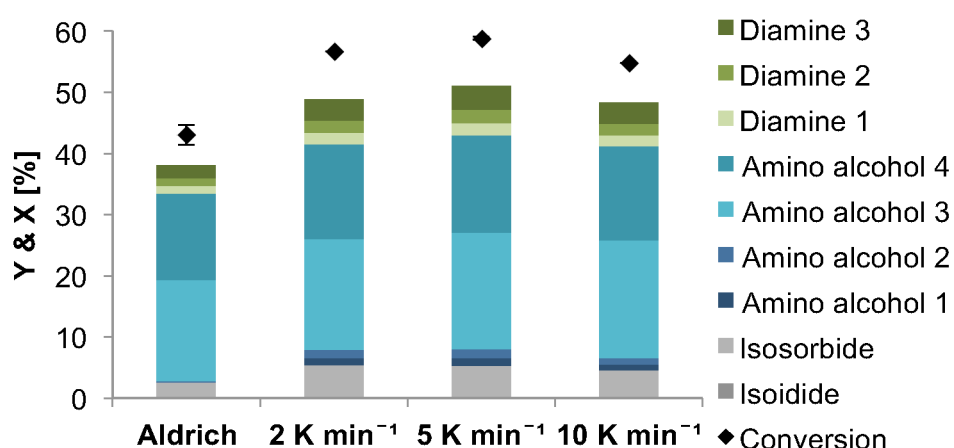


Figure 12. Screening of different heating rates of the reduction in the synthesis of Ru/C catalysts using A Supra EUR as support material in comparison to the commercial Ru/C by Sigma Aldrich. Reaction conditions: 170 °C, 2 mol-% catalyst, 1 g isomannide, 5 g aq. ammonia solution, 10 bar H₂ (at RT), 500 rpm, and 6 h reaction time.

Again, using freshly synthesised catalysts, higher yields can be obtained than with the commercial Ru/C catalyst for the same reasons as stated above. When comparing the various heating rates applied in the catalyst reduction, the conversions and yields differ only marginally and the differences are in the range of the experimental error. Thus, the heating rate of the catalyst reduction has no significant influence on the catalyst's performance.

The reduction temperature on the other hand has an influence on the catalyst's performance as can be seen in Figure 13. There is no difference in the conversion and total yields when applying the synthesised catalysts, which were reduced at 300 or 350 °C. Moreover, these two catalysts lead once more to better results than the commercial Ru/C. Interestingly, the

catalyst reduced at 400 °C leads to a similar conversion as the other two freshly synthesised catalysts. However, the total yield of the amination products is significantly lower and comparable to the yield obtained with the commercial Ru/C catalyst. The discrepancy might be due to increased adsorption on the high surface area support. In this case also no amino alcohols 1 or 2 can be obtained. The reduction temperature of 400 °C is quite harsh and might lead to the formation of larger nanoparticles. Thus, the same hypothesis as for the commercial catalyst mentioned above can be applied. Hence, the size of the nanoparticles was investigated.

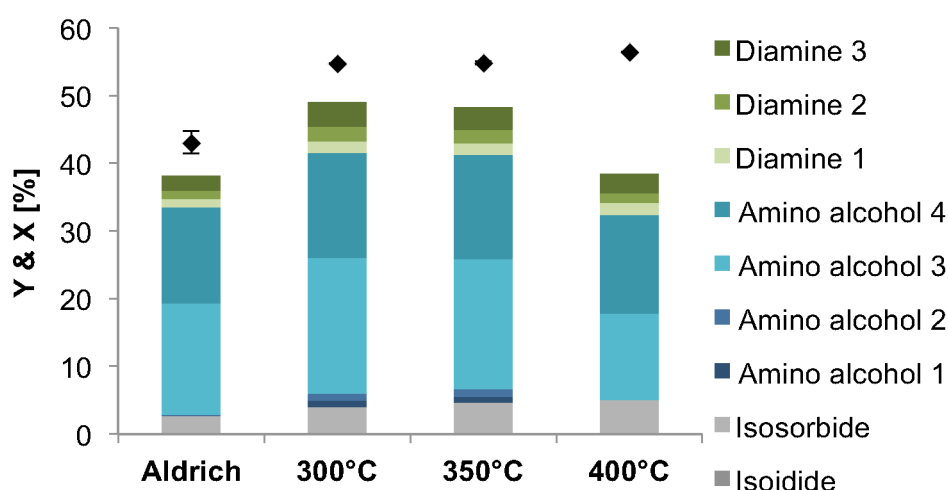


Figure 13. Screening of different reduction temperatures in the synthesis of Ru/C catalysts using A Supra EUR as support material in comparison to the commercial Ru/C by *Sigma Aldrich*. Reaction conditions: 170 °C, 2 mol-% catalyst, 1 g isomannide, 5 g aq. ammonia solution, 10 bar H₂ (at RT), 500 rpm, and 6 h reaction time.

A common method to determine the size of nanoparticles is powder X-ray diffraction (XRD) measurements using the Scherrer equation.^[165] Therefore, exemplarily XRD measurements of the commercial Ru/C catalyst as well as the synthesised Ru/C catalyst using A Supra EUR as support material, 10 K min⁻¹ as heating rate, and 350 °C as reduction temperature were performed. The corresponding XRD patterns can be found in the appendix (Figure A 1 and Figure A 2). Yet, only broad reflexes corresponding to the amorphous support material and a small reflex, which can be attributed to graphite, can be seen in the XRD diffraction pattern. By means of ICP-OES measurements, the ruthenium content was confirmed and under the applied conditions in the reduction step it is highly unlikely that the metal precursor was not reduced to Ru(0). Thus, the absence of discrete reflexes for ruthenium is an indication of very small particles below 10 nm.^[165]

Another way for the determination of the mean ruthenium particle size is through the chemisorption of carbon monoxide. In this procedure the catalysts undergo a pre-treatment step in which all potential oxidised species are reduced. This pre-treatment is necessary to

determine the correct size of the nanoparticles. Afterwards, the catalysts are treated with pulses of carbon monoxide. The detailed description of the procedure can be found in chapter 5.5.5.5. The size of the nanoparticles can be calculated based on the amount of adsorbed carbon monoxide. Table 1 shows the particle sizes for the measured catalysts based on this procedure.

Table 1. Overview of the ruthenium nanoparticle sizes depending on the parameters of the catalyst synthesis and the analysis method.

Catalyst	Aldrich	1	2	3	4	5	6
Support Material	-	A Supra EUR	A Supra EUR	A Supra EUR	A Supra EUR	A Supra EUR	RX3 Extra
Reduction Temperature [°C]	-	300	350	400	350	350	350
Heating Rate [K min⁻¹]	-	10	10	10	2	5	10
NP Size by CO Adsorption [nm]	1.2 (±0.07)	2.0 (±0.4)	1.2	2.0	1.1	1.8	1.3
NP Size by TEM [nm]	1.7 (±0.3)	1.3 (±0.2)	1.2 (±0.2)	1.5 (±0.3)	-	1.2 (±0.2)	-

The nanoparticles in the investigated samples have a mean size far below 10 nm as already assumed after the XRD measurements. More precisely, they are between 1.1 and 2.0 nm small. The mean nanoparticle size of the commercial catalyst was obtained from three independent measurements with different samples of the same batch with a standard deviation of ±0.07 nm. The results for the synthesised catalysts were collected from single measurements except for catalyst 1. In the first measurement for this catalyst an unexpected large mean nanoparticle size of 2.5 nm was obtained. Thus, two additional measurements were conducted with different samples of the same batch leading to a mean value of 2.0 nm with a large standard deviation of ±0.4 nm. Therefore, a broad size distribution of the ruthenium nanoparticles is possible. In general, no clear correlation between the synthetic method and the nanoparticle size obtained by the virtue of carbon monoxide adsorption can be made.

To verify the results, scanning transmission electron microscopy (STEM) pictures were taken of some of the catalysts. Figure 14 shows two exemplary STEM pictures. Further pictures can be found in appendix Figure A 3 to Figure A 7. It can be seen that the ruthenium

nanoparticles are uniformly distributed. The results of the size evaluation (measurements of 50 to 90 nanoparticles depending on the sample) are also displayed in Table 1 and range from 1.2 to 1.7 nm. Noticeably, the ruthenium nanoparticle sizes obtained by the two methods differ except for catalyst 2. In most cases the mean value of the nanoparticles measured in the STEM pictures are smaller than the size average gained by the carbon monoxide adsorption measurements. Considering the nanoparticles sizes obtained by STEM, the lowest yields were achieved with the catalyst containing larger ruthenium nanoparticle sizes, the commercial catalyst with 1.7 nm and catalyst 3 with 1.5 nm in average. Especially when looking at the size distributions (Figure A 3 to Figure A 7), it can be seen that in the investigated samples of these catalysts the largest nanoparticles (> 2 nm) can be found. Thus, the decrease in catalytic activity might be due to an increase in ruthenium nanoparticle size. However, it has to be considered that STEM is a local method and even with several pictures of one sample only a small part of the catalyst can be represented. Thus, a bimodal or significantly varying size distribution leading to bigger mean values as obtained by means of carbon monoxide adsorption cannot be excluded. Yet, so far, very small ruthenium nanoparticle seem to facilitate the isohexide amination reaction.

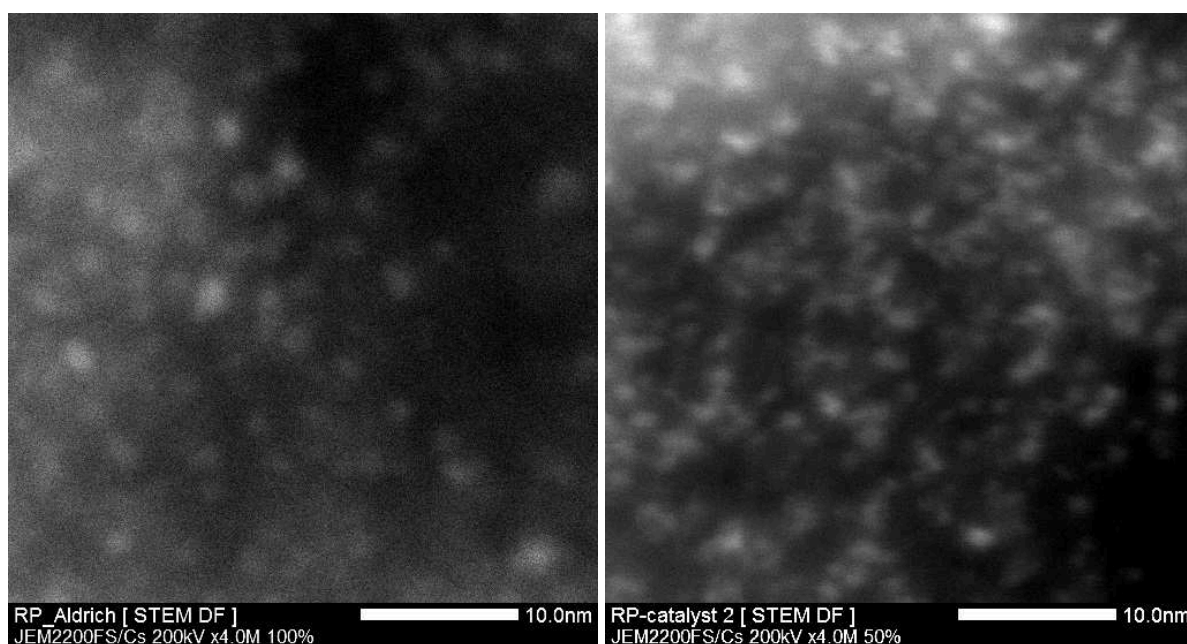


Figure 14. Exemplary STEM DF pictures of the commercial catalyst (left) and the synthesised catalyst 2 (right).

3.1.3 Investigation of the Hydrogen Autotransfer Mechanism

Hydrogen autotransfer is a possible catalytic mechanism for the direct amination of secondary alcohols as already mentioned in chapter 2.3. Therefore, it was investigated whether the amination of isohexides follows this mechanism when using a heterogeneous Ru/C catalyst.^[160] In this case the amination reaction should be, in principal, independent from external hydrogen. Unfortunately, without external hydrogen pressure no amination and only negligible amounts of isomerisation products can be detected under the applied reaction conditions (Figure 15). However, the detected low amount (1 %) of isoidide is most likely already in the isosorbide feed since the used isosorbide has a purity of 98 %. Reference GC measurements of pure isosorbide revealed an isoidide content of at least 0.3 %. The observed conversion can be attributed either to adsorption of the substrate on the catalyst or degradation of the substrate. In general, with Ru/C as catalyst and when hydrogen is applied, the reaction solution after the reaction is clear and colourless. However, after the reaction without hydrogen the solution was yellow to orange indicating the formation of humins. Thus, the degradation of isosorbide is at least partially the reason for the observed conversion.

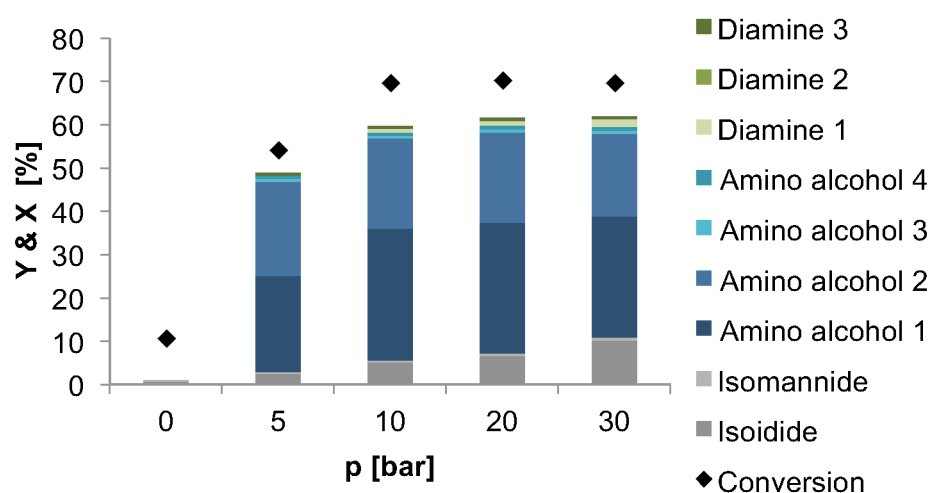


Figure 15. Pressure dependence of the amination of isosorbide. Reaction conditions: 170 °C, 2 mol-% Ru/C, 1 g isosorbide, 5 g aq. ammonia solution, 500 rpm, and 24 h reaction time. All denoted pressures are the pressures at RT. Results were obtained in autoclaves with an internal thermocouple.

Applying only 5 bar hydrogen pressure at room temperature the amination reaction occurs. When the pressure is increased to 10 bar an increase in conversion from 54 to 70 % and total yield from 49 to 60 % can be obtained. However, a further increase to 20 or 30 bar hydrogen pressure does not influence the conversion or total yield. Yet, there is a slightly lower amount of amination products and an increased amount of isomerisation products, mostly isoidide, formed. For more information on the isomerisation of isohexides, please see chapter 3.2. As already discussed in chapter 3.1.1, the *exo*-configured hydroxy groups are less reactive in the amination reaction. Therefore, it is beneficial to keep the isomerisation to

a minimum with a maximum amount of amination products. Thus, for the amination of isosorbide, 10 bar hydrogen pressure at room temperature is favourable.

Figure 16 shows the pressure dependence of the amination of isomannide. The differences in conversion and total yield between the amination of isosorbide in Figure 15 and of isomannide in Figure 16 can primarily be attributed to the lower reaction temperature for the amination of isomannide at 160 °C instead of 170 °C. Additionally, the results starting from isosorbide were obtained in different autoclaves than the ones starting from isomannide. The autoclaves in the isosorbide experiments (Figure 15) have a thermocouple inside a capillary, which reaches into the autoclave, allowing for better temperature control than for the autoclaves in the isomannide experiments (Figure 16) where the thermocouple was attached to the outer heating block.

Nevertheless, the trend concerning the variation of the hydrogen pressure should be the same. Intriguingly the conversion and total yield are increasing with increasing hydrogen pressure for the isomannide experiments in contrast to the isosorbide experiments. However, this difference is majorly due to the isomerisation side reaction. At 40 bar hydrogen pressure (at RT) 11 % isosorbide and 1 % isoidide are produced. Therefore, it is reasonable that amino alcohols 1 and 2 are formed in this experiment with 3 and 4 %, respectively.

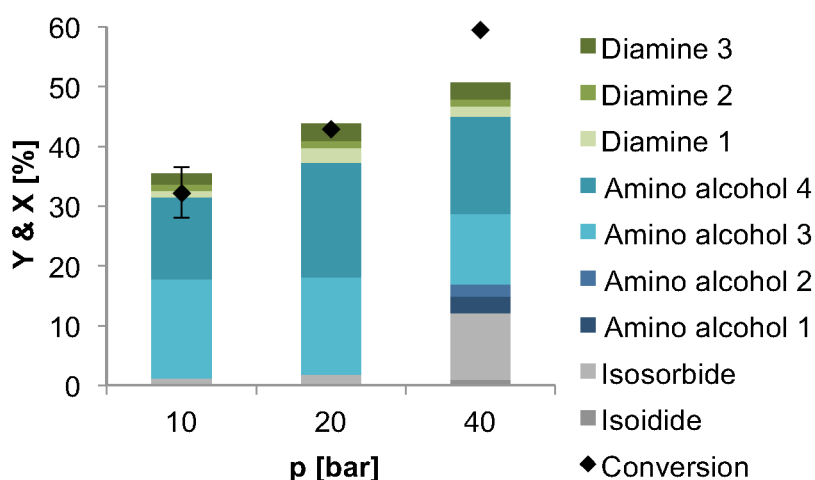


Figure 16. Pressure dependence of the amination of isomannide. Reaction conditions: 160 °C, 2 mol-% Ru/C, 1 g isomannide, 5 g aq. ammonia solution, 500 rpm, and 24 h reaction time. All denoted pressures are the pressures at RT. Results were obtained in autoclaves with an external thermocouple.

When the isomerisation products are not considered (Figure 17), only from 10 to 20 bar a slight increase in the total yield of amination products is observed while a further increase to 40 bar hydrogen pressure leads to a slight decrease. Thus, it is favourable to work at lower hydrogen pressures to avoid the isomerisation and maximise the yield of the amination products.

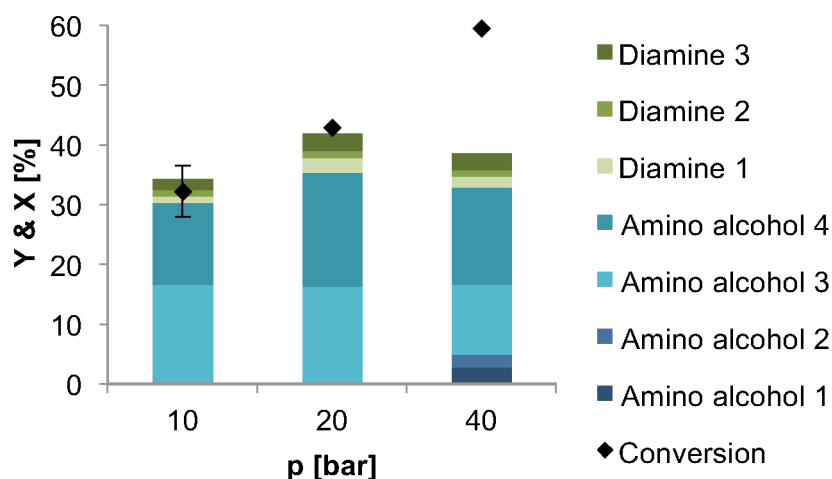


Figure 17. Pressure dependence of the amination of isomannide as in Figure 16 but without the obtained isomerisation products. Reaction conditions: 160 °C, 2 mol-% Ru/C, 1 g isomannide, 5 g aq. ammonia solution, 500 rpm, and 24 h reaction time. All denoted pressures are the pressures at RT. Results were obtained in autoclaves with an external thermocouple.

The increase between 10 and 20 bar in contrast to the isosorbide experiment can likewise be explained by the autoclaves used. The once used in the isosorbide experiments have not only a better temperature control but also a greater volume (45 mL in comparison to 20 mL). Therefore, if in both cases 5 mL reaction solution and 10 bar of hydrogen are applied the effective amount of hydrogen is larger in the 45 mL autoclave with the larger gas volume.

The amount of hydrogen is calculated in first approximation using the ideal gas law. When 5 bar hydrogen pressure is applied in the 45 mL autoclave, the result is approximately 8 mmol hydrogen, i.e. 16 mmol for 10 bar. Between these results a difference in the total yield and conversion can be obtained but not when the pressure is further increased. When calculating the amount of hydrogen for the 20 mL autoclave, the result for 10 bar is approximately 6 mmol; thus, 12 mmol for 20 bar. This difference could explain why the conversion as well as the total yield is increasing from 10 to 20 bar in the isomannide experiments in contrast to the isosorbide experiments. Referencing the hydrogen amount to the amount of substrate, there are 1.2 and 2.3 eq. (45 mL autoclave) as well as 0.9 and 1.7 eq. (20 mL autoclave) of hydrogen. For a better overview, all calculated values are summarised in Table 2.

Table 2. Overview of the calculated amounts of hydrogen depending on the used autoclave and pressure in first approximation (5 mL reaction solution, 1 g isohexide (1 eq.), and 0.2769 g Ru/C catalyst).

Autoclave	45 mL		20 mL	
Gas Volume [mL]	40		15	
Pressure [bar]	5	10	10	20
Amount of Hydrogen [mmol]	8	16	6	12
Equivalents of Hydrogen	1.2	2.3	0.9	1.7

It can be concluded that an excess of hydrogen of 1.7 to 2.3 eq. is necessary to eliminate its influence on the reaction. Nevertheless, a small amount of hydrogen is already sufficient to enable the amination reaction to a large extent. In fact, less than two equivalents of hydrogen are sufficient. Thus, the ratio between hydrogen and the involved hydroxy and the therefore to be reduced imine groups, is still substoichiometric. Hence, the hydrogen is most likely primarily used to reactivate the catalyst under reaction conditions and to saturate the surface of the catalyst with hydrogen.

As discussed already in chapter 2.3, the hydrogen autotransfer mechanism was so far only reported for smaller molecules when solid catalysts were applied. However, in case of the isohexides, it is conceivable that the possibility of contact of the sterically demanding imine molecule with hydrogen on the surface of the catalyst has to be increased to enable the re-hydrogenation step towards the amine. Therefore, a certain coverage of the active metal surface becomes necessary.

In order to investigate if the additional hydrogen is only required to reactivate the catalyst, a freshly synthesised Ru/C catalyst, which was handled under inert gas atmosphere throughout, was applied in catalysis. Both the catalyst and the substrate were weighed into the autoclave in a glovebox under argon atmosphere and the aq. ammonia solution was added under counterflow of argon to keep the oxygen content to a minimum. The aq. ammonia solution was not degassed to maintain the ammonia content of 25 %. Starting from isomannide and without additional hydrogen, minor amounts of approximately 1 % amino alcohols and 2 % isosorbide could be observed after 24 h reaction time at standard conditions. The conversion in this case was 26 %. Thus, in general, the heterogeneously catalysed amination of isohexides using Ru/C as catalyst seems possible, although the conversion due to leaching of the active metal species cannot be ruled out completely. However, only minor leaching of ruthenium was observed, at least for the commercial Ru/C catalyst, as will be discussed in more detail in chapter 3.1.5. Nevertheless, the reaction kinetics in this experiment were slow and the degradation of the substrate was preferred, as

indicated by the yellow colour of the reaction solution after the reaction as well as the unclosed mass balance of 23 %. Furthermore, also adsorption of the reactants on the surface of the catalyst can be a reason for the latter. Thus, the necessary amount of additional hydrogen is most likely important to reach a certain coverage of the active metal surface enhancing the reaction, especially the re-hydrogenation. This means, that the amount of hydrogen is dependent from the amount of catalyst rather than the amount of substrate and should be calculated per gram of Ru/C catalyst. Under the applied conditions the estimated limited value would be between 43 and 58 mmol g⁻¹. To verify this assumption the pressure dependence of the amination was investigated for a larger amount of catalyst, more precisely the catalyst amount was doubled. The autoclaves with the internal thermocouple were used, and to keep all parameters equal the amount of substrate and aq. ammonia solution was also doubled. The experiments were performed for 6 h, because in the progress of the project it was discovered that shorter reaction times are also sufficient for reaching a reasonable conversion and yield. The results, starting from isomannide as the substrate, are shown in Figure 18. Additionally, the result for a lower amount of substrate and catalyst with 10 bar hydrogen pressure (at RT) and, therefore, approximately 58 mmol g⁻¹ hydrogen after 6 h reaction time is also displayed and is indicated using an asterisk.

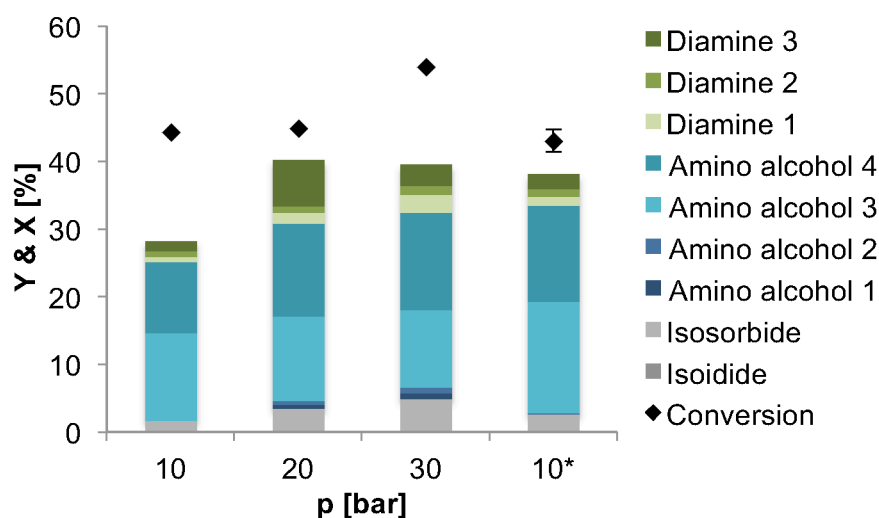


Figure 18. Pressure dependence of the amination of isomannide. Reaction conditions: 170 °C, 2 mol-% Ru/C, 2 g isomannide, 10 g aq. ammonia solution, 500 rpm, and 6 h reaction time. All denoted pressures are the pressures at RT. Results were obtained in autoclaves with an internal thermocouple. *Same reaction conditions except for 1 g isomannide and 5 g aq. ammonia solution.

When using a hydrogen pressure ranging from 10 to 20 bar, an increase in yield can be observed; whereas, there is no further increase from 20 to 30 bar. The amount of hydrogen per gram of catalyst is estimated using the ideal gas law. Thereby, the decreased gas phase because of the larger volume of the reaction solution is taken into account and the results are summarised in Table 3.

Table 3. Overview of the calculated amounts of hydrogen per gram catalyst depending on the gas volume and pressure in first approximation. (10 mL reaction solution, 2 g isomannide, and 0.5538 g Ru/C catalyst in the experiments with 35 mL gas volume. For 40 mL gas volume all parameters were bisected.)

Gas Volume	35 mL			40 mL
Hydrogen Pressure [bar]	10	20	30	10
Amount of Hydrogen [mmol]	14	28	42	16
Amount of Hydrogen per Gram Catalyst [mmol g⁻¹]	26	51	77	58

No influence on the amination activity could be observed for ratios of 50 mmol g⁻¹ or higher. The fact that with 10 bar hydrogen (58 mmol g⁻¹) but with a lower amount of substrate and catalyst, similar results can be obtained as with 20 bar at a larger scale reinforces this assumption.

In conclusion, to achieve reasonable yields and conversions the requirements for a HAT concept are not given in the case of a solid Ru/C catalyst, although no additional hydrogen is consumed overall. Still, because hydrogen is needed only in a low pressure range, the amination of isohexides in aqueous ammonia is a benign reaction path towards biogenic amines.

3.1.4 Investigation of Reaction Parameters

In this chapter, the influence of different reaction parameters on the amination of isomannide is discussed.^[160]

Upon temperature variation, the conversion and yield increase significantly with rising temperature, but only up until 170 °C (Figure 19). The differences from 50 % conversion and 47 % total yield at 170 °C to 52 % conversion and 52 % total yield at 180 °C are rather low. These results were obtained using the 20 mL autoclaves. Therefore, it has to be noted that the results were gained in the hydrogen-dependent regime (cf. 3.1.3). However, all results were obtained using the same amount of catalyst as well as the same hydrogen pressure. Thus, they can be compared among each other.

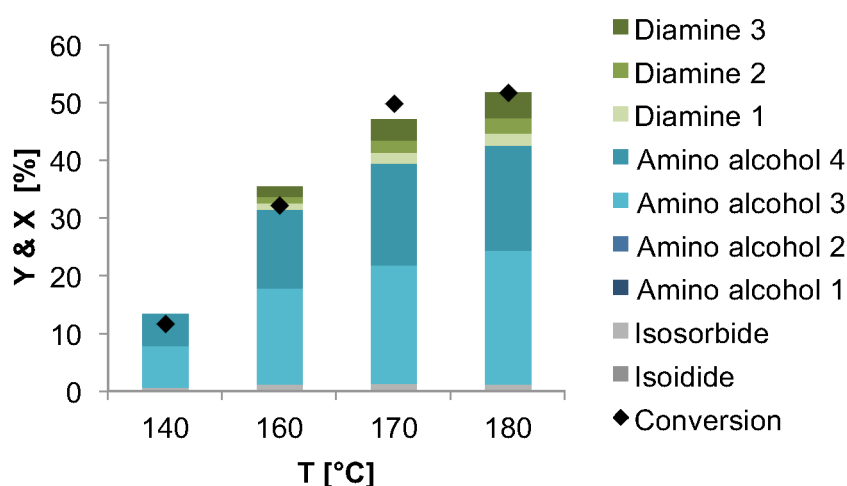


Figure 19. Screening of different reaction temperatures in the amination of isomannide. Reaction conditions: 2 mol-% Ru/C, 1 g isomannide, 5 g aq. ammonia solution, 10 bar H₂ (at RT), 500 rpm, and 24 h reaction time.

In the attempt to reach full conversion towards amine products, different approaches at 180 °C reaction temperature were investigated (Figure 20). Leftmost in Figure 20 (a) the results obtained after 24 h reaction time at 180 °C are displayed for comparison. After prolonging the reaction time to 48 h (b), the conversion increases to 65 % while the total yield stays constant and only the product distribution changes slightly. The amount of diamines is increased while the amount of amino alcohols decreases. Furthermore, also by adding fresh catalyst (c), only a minor increase in the total yield and no significant increase in conversion can be observed. Therefore, it is conceivable that once a specific amount of amination products is present in the solution, they adsorb on the active metal of the catalyst and deactivate even a freshly added catalyst.

To rule out a limitation by the present amount of ammonia, additional ammonia solution was added during the reaction course (**d**), leading to a slight increase in the total yield to 63 %. Through the additional ammonia the concentration in the solution is altered changing also the adsorption equilibrium, which may be one reason for the enhanced total yield. Moreover, to enable a higher ammonia concentration a lower amount of substrate and catalyst are applied in this experiment. Therefore, it is the only one of the experiments displayed in Figure 20, which is not performed in the hydrogen-dependent regime based on the hypothesis explained above (with a hydrogen amount per gram catalyst of 43 mmol g^{-1} instead of 22 mmol g^{-1}). This fact may be another reason for the slightly better results.

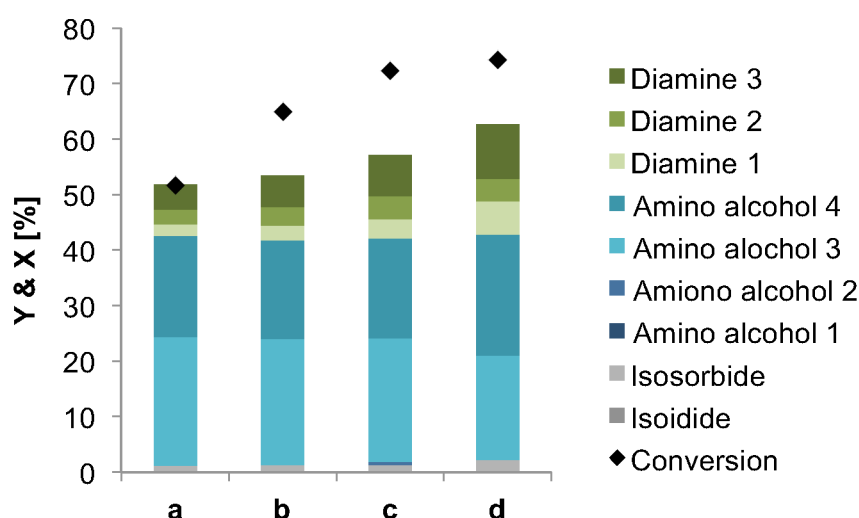


Figure 20. Screening of different parameters. Reaction conditions: 180°C , 2 mol-% Ru/C, 1 g isomannide, 5 g aq. ammonia solution, 500 rpm, and 10 bar H_2 . a) 24 h reaction time b) 48 h reaction time c) 24 h with 2 mol-% catalyst then additional 1 mol-% was added and run for another 24 h d) 5 h with 0.5 g isomannide in 2.5 g aq. ammonia solution then additional 2.5 g aq. ammonia solution was added and run for another 16 h.

Figure 21 displays the conversion and yield in dependence on the applied amount of substrate. The increase in conversion and total yield could be due to the larger excess of ammonia available in the experiment with the lower substrate concentration. However, simultaneously with the lowering of the substrate concentration, the amount of catalyst was reduced in order to stay at 2 mol-% catalyst ratio. Thus, the result on the right in Figure 21 was obtained without being limited by the present hydrogen amount (hydrogen amount per gram catalyst: 43 mmol g^{-1}), which is not the case for the result with a higher substrate concentration where also a higher amount of catalyst is applied (hydrogen amount per gram catalyst: 22 mmol g^{-1}). This variation could be another reason for the differences in conversion and yield. Furthermore, also the concentration of the amination products has to be considered. As already stated above, the catalyst seems to be deactivated through the adsorption of amination products on the active metal surface, once a certain amount of those products is present in the reaction mixture. In case of the different substrate concentrations,

at the same conversion, the absolute amount of amination products is smaller at lower substrate concentrations. Hence, it is conceivable that the deactivation in case of the higher substrate concentration is more severe leading to lower conversion and yield.

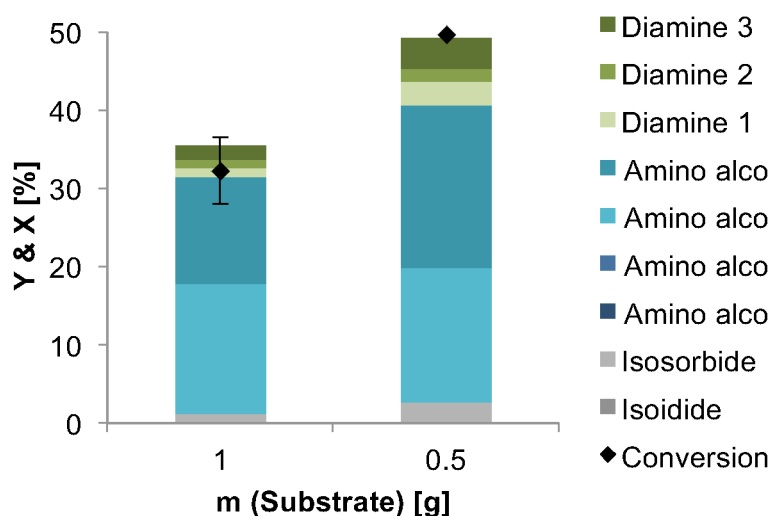


Figure 21. Comparison of different substrate concentrations in the amination of isomannide. Reaction conditions: 160 °C, 2 mol-% Ru/C, 5 g aq. ammonia solution, 10 bar H₂ (at RT), 500 rpm, and 24 h reaction time.

To get a clearer insight into how the amount of ammonia affects the amination reaction, experiments with varying amounts of ammonia at constant substrate and catalyst concentration would be necessary. It is not practical to perform these experiments with aqueous ammonia solution as the ammonia source. Dosing liquid ammonia to an aqueous substrate solution would be an option. Preliminary experiments were performed using a dosage pump to achieve different ammonia concentrations (Figure 22). At this point the GC analysis was not yet fully developed and only ratios of the different substances in the product mixture based on their area in GC could be obtained. The amount of ammonia within the autoclave was weighed out since the dosage is not yet very reliable in batch mode, especially when dosing only a few grams. This imprecision makes it difficult to reproduce each experiment. Still, this procedure seems promising for a continuous process. In Figure 22 the results labelled “Standard” are obtained with 5 g aqueous ammonia solution (11 eq. ammonia with respect to the substrate). The other two experiments were conducted in 5 g water and the respective amounts of ammonia were gained by dosing liquefied ammonia. Experimental details can be found in chapter 5.3.1.2. It can be seen that there is not much difference in the product distribution regardless of the ammonia source or the ammonia concentration. When comparing normalised results, there is the risk that the ratio of the products is distorted if the mass balance is different in the compared experiments. However, neither the GC analysis nor the colour of the product solution suggest more substrate decomposition in one experiment or the other, indicating no differences in the mass balance.

Nevertheless, to prove the assumption, these experiments have to be repeated with full analysis that gives more reliable results. To additionally enhance the reliability of the ammonia concentration through liquefied ammonia dosing, the experiments should be preferably done in a continuous system.

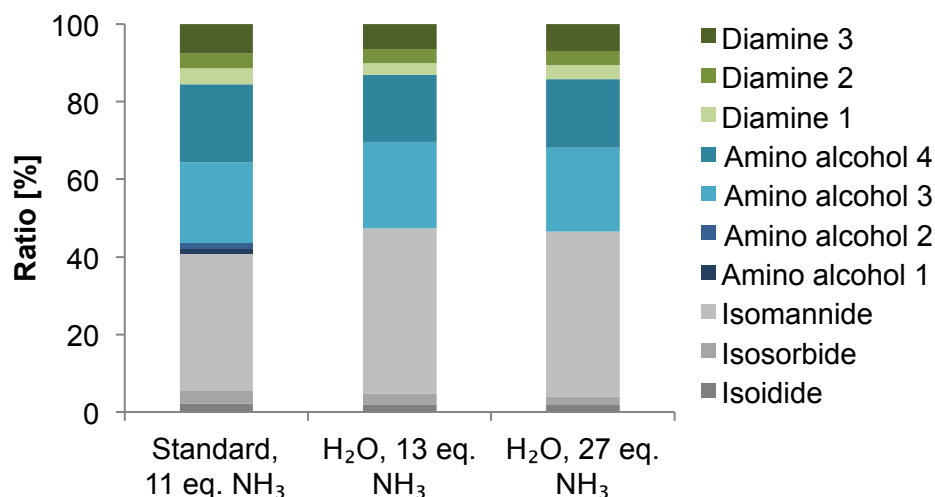


Figure 22. Screening of different amounts of ammonia in the amination of isomannide. Reaction conditions: 170 °C, 1 g isomannide, 5 g solvent (aq. ammonia solution or H₂O), 10 bar H₂ (at RT), 500 rpm, and 24 h reaction time. Standard labels results obtained with aq. ammonia.

Figure 23 displays the results gained by using different amounts of catalyst. Interestingly, the conversion and yield do not increase linearly with increasing catalyst amounts. Especially since with 1 and 2 mol-% catalyst, the conversion and yield are quite similar. To exclude that the result using 1 mol-% is an outlier, this experiment was repeated for a second time and the error bar displayed in Figure 23 depicts the deviation of the conversion.

One reason for this behaviour could be the deactivation of the catalyst through product adsorption, assuming that a certain amount of product is produced faster when a larger amount of catalyst is used. However, considering the influence of the hydrogen pressure, higher catalyst loadings require a larger amount of hydrogen (cf. chapter 3.1.3). Hence, only the results gained with 1 mol-% catalyst are not limited by the amount of hydrogen. Thus, to elucidate the influence of the amount of catalyst, additional experiments should be conducted with an excess of hydrogen.

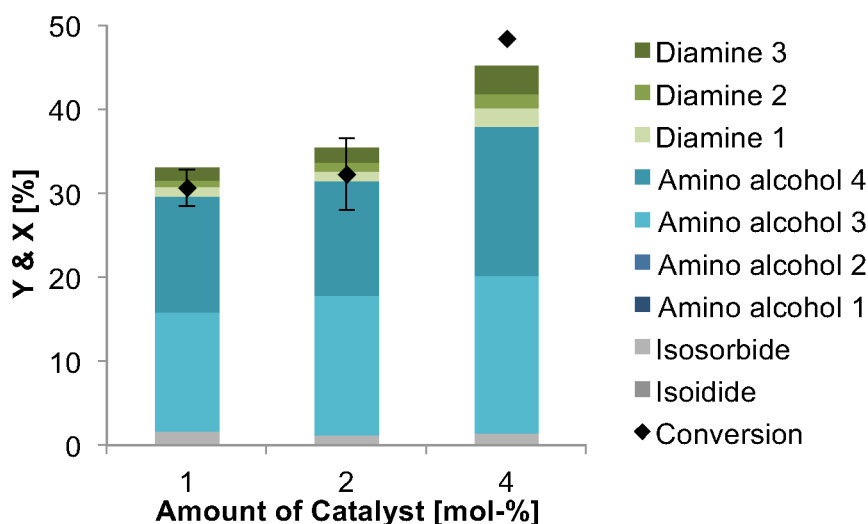


Figure 23. Screening of different amounts of catalyst in the amination of isomannide. Reaction conditions: 160 °C, 1 g isomannide, 5 g aq. ammonia solution, 10 bar H₂ (at RT), 500 rpm, and 24 h reaction time. For clarity only the error bar for the conversion is shown.

The results of the amination reaction after different reaction times are displayed in Figure 24. The enhanced conversion and yields, even at shorter times in comparison to the results showed in the other figures in this chapter, are once more due to the use of different autoclaves. In this case, the 45 mL autoclaves were used (for details please see chapter 5.3.1.1). Thus, a better temperature control and no limitation of the amount of hydrogen are given leading to higher conversion and yield.

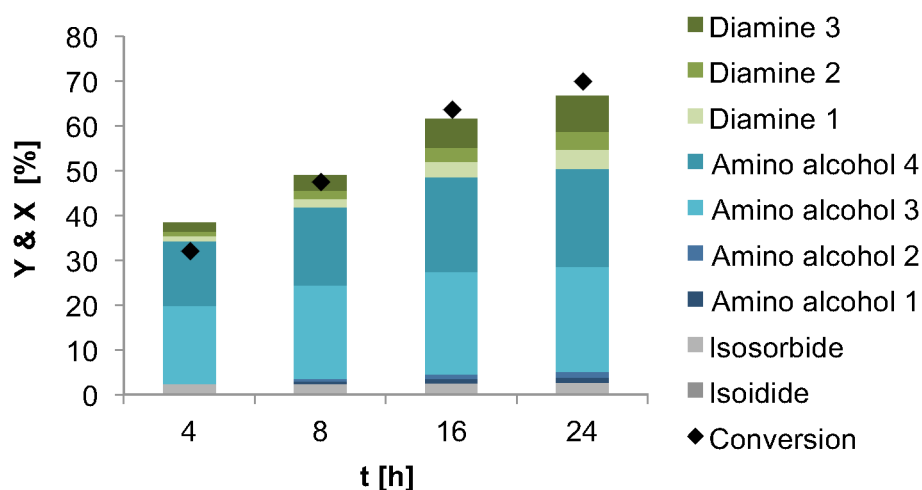


Figure 24. Screening of different reaction times in the amination of isomannide. Reaction conditions: 160 °C, 2 mol-% Ru/C, 1 g isomannide, 5 g aq. ammonia solution, 500 rpm, and 10 bar H₂ (at RT).

In Figure 25 the same results as in Figure 24, summarised in product categories, are displayed in a yield/conversion-time profile for a better overview. Since all results were obtained in single batch experiments without sampling, the dashed line is only added to guide the eye. The yield/conversion-time profile shows that the amino alcohols are formed

first and subsequently the diamines are produced. Hence, the amination reaction is a consecutive reaction. Additionally, based on these results a first estimation about the initial reaction rate with $2 \text{ mol kg}^{-1} \text{ h}^{-1}$ can be made (amount of amine products produced per kilogram catalyst and hour). The rate decreases with increasing time. This behaviour is most likely due to the already described catalyst deactivation by product adsorption.

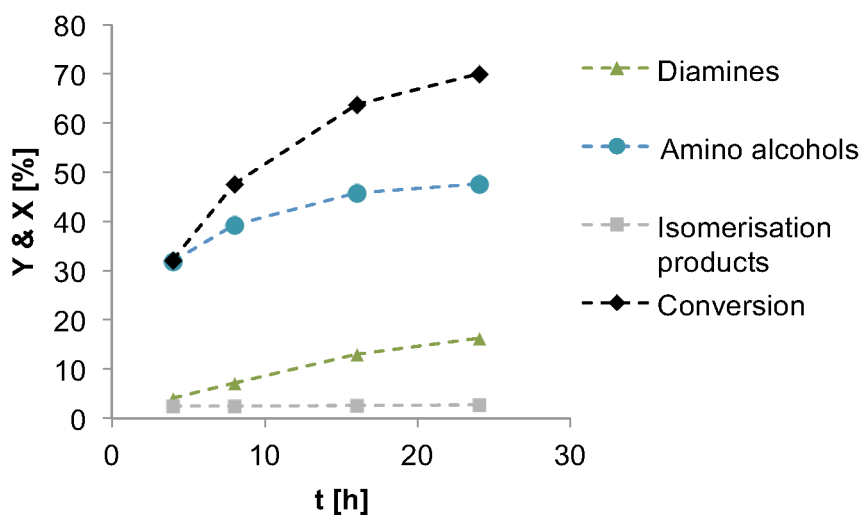


Figure 25. Yield/Conversion-time profile of the amination of isomannide. Same data as in Figure 24 displayed in correct time intervals and summarised in the product categories for a better overview. Reaction conditions: 160 °C, 2 mol-% Ru/C, 1 g isomannide, 5 g aq. ammonia solution, 500 rpm, and 10 bar H₂ (at RT).

3.1.5 Stability and Deactivation of the Commercial Ru/C catalyst

In chapter 3.1.4 it was already mentioned that catalyst deactivation was observed. Recycling tests should shed light on the stability of the commercial Ru/C catalyst.^[160] Furthermore, through recycling the nature of the deactivation is also investigated. Figure 26 shows the results of the recycling tests.

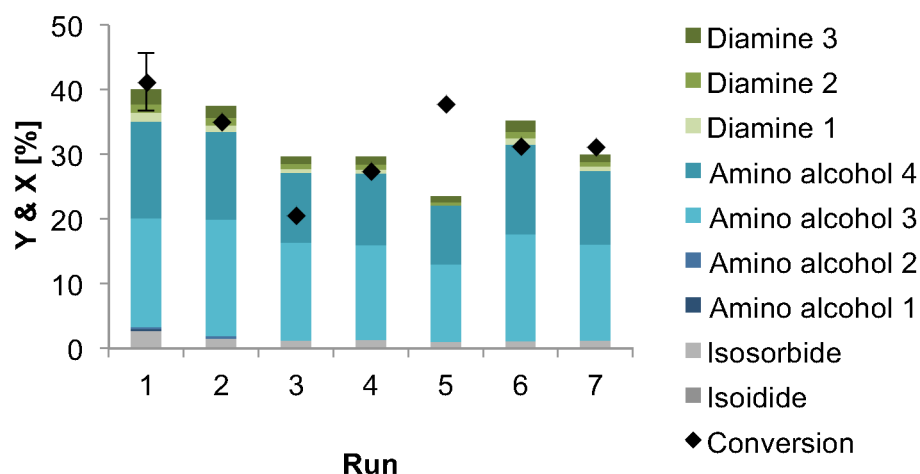


Figure 26. Recycling of the commercial Ru/C catalyst in the amination of isomannide. Reaction conditions: 150 °C, 2 mol-% Ru/C, 2 g isomannide, 10 g aq. ammonia solution, 10 bar H₂ (at RT), 500 rpm, and 24 h reaction time. The amount of substrate and solvent was adapted to the residual amount of catalyst in each run.

It can be seen that the catalyst is recyclable at least seven times under the applied conditions. Washing with water and ethanol restores the catalytic activity. Thus, the proposed catalyst deactivation through product adsorption is reversible. The experimental details are described in chapter 5.3.1.3. Recycling experiments in batch mode are not as precise as long-term experiments in a continuous reaction system as foundation for a statement about catalyst stability. Yet, seven consecutive runs are a good hint, that the catalyst is stable.

Some of the data points in the recycling study are certainly defective. Especially the third run in which the conversion is much lower than the total yield that is per definition not possible. However, for the proof of concept of the recyclability of the commercial Ru/C catalyst this is of little importance. From the first to the third run, the conversion and yield are decreasing but after that they commute around one value. This slight decrease in activity is a typical behaviour for a catalyst in the conditioning phase. Also in industry the catalysts often lose some of their activity in the beginning before a steady state phase is reached.

Exemplary product solutions after one run were investigated by ICP-OES and an average ruthenium content of <1 ppm was obtained.^[160] This value correlates to a loss of metal below 0.05 %, indicating minor leaching of the active metal. Considering the hydrothermal and highly basic conditions, the detected amount is surprisingly small. Therefore, the Ru/C

catalyst shows a comparably high stability in the amination reaction of isohexides. Nevertheless, the application in a continuous system is desirable to give a comprehensive statement on the catalyst's stability.

Furthermore, the catalyst was characterised before and after its use.^[160] Thus, a deeper understanding not only of the stability of the catalyst but also about its deactivation can be gained. ICP-OES measurements of the catalysts show that the loading of the metal decreases only marginally from 4.1 wt.-% (± 0.2 wt.-%) to 4.0 wt.-%, a decrease which is within the error range of the method.

Nitrogen physisorption measurements (cf. 5.5.5.1) reveal specific surface areas of $696 \text{ m}^2 \text{ g}^{-1}$ for the fresh catalyst and $600 \text{ m}^2 \text{ g}^{-1}$ for the used one. The decrease in specific surface area can be attributed to adsorption of reactants, which cannot be washed off.

Additionally, thermogravimetric analysis (TGA) was conducted of the fresh as well as of the spent catalyst. For details of the method see chapter 5.5.5.4. The commercial catalyst has a metal loading of 5 wt.-% (4.1 wt.-% according to ICP-OES as mentioned above). Thus, a residual mass of 4 to max. 5 % is expected assuming the activated carbon is burned completely. When the residue is a RuO_2 or RuO_4 species, this mass would increase slightly to approximately 7 to 8 %. Yet, the residual mass of the fresh Ru/C catalyst is 22 % without considering the initial loss of water (Figure 27). The additional residue can most likely be explained by ash, which is an impurity of the support material. Unfortunately, the supplier *Sigma Aldrich* did not provide information concerning the ash content of the activated carbon support material.

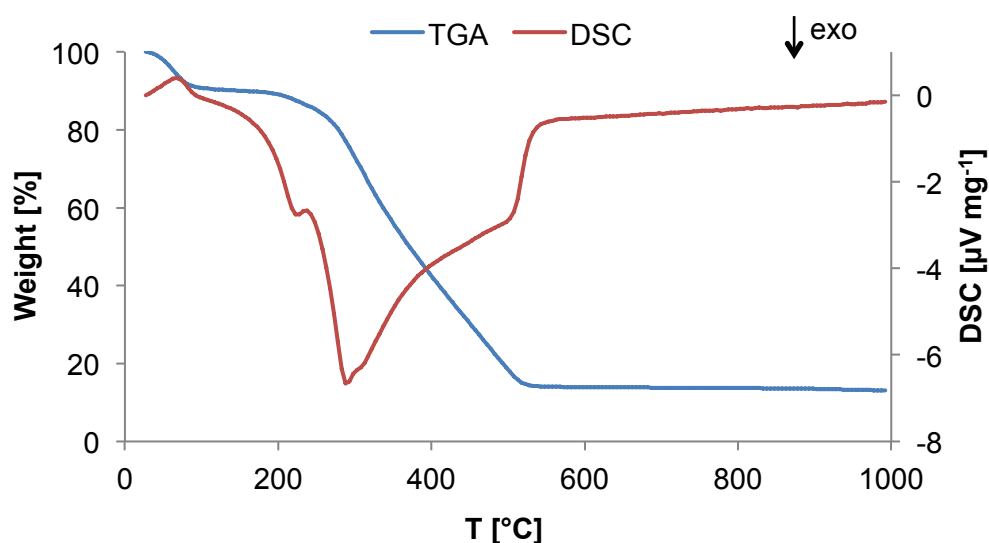


Figure 27. TGA and DSC data of the fresh commercial 5 wt.-% Ru/C catalyst.

Ash can also be observed in the A Supra EUR activated carbon used as support in most of the freshly synthesised catalysts. TGA shows 9 % residual mass for the mere support material (Figure 28) and 15 % for the synthesised 5 wt.-% Ru/C catalyst (catalyst 2; Figure 29). Considering the 9 % ash content the residue correlates to the ruthenium loading of 5.3 wt.-% as analysed by ICP-OES.

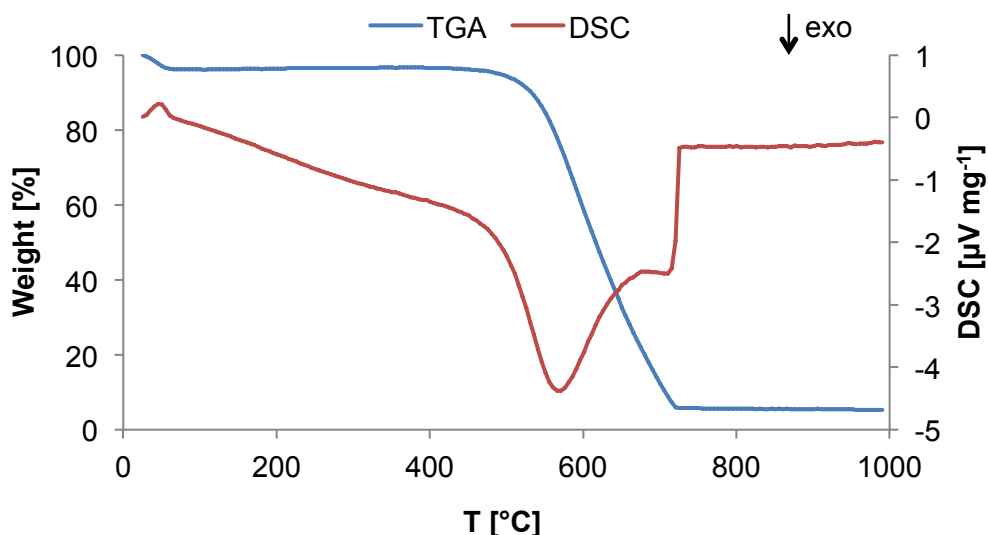


Figure 28. TGA and DSC data of the activated carbon A Supra EUR.

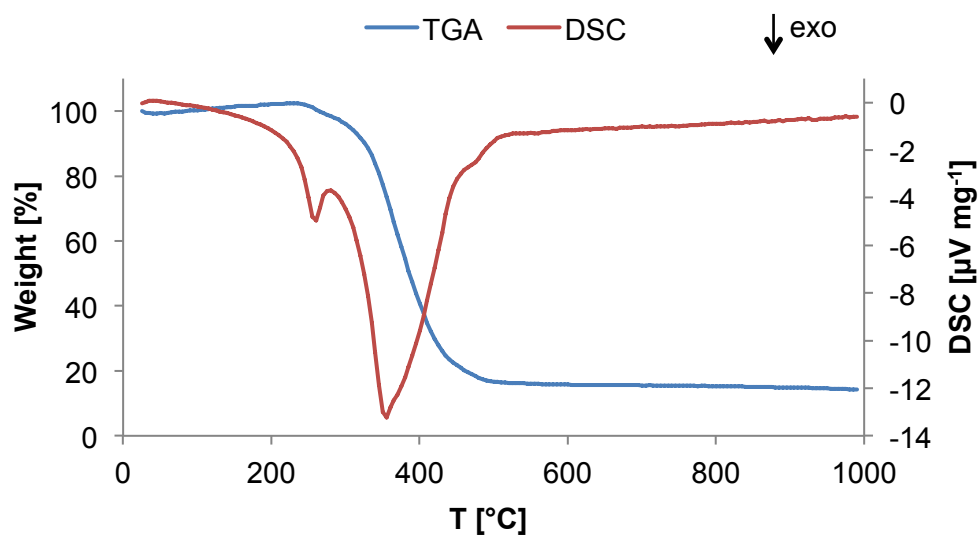


Figure 29. TGA and DSC data of the fresh 5 wt.-% Ru/C catalyst synthesised using A Supra EUR as support material.

The spent commercial catalyst was investigated twice by means of TGA: washed and unwashed. The washing procedure included washing with 100 mL water and 50 mL ethanol. Both catalysts, the washed and unwashed, were dried at 120 °C over night prior to the analysis.

For the spent and washed catalyst the same residual mass of 22 % was determined (Figure 30) as for the fresh catalyst, whereas, the mass loss with 15 % residual mass was enhanced for the unwashed spent catalyst (Figure 31). Thus, more of the weighed-in substance was thermally decomposed. Therefore, organic compounds were most likely adsorbed on the catalyst. This circumstance shows once more that reactants do adsorb onto the catalyst but most of them can be washed off. Additionally, burning them off could be another possibility to reactivate the catalyst.

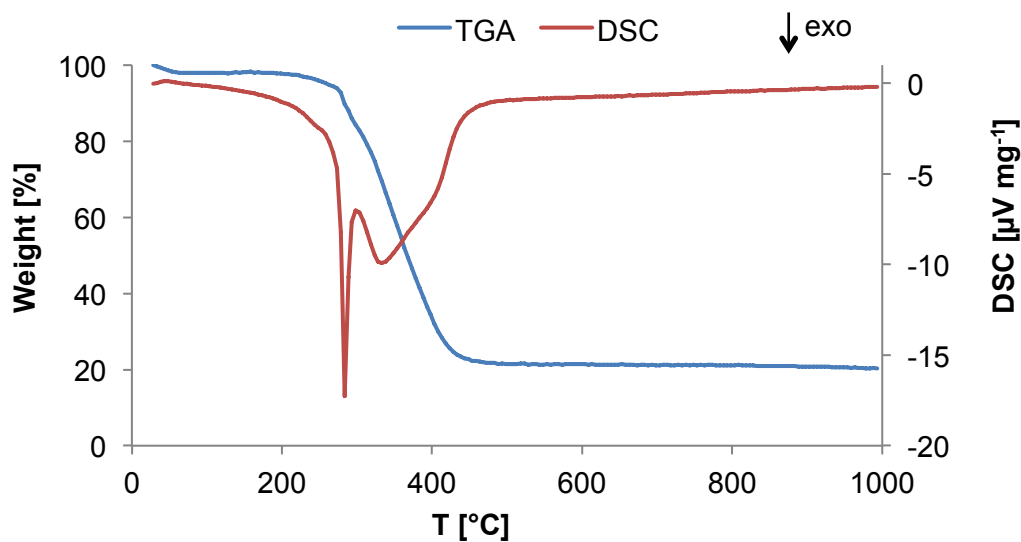


Figure 30. TGA and DSC data of the used and subsequently washed commercial Ru/C catalyst.

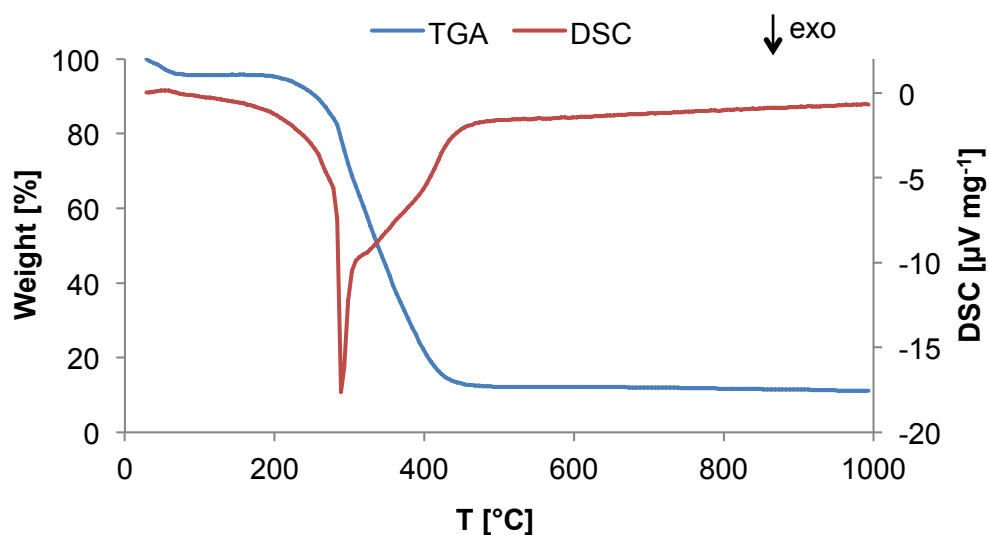


Figure 31. TGA and DSC data of the used commercial Ru/C catalyst without washing.

3.2 Catalytic Isomerisation of Isohexides

Some of the experimental data used in this chapter was collected and partially processed in the bachelor thesis by Anja Fink, entitled “Kinetic Investigation of Biogenic Sugar Alcohol Isomerisation”, RWTH Aachen 2014, under my supervision.

The production of isoidide, starting directly from biomass analogue to the other isomers, is not suitable since its precursor L-idose is not abundant in nature. Thus, a possible synthesis route to gain access to isoidide lies in the catalytic isomerisation of the more abundant stereoisomers isosorbide and isomannide (Figure 32).

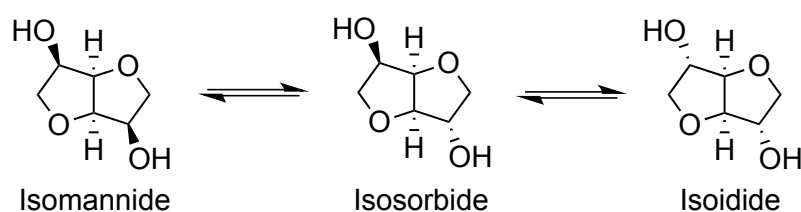


Figure 32. Isohexide isomerisation.

In this work the isomerisation of isosorbide and isomannide was investigated using a commercial Ru/C catalyst (*Sigma Aldrich*). When compared to the work of LE NÔTRE *et al.*^[73] the reaction conditions could be improved. Thus, a lower temperature of 160 °C instead of 220 °C and also a decreased hydrogen pressure from 40 to 25 bar were applied. Starting from isosorbide after 2 h the reaction mixture consists of 54 % isoidide, 26 % isosorbide, and 3 % isomannide according to high-performance liquid chromatography (HPLC) analysis (for details see chapter 5.5.3). These values correspond to a normalised ratio of 65:31:4 for isoidide, isosorbide, and isomannide, respectively, which is comparable to the reported normalised equilibrium ratios.^[29, 32, 73] The error of the HPLC analysis is rather high (up to 15 %). In the 2 h reaction time, the heating phase is included (approximately 20 min) but not the cooling period, which was accelerated by an ice bath. Similar to the literature^[73] under neutral conditions a severe loss in carbon balance of approximately 20 % was observed. Interestingly, when a sample of the reaction mixture was taken after 2 h at reaction temperature, a different product spectrum was obtained. At 160 °C this sample contains 47 % isoidide, 40 % isosorbide, and 6 % isomannide in the reaction mixture. When comparing the results obtained from the solution at room temperature after the reaction with the ones from the sample taken under reaction conditions (Figure 33), it can be noted that especially the amount of isosorbide decreases in the cooling process whereas the amount of isoidide slightly increases. Additionally, in the sample taken at reaction temperature, the

mass loss was approximately 7 %. Thus, it is significantly enhanced during the cooling process from 7 to ca. 17 %. This behaviour is unusual and is investigated in more detail.

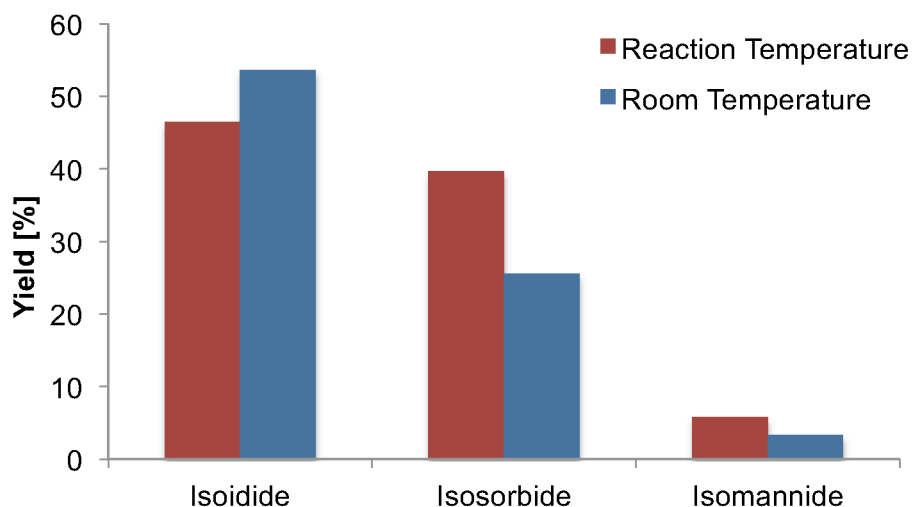


Figure 33. Comparison of the isohexide yields for samples taken at reaction temperature (160 °C) and at room temperature.

For the kinetic investigations (for details see chapter 3.3), the course of the reaction was followed by taking samples at different times until the equilibrium was reached. Subsequently the autoclave was cooled directly after the last sample was taken and the composition of the residue in the autoclave was examined. At all investigated temperatures (140, 150, and 160 °C) and independent of the starting material (isosorbide or isomannide), there is an increase in mass loss from the last taken sample under reaction conditions to the sample taken from the cooled product mixture. The difference was typically around 10 % (Table A 2). Once more, the amount of isosorbide is notably decreased in the product mixture.

LE NÔTRE *et al.* suggested that the mass loss is due to hydrodeoxygenation side reactions as discussed in chapter 2.1.1.3.^[73] The existence of these side reactions can most likely explain the observed mass loss under reaction conditions. However, since the mass loss is rising during the cooling process an increased occurrence of side reactions under this condition is unlikely. Another explanation for this additional mass loss could be adsorption which is actually much more probable. The enthalpy change for physical adsorption processes is negative, indicating an exothermic process.^[166] Thus, adsorption is enhanced with lower temperatures and, therefore, more pronounced after the reaction mixture is cooled down. Strikingly, the amount of isosorbide decreases the most. Thus, it seems to adsorb selectively. In fact, an adsorption experiment was conducted with an equimolar solution of isosorbide and isomannide and the activated carbon A Supra EUR as adsorbent in which this behaviour could also be observed. At 20 °C more isosorbide than isomannide was adsorbed onto the activated carbon (cf. Figure A 8 in the appendix). The order of magnitude of the loss

of isosorbide during the cooling period after the isomerisation reaction correlates to the amount of adsorbed isosorbide in the adsorption experiment. Yet, it has to be considered that the results were not measured at the same equilibrium concentrations and with different adsorbents. Therefore, the comparison with the adsorption data is only an estimation.

It is known that hydrophobic and, therefore, non-polar adsorbent materials adsorb substrates with lower polarity selectively.^[167-168] In order to estimate the different polarities of the dianhydrohexitol isomers, their dipole moments were obtained through DFT calculations (Table 4).

Table 4. Calculated dipole moments of the dianhydrohexitol isomers. The DFT calculations including structure optimisations (GAMESS,^[169] B3LYP,^[170-171] 6-31G^[172-173]) were performed by M. Rose.**

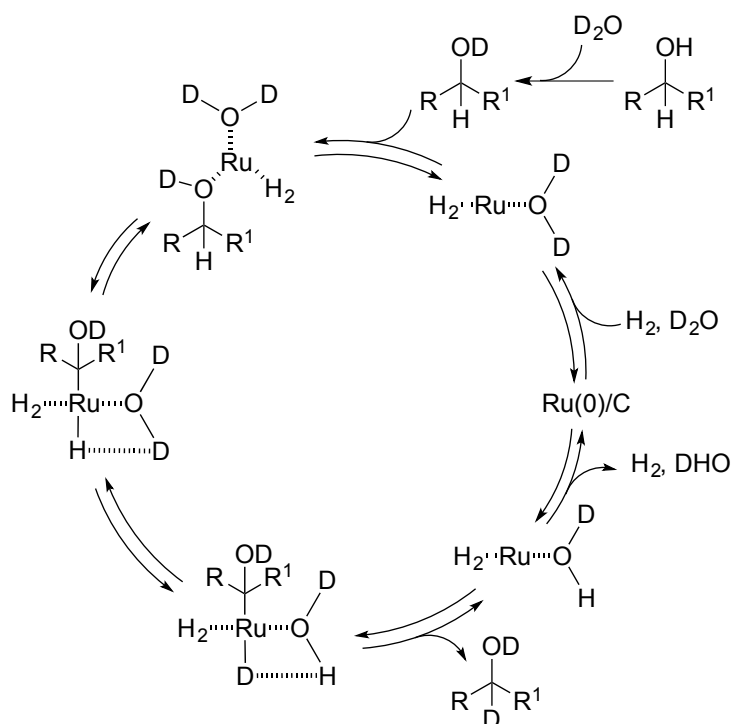
Isomer	Isomannide	Isosorbide	Isoidide
Dipole Moment [D]	3.17	1.65	1.91

Isomannide has the largest dipole moment with 3.17 D and, thus, the highest polarity. Whereas, isosorbide and isoidide exhibit significantly lower dipole moments indicating lower polarity. The applied catalyst with activated carbon as support material and the A Supra EUR activated carbon, applied in the adsorption experiment, are hydrophobic materials.^[167] Therefore, the trend in adsorption behaviour can be explained by the polarity of the molecules. Isosorbide with a lower polarity is preferentially adsorbed in contrast to isomannide. Interestingly, the effect is not that pronounced for isoidide although the difference in polarity by virtue of the dipole moment in relation to isosorbide is relatively small.

3.2.1 Investigation of the Reaction Mechanism

In chapter 2.1.1.3, three different possible reaction mechanisms are described for the isomerisation of isohexides. In all papers dealing with this topic, the dehydrogenation/rehydrogenation mechanism with the ketone intermediate is proposed as the most probable one.^[29, 32, 73] Herein the mechanism is to be investigated using deuterium labelling.

Generally, deuterium labelling can be very useful in the process of determining reaction mechanisms. A possible way to obtain molecular deuterium is to use deuterium oxide as convenient source. For this, beside a metal catalyst such as Pd/C molecular hydrogen is needed.^[174-176] After stirring at room temperature for 24 h, a total exchange between H₂ and D₂O occurs leading to D₂. Additionally, SAJIKI and co-workers proposed the direct exchange of a proton attached to a molecule with deuterium provided by deuterium oxide through direct C–H activation using transition metal-based catalysts like palladium or ruthenium.^[176-179] Scheme 16 shows the proposed mechanism exemplarily for ruthenium.



Scheme 16. Mechanism of the deuteration through direct C–H activation as proposed by SAJIKI and co-workers.^[179]

Nevertheless, low pressures of molecular hydrogen are required. The authors suggest that the role of the molecular hydrogen is to activate the metal species. However, with molecular hydrogen present, it is difficult to determine whether the deuterium is exchanged directly between deuterium oxide and the compound or molecular deuterium is produced first. The same group identified heterogeneous palladium, platinum, iridium, rhodium or ruthenium

catalysts as suitable catalysts for the deuteration of alkanes^[178], alcohols,^[180] and sugar compounds.^[179]

At mild conditions of 50-80 °C and 1 atm hydrogen pressure, a regioselective deuteration of alcohols and sugar compounds can be observed after 24 h using a Ru/C catalyst.^[179-181] Only protons attached to hydroxy-substituted carbons are exchanged by deuterium; whereas, protons attached to ether-substituted carbons or the backbone remain. SAJIKI and co-workers observed racemisation in simple aliphatic alcohols during this procedure. Thus, they suggested a dehydration/re-hydrogenation mechanism.^[180] For more complex alcohols like the sugar compounds, however, a direct C–H activation for the H-D exchange is proposed since no epimerisation was observed.^[181] The authors attributed this to the disadvantageous steric strain of the corresponding ketone. For the deuteration of alkanes the same mechanism, the C–H activation, is proposed.^[178] Yet, to exchange the protons through deuterium provided by deuterium oxide, harsher conditions of 160 °C are needed. At this temperature, 1 atm hydrogen pressure, and after 24 h most of the protons in various alkanes are exchanged using an Rh/C catalyst. With Pd/C, similar results were obtained at the alkyl side chains of alkyl-substituted aromatic compounds with the mere exception of protons of attached methoxy or ethoxy groups. In this case almost no exchange occurs at 110 °C.^[177]

To elucidate the mechanism of the isohexide isomerisation, a deuterium labelling experiment of isomannide with deuterium oxide as the deuterium source and the solvent was conducted under the typical conditions, i.e. 160 °C, 25 bar hydrogen pressure (at RT) for 3 h using a commercial Ru/C catalyst. In case of the proposed dehydrogenation/re-hydrogenation mechanism only the protons of the hydroxy groups and of the hydroxy-substituted carbons should be exchanged. However, under the applied conditions all isohexide-based signals in the ¹H and ¹³C NMR spectrum vanished (Figure 34 and Figure 35). Therefore, all protons of the isohexides backbone have to be exchanged by deuterium. This result is contradictory to the ones reported in literature. Yet, the reaction temperature in the present case is higher than in the already published results using alcohols and sugar compounds as reagents. Thus, the potential higher activation barrier for the proton-deuterium exchange at the backbone can be overcome. In fact, with 160 °C the reaction temperature is in the same range as in the literature examples where the deuteration of alkanes is possible.

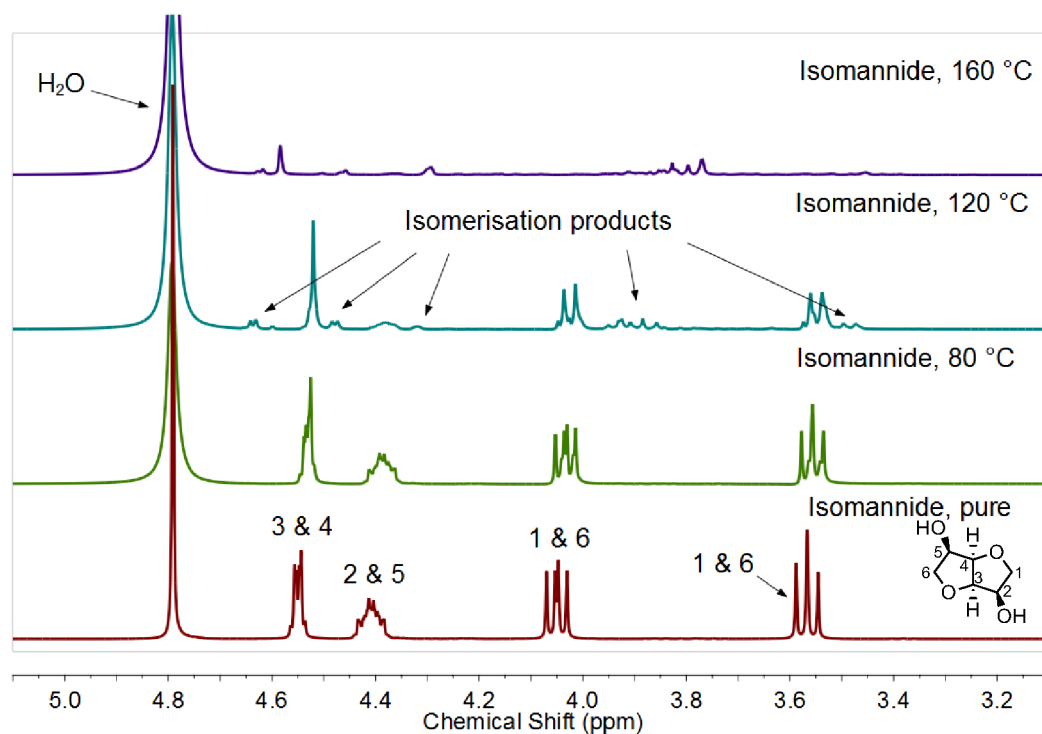


Figure 34. ^1H NMR (close-up) of pure isomannide as well as of the product solutions after isomerisation using Ru/C and 25 bar H_2 pressure after 3 h at the indicated temperatures. D_2O was used as the solvent and the deuterium source. The numbers depict the corresponding carbon atom number.

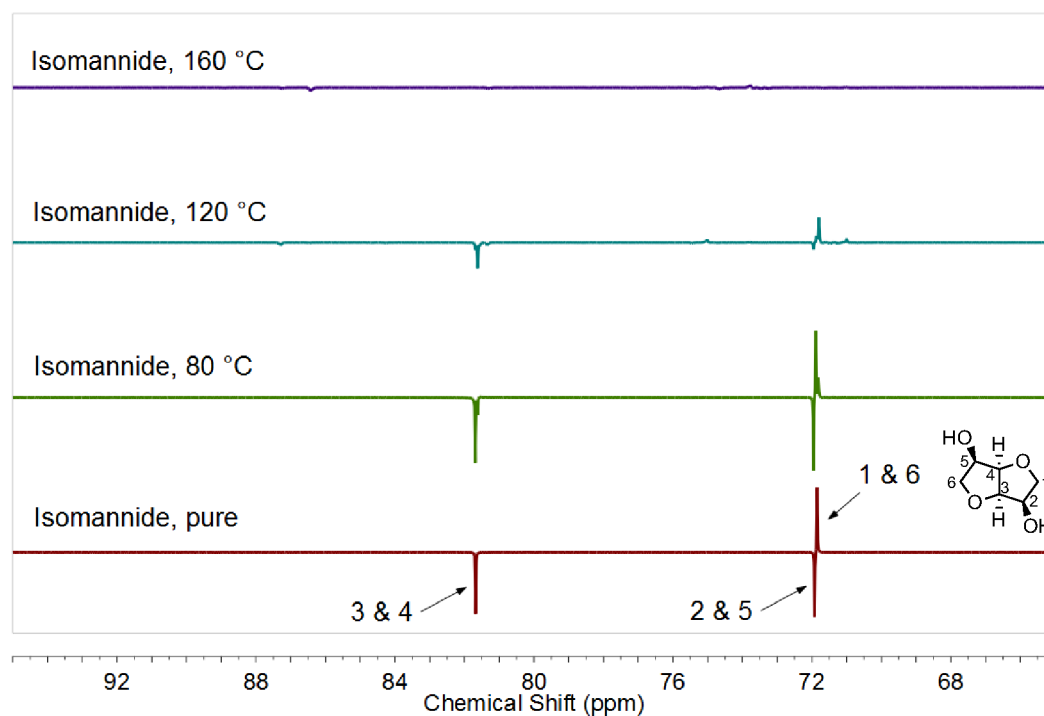
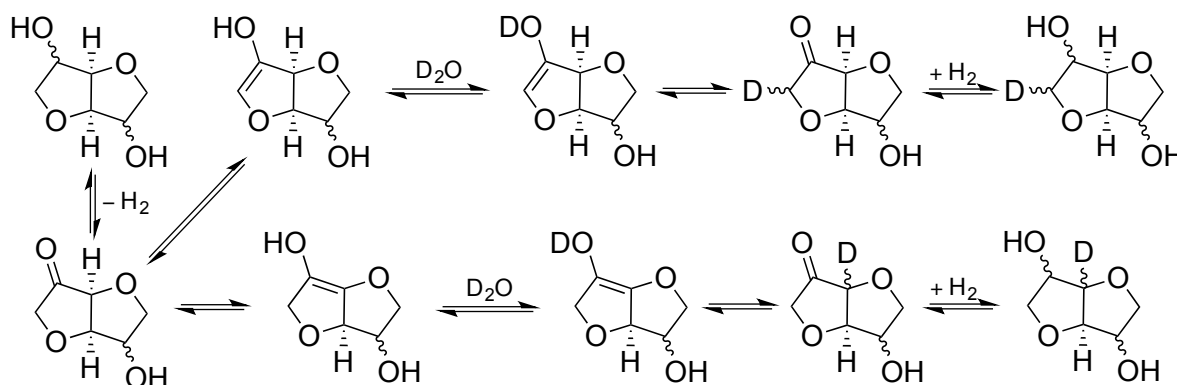


Figure 35. APT ^{13}C NMR (close-up) of pure isomannide as well as of the product solutions after isomerisation using Ru/C and 25 bar H_2 pressure after 3 h at the indicated temperatures. D_2O was used as the solvent and the deuterium source. The numbers depict the corresponding carbon atom number.

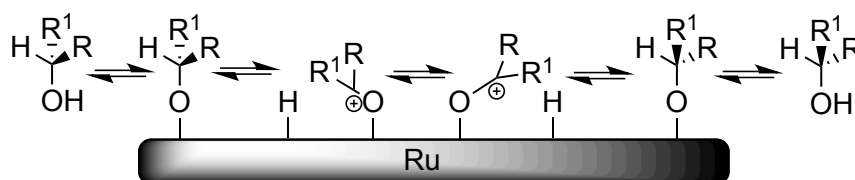
Additionally, also 120 and 80 °C reaction temperature have been screened (Figure 34 and Figure 35). At 80 °C neither isomerisation nor H-D exchange could be observed after 3 h. Increasing the temperature to 120 °C leads to isomerisation; although, after 3 h the equilibrium was not yet reached because of a lower reaction rate at lower temperatures. Moreover, deuterium exchange can be observed after this time but to less extent. At 120 °C the signals originating from the protons attached to the hydroxy-substituted carbon atoms (2- and 5-position) vanish preferentially in the ^1H NMR, and the same is true for the respective carbon signal in ^{13}C NMR. Thus, the exchange of the protons at 2- and 5-position is favoured indicating a dehydrogenation/re-hydrogenation mechanism at this temperature. Furthermore, no H-D exchange can be observed in the absence of molecular hydrogen, which is consistent with the literature results.^[176]

There are two possible pathways explaining the total H-D exchange in the isohexide molecules at 160 °C. One option could be a keto-enol tautomerisation after the initial dehydrogenation step (Scheme 17). Protons of hydroxy groups easily exchange with deuterium. Thus, if the hydroxy group proton is exchanged in the enol-form the deuterium can be transferred to the positions 3 and 4 or 2 and 6, respectively.



Scheme 17. Potential route for the complete deuteration through a keto-enol tautomerisation after the dehydrogenation step.

In addition, a direct C–H bond activation as proposed by SAJIKI and co-workers^[178-179] could lead to the total deuterium exchange. Taking this possibility into consideration, also the isomerisation could proceed through a direct C–H bond activation as shown in Scheme 18.



Scheme 18. Potential mechanism for the isomerisation of isohexides through C–H activation.

Thereby, the molecule is bound to the oxophilic ruthenium surface through the oxygen of the hydroxy group. The cleavage of C–H bonds can proceed in a homolytic or heterolytic fashion.^[182] Although both pathways are possible working in water it is conceivable that the protic environment facilitates a heterolytic C–H cleavage. In this case, the cleavage would lead to a hydride and a prochiral carbenium ion. The latter can then rotate along the C–O bond as well as along the Ru–O bond. Therefore, an inversion of the stereocentre can be obtained after the re-addition of the hydride.

However, both mechanisms remain possible. Therefore, comparable experiments with dimethyl isosorbide (DMI) were performed. Using this ether derivative as substrate no isomerisation as well as deuterium exchange should occur if the dehydrogenation/re-hydrogenation (for the H–D exchange with additional keto–enol tautomerisation) is the exclusive path. At first, solely the isomerisation was investigated, i.e. the reaction was performed in water instead of deuterium oxide. Unfortunately, a broad product spectrum was obtained from which approximately half of the products could be assigned by means of gas chromatography – mass spectrometry (GC–MS) (cf. appendix Figure A 9). Besides residual starting material DMI, monoethers were the main products. Additionally, one isohexide, presumably isosorbide, was observed. Therefore, ether cleavage occurs for a major part. Using GC, methane was detected in the gas phase evidencing hydrogenolysis.

A closer look on the product distribution reveals three monoethers but DMI itself can only be cleaved into two. Consequently, they had to be isomerised. So far, it could not be identified whether the hydroxy or ether moiety was isomerised. The first option is more likely. However, the isomerisation of the ether moiety cannot be excluded. Moreover, a smaller peak possessing the same molar mass as DMI was detected. Since a re-etherification after the cleavage by hydrogenolysis and isomerisation is highly implausible, DMI itself had to be isomerised. A simple dehydrogenation/re-hydrogenation mechanism cannot explain this transformation. Therefore, the above-mentioned direct hydride exchange by C–H bond activation has to be involved. An analogue mechanism via a prochiral carbenium ion as displayed in Scheme 18 can be assumed. Therefore, in general the isomerisation cannot only occur through dehydrogenation/re-hydrogenation but also through a direct C–H bond activation.

Additionally, deuterium exchange was studied using DMI as substrate. Once more, without the application of molecular hydrogen, no exchange can be observed. Furthermore, experiments at 80, 120, and 160 °C were performed using molecular hydrogen. At 80 and 120 °C no differences in the ^1H and ^{13}C NMR spectra in comparison to the spectra of pure DMI can be noticed (Figure 36 and Figure 37). Therefore, no H-D exchange occurs. After 3 h at 160 °C, however, mostly all signals vanish in the ^1H as well as in the ^{13}C NMR spectra (Figure 36 and Figure 37). Consequently, all protons were exchanged under the applied conditions. Since not all methoxy groups were cleaved by hydrogenolysis, the signals in the NMR spectra (160 °C) originating from the methoxy groups vanish, also because of H-D exchange, which was not observed to this extent in the literature. Furthermore, the full exchange, especially of the DMI and its observed isomer, cannot be explained by keto-enol tautomerisation after dehydrogenation. Thus, the deuteration has to proceed through the direct C–H activation as suggested by SAJIKI and co-workers. However, the role of the necessary molecular hydrogen is not yet clear. One possibility could be the activation of the ruthenium catalyst. As mentioned above in the discussion about the amination of isohexides, the surface of the metal catalyst can be oxidised and thus, passivated. The molecular hydrogen is then be needed to reduce the active metal under reaction conditions. Furthermore, another explanation, again similar to that discussed in chapter 3.1, could be a potential need of a certain surface coverage of the metal catalyst with hydrogen to facilitate a fast exchange.

Taking everything into consideration, it seems reasonable to assume a dehydrogenation/re-hydrogenation mechanism at lower temperatures (< 160 °C), while at higher temperatures (> 160 °C) the barrier for the C–H bond activation can be overcome and a direct hydride exchange can be enabled as a in parallel occurring pathway.

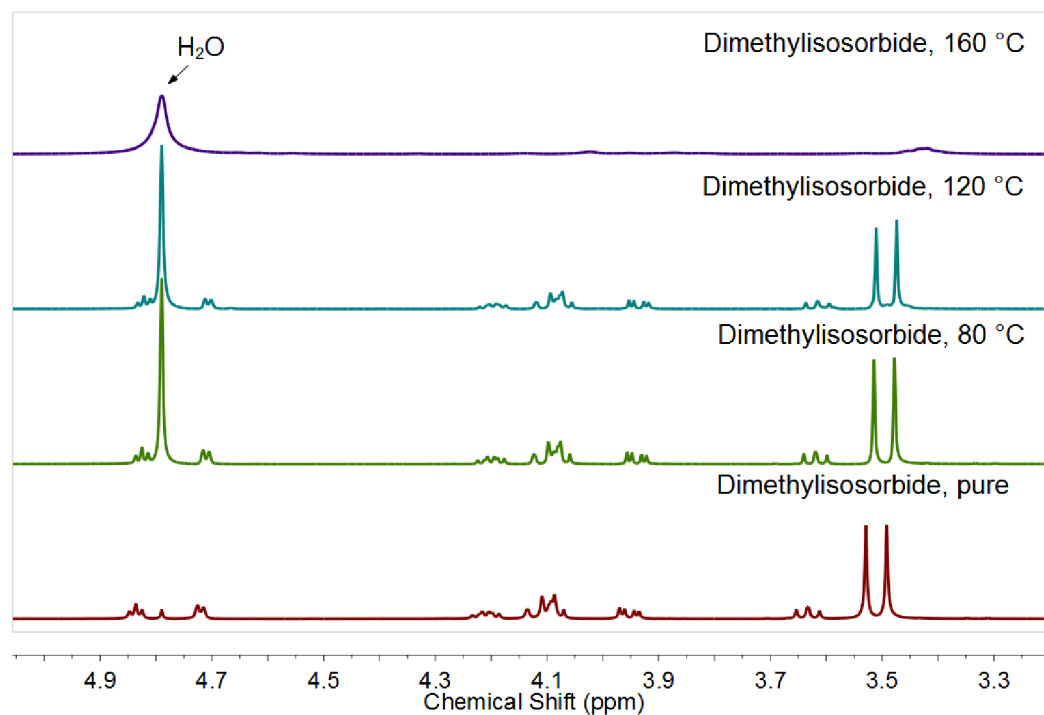


Figure 36. ^1H NMR (close-up) of pure dimethyl isosorbide (DMI) as well as of the product solutions after isomerisation using Ru/C and 25 bar H_2 pressure after 3 h at the indicated temperatures. D_2O was used as the solvent and the deuterium source.

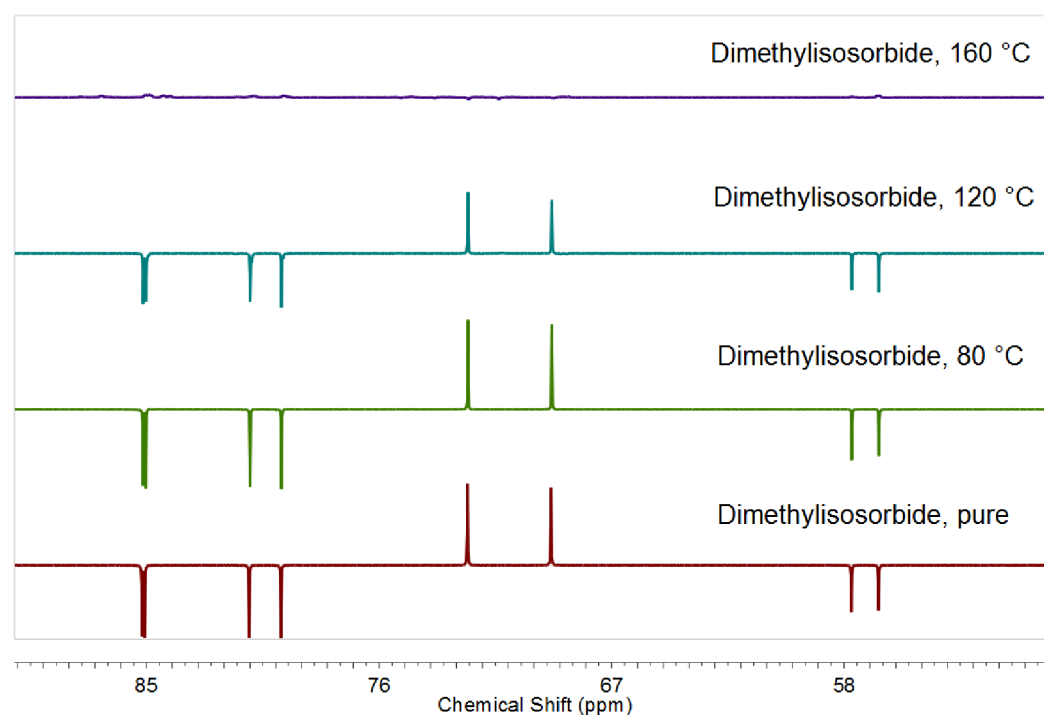


Figure 37. APT ^{13}C NMR (close-up) of pure dimethyl isosorbide (DMI) as well as of the product solutions after isomerisation using Ru/C and 25 bar H_2 pressure after 3 h at the indicated temperatures. D_2O was used as the solvent and the deuterium source.

3.2.2 Investigation of an Unknown Compound

A surprising discovery was made while collecting the data for the kinetic investigations. At the beginning of the reaction, a major amount of a fourth compound was observed regardless of whether the starting material was isosorbide (Figure 38) or isomannide (Figure 39). Yet, this was more pronounced in the experiments using isosorbide at 160 °C. Unfortunately, in the HPLC analysis the peak of the unknown substance was not baseline-separated from the isosorbide peak but an explicit shoulder. Furthermore, the lack of a pure sample of this compound made it impossible to determine the corresponding calibration factor. Therefore, the concentration of the unknown substance is defective. However, it can be seen that the concentration of this compound decreases rapidly in the beginning of the reaction and then remains at almost zero. In this case the time 0 min depicts the moment the reaction temperature was reached. The heating phase takes approximately 20 min. Thus, it behaves like an intermediate, which is formed during the heating phase of the reaction. Therefore, it is labelled “Intermediate” in Figure 38 and Figure 39.

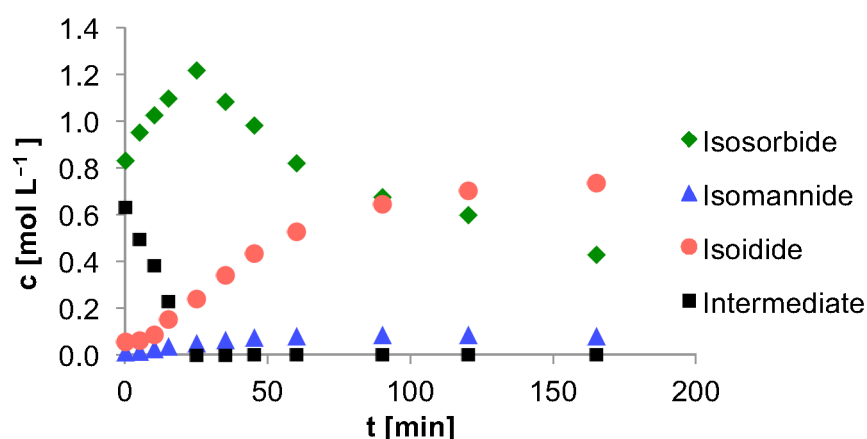


Figure 38. Concentration-time profile of the isohexide isomerisation at 160 °C starting from isosorbide. The moment the reaction temperature was reached was set to 0 min. Reaction conditions: 5.4 g isosorbide, 18 g water, 1 mol-% Ru/C, and 500 rpm.

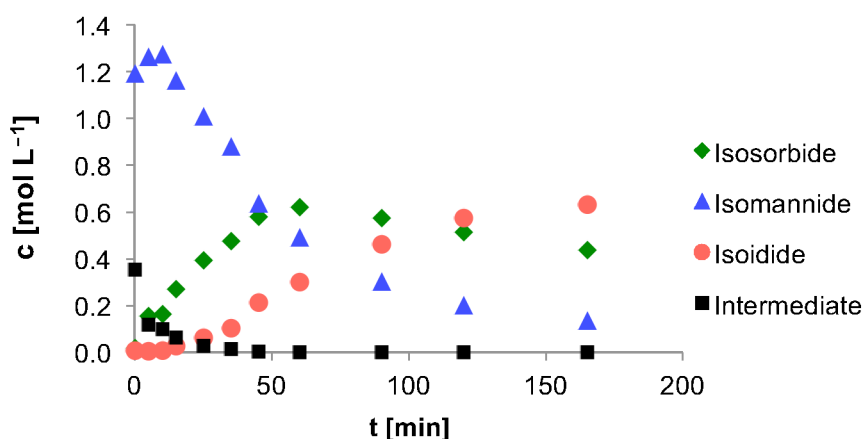


Figure 39. Concentration-time profile of the isohexide isomerisation at 160 °C starting from isomannide. The moment the reaction temperature was reached was set to 0 min. Reaction conditions: 5.4 g isomannide, 18 g water, 1 mol-% Ru/C, and 500 rpm.

Keeping the postulated dehydrogenation/re-hydrogenation mechanism in mind (cf. chapter 2.1.1.3) and considering the compound's behaviour in the reaction course, the fourth compound was assumed to be the ketone intermediate. However, neither in IR nor in ^1H or ^{13}C NMR evidence for a carbonyl compound was found. GC-MS after derivatisation revealed the same molecular mass for all four compounds. Therefore, the unknown substance is most likely a fourth isohexide stereoisomer.

Searching the literature for a fourth dianhydrohexitol isomer, only three patent applications can be found that mention four isohexides.^[183-185] Besides the well-known isomannide, isosorbide, and isoidide the authors name isogalactide as a fourth dianhydrohexitol. However, none of these reports show a structure of this molecule. Considering the structures of the known isohexide isomers, the only possibility for another isomeric structure is a different configuration of the hydrogen atoms attached to the bridgehead atoms. They show *cis* configuration for isomannide, isosorbide, and isoidide. Thus, they need to have a *trans* configuration in isogalactide (Figure 40). In this case, the molecule is not “V”-shaped anymore but the two rings are slightly twisted. Although the final proof of the structure is not given, the observed new compound will be named *isogalactide* in this work for simplification.

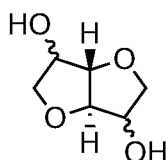
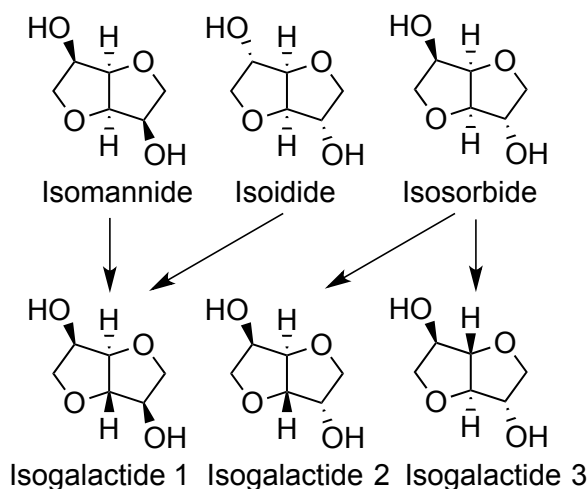


Figure 40. Potential structure of isogalactides.

A closer look on the structure indicates that there is not only one isogalactide structure but three isogalactide isomers. Depending on which of the three well-known isohexide isomers is the starting point, a different compound with the bridgehead protons in *trans* configuration

can be obtained (Scheme 19). Interestingly, in the HPLC analysis only one other compound with the same retention time can be detected regardless of the starting material being isomannide or isosorbide. Yet, the separation of isomers is challenging. Thus, the isogalactide isomers could have the same retention time using the current method.



Scheme 19. Possible isogalactide isomer structures.

A more detailed investigation of the compound concerning its structure was not yet possible since it was thus far only obtained in the mixture together with the other isomers. In NMR spectra most of the signals of the different compounds are overlapping. With the small amounts from the sampling for the kinetic investigations, separation was not possible. A first attempt to obtain a larger amount of isogalactide was performed. The reaction solution containing isomannide was heated to 150 °C in an autoclave. Once the desired temperature was reached, the reaction was directly stopped and the cooling process was accelerated with an ice bath (as in the isomerisation experiments described above). However, there is a substantial difference in comparison to the results from the samples taken at reaction temperature. At room temperature after the short reaction time no significant amount of isogalactide can be observed but mainly starting material. In order to get a better understanding of this behaviour, an experiment with isomannide as substrate was performed in which a sample was taken once the reaction temperature was reached. Directly after that the reaction was stopped and cooled with an ice bath. Subsequently, another sample from the product mixture was taken and both were analysed by HPLC. As shown in Figure 41, at reaction temperature significant amounts of isogalactide are present, whereas, the product mixture after the cooling consists mainly of the substrate and isosorbide. Thus, during the cooling procedure the isogalactide is converted to the well-known isomers. The big error in the mass balance for the sample at 150 °C is most likely caused by the lack of the corresponding calibration factor. For the analysis, the calibration factor for isogalactide was

approximated with the mean value of the calibration factors of the other three isohexide isomers. The yield of over 100 % suggests that the amount of isogalactide is overestimated.

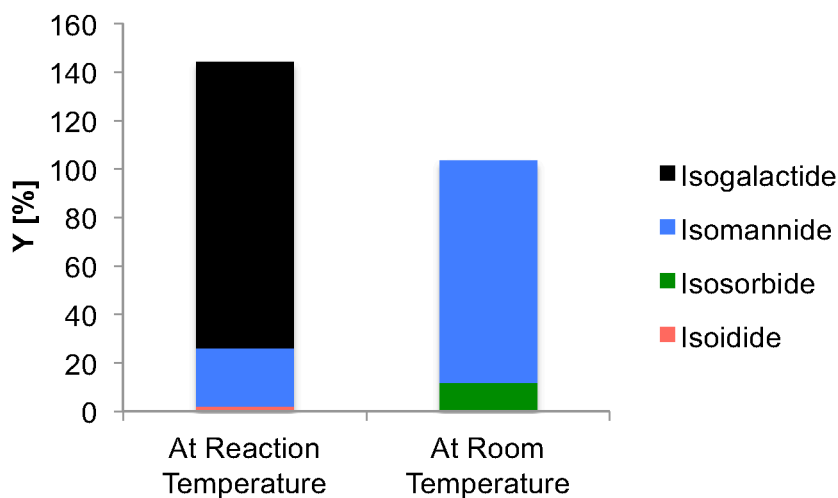
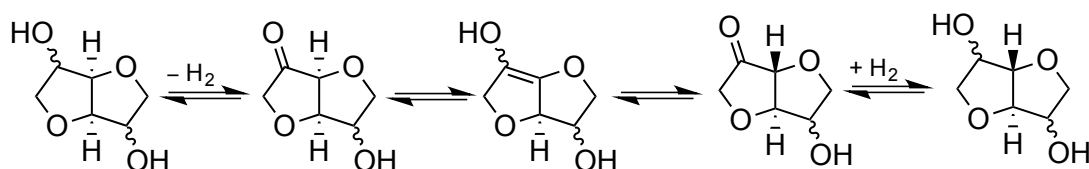


Figure 41. Product distribution directly after the reaction temperature of 150 °C was reached and after the cooling process.

It seems that the activation barrier to form isogalactide is lower than it is for the other isomers, leading to an increased formation of this compound during the heating phase. However, it is presumably not thermodynamically favoured. In fact, it never occurs in the thermodynamic equilibrium at the investigated temperatures. Thus, it is most likely easily converted back to the well-known isomers during the cooling period when the catalyst is still present. The samples taken from the reaction mixtures cool down rapidly and the catalyst can be separated faster. Therefore, the isogalactide can be preserved. Considering these facts, a continuous production is probably the most promising approach to gain isogalactide in a larger amount.

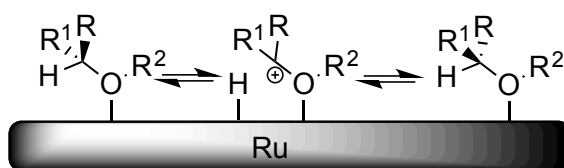
Once pure isogalactide can be obtained the configuration of the bridgehead protons could be determined by a change in the 3J -coupling in the ^1H -NMR spectrum. Most likely it will increase ($^3J_{\text{trans}} > ^3J_{\text{cis}}$).^[186] As for the identification of the total configuration 2D NMR, more precise nuclear Overhauser effect spectroscopy (NOESY) can be an appropriate technique.

For the formation of the isogalactide isomers starting from the known isohexides there are two possible pathways. One possibility is its production through a keto-enol tautomerisation after the dehydrogenation step (Scheme 20) similar to the H-D exchange discussed in the last chapter. The α -carbon atom is prochiral in the enol form. Thus, when converted back to the keto form the configuration can change with respect to the starting material and leading to the isogalactide after hydrogenation.



Scheme 20. Possible mechanism towards isogalactide through keto-enol tautomerisation.

Another option is a direct hydride exchange, converting one of the well-known isohexides into one of the isogalactide isomers also as discussed in the last chapter for the deuteration of the isohexides. In this case the molecule is most likely bound to the ruthenium surface through the oxygen of the ring, and the cleavage at the C3- or C4-carbon atom leads to the hydride and the prochiral carbenium ion. The molecule can rotate along the Ru–O bond. Thus, an inversion of the stereocentre can be obtained. However, the fact that for a direct C–H activation a higher temperature is needed and that the isogalactide is preferentially produced in the heating phase of the reaction and, therefore, at lower temperatures has to be considered. Consequently, the first option is much more likely the mechanism for the formation of isogalactide.



Scheme 21. Possible mechanism towards isogalactide through direct C–H activation.

3.3 Kinetic Modelling of the Catalytic Isohexides Isomerisation

Some of the experimental data used in this chapter was collected and partially processed in the bachelor thesis by Anja Fink, entitled “Kinetic Investigation of Biogenic Sugar Alcohol Isomerisation”, RWTH Aachen 2014, under my supervision.

For a deeper understanding of the herein reported isohexide isomerisation the kinetics of this reaction were investigated. Therefore, the concentration-time profiles were collected with isomannide and isosorbide as starting material to compare the results. The applied catalyst is a commercial Ru/C catalyst, as in the other isomerisation experiments, and three reaction temperatures (140, 150, and 160 °C) were investigated to determine the activation energies according to the Arrhenius equation (equation 1).^[187] In this temperature range an efficient and reliable collection of the concentration-time profiles is possible. At lower temperatures the reaction becomes considerably slow. The high reaction rate at higher temperatures reduces the resolution at the beginning of the reaction, since the sampling frequency is limited by the experimental setup. Additionally, with higher temperatures an enhanced formation of side reactions and substrate decomposition occurs.

$$k = A \cdot e^{-\frac{E_A}{R \cdot T}} \quad (1)$$

Herein k is the rate constant, A the pre-exponential factor, E_A the activation energy, R the ideal gas constant, and T the temperature.

3.3.1 Mass Transport Limitations

In heterogeneously catalysed reactions, the reaction velocity is not only influenced by parameters like temperature, pressure, and substrate concentration but also by amount and type of catalyst, as well as by transport processes at the interfaces and inside all involved phases. The latter might be even the rate-determining step. In three-phase systems (gas-liquid-solid), like in the present case, possible mass transport limitations occur at the interface of the gas and liquid, in the diffusion of the substrate from the liquid bulk to the catalyst's outer surface (film diffusion), and within the catalyst (pore diffusion of the substrate). Therefore, a distinction between micro- and macrokinetics is necessary. While microkinetics define the kinetics of the single reaction steps, macrokinetics describe the interaction of the kinetics of the transport processes with the microkinetics. Consequently, all mass transport limitations have to be eliminated in order to investigate the microkinetics of a reaction. Therefore, experiments were performed to rule out that the isohexide isomerisation is affected by mass transport limitations under the applied conditions.

The reaction velocity of a reaction, which is limited by mass transfer at the gas liquid interface, does not increase when the amount of catalyst is increased since all of the available dissolved gas is immediately converted. Thus, the transport of the gas into the liquid phase is rate determining. Therefore, experiments with varying amounts of catalyst were performed. As an expression of the rate velocity, the conversion and yield were chosen. Figure 42 shows that both conversion and yield are linearly increasing with the amount of catalyst. Yet, when comparing the results for 1 and 2 mol-% catalyst amount, there is no doubling of the conversion and yield as expected. This lower increase indicates that the system is influenced by transport limitation when 2 mol-% or more of the catalyst is used. The unclosed mass balance can be attributed to the error of the HPLC analysis. Since 1 mol-% is the standard amount of catalyst for the isomerisation experiments, gas-liquid mass transport limitation can be disregarded.

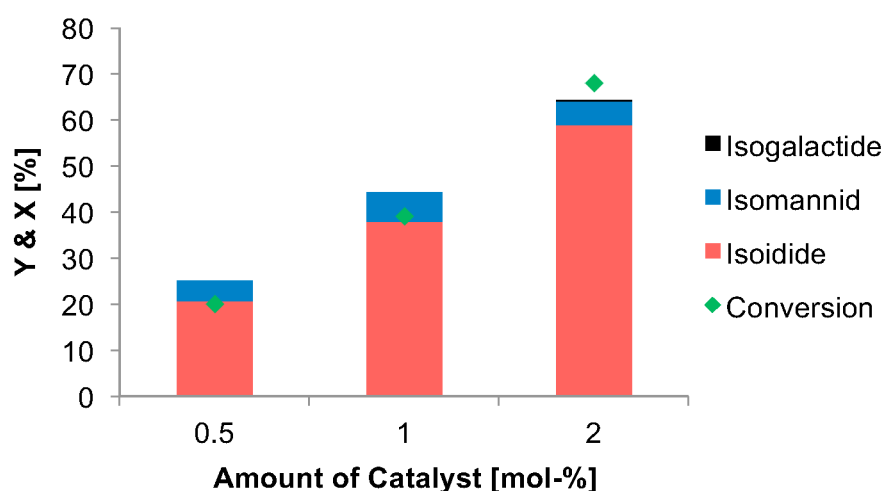


Figure 42. Screening of different amounts of catalyst (Ru/C) in the isomerisation of isosorbide. Reaction conditions: 1.5 g isosorbide, 5 g H₂O, 25 bar H₂ (at RT), 160 °C, 500 rpm, 30 min.

A reaction is limited by substrate diffusion to the catalyst in the liquid phase when the reaction velocity and, therefore, conversion and yield, increase with increasing stirrer speed. Yet, if there is no increase of conversion and yield with higher stirrer speed, the stirring intensity is high enough so that mass transport can be neglected in this case. Figure 43 shows a variation of the stirrer speed, and the conversion and yield as expression of the reaction velocity are in a similar region for all three cases. However, there is a rather big error in the HPLC analysis (up to 15 %) leading to the defective mass balance, especially for the experiment with 1000 rpm stirrer speed. Nevertheless, conversion and yield are not directly increasing with higher stirrer speed. Moreover, a decrease from 250 rpm to 500 rpm can be observed. Therefore, it can be assumed that a limitation through the stirring intensity can be neglected.

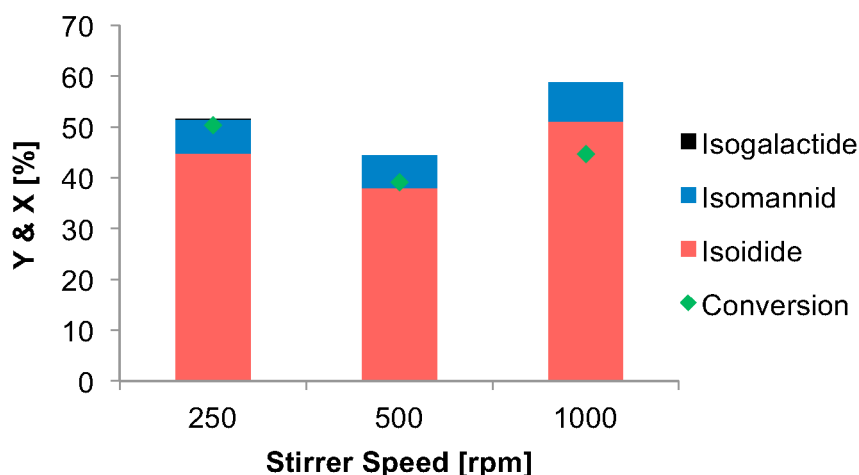


Figure 43. Screening of different stirring speeds in the isomerisation of isosorbide. Reaction conditions: 1.5 g isosorbide, 5 g H₂O, 1 mol-% Ru/C, 25 bar H₂ (at RT), 160 °C, 30 min.

A mass transport limitation through pore diffusion can be excluded if there is no change in reaction velocity for different catalyst particle sizes. However, in the present case the catalyst was already a fine powder with an average particle size of 19 μm .^[188] To determine if pore diffusion limitation has to be considered, the Weisz modulus Ψ was calculated using equation 2.^[189]

$$\Psi = \frac{L_{ch}^2 r_{eff}}{c_s D_{eff}} \quad (2)$$

Herein L_{ch} is the characteristic length of the catalyst, r_{eff} is the effective reaction rate, c_s is the concentration of the substrate on the catalyst surface, and D_{eff} is the effective diffusion coefficient. For values of $\Psi < 1$, mass transport limitation through pore diffusion can be disregarded.^[189]

L_{ch} is the ratio of catalyst volume and external surface. It is assumed that the catalyst particle has a spherical shape. Thus, in the present case the value of L_{ch} was estimated to be $3.2 \cdot 10^{-6}$ m. The effective reaction rate r_{eff} was calculated to be $9.03 \text{ mol s}^{-1} \text{ m}^{-3}$ based on the results of the isomerisation reaction after two hours. The concentration of the substrate on the catalyst surface c_s is assumed to be equal to the bulk concentration and the effective diffusion coefficient can be calculated using the following correlation:^[190]

$$D_{eff} = \frac{\varepsilon}{\tau} D \quad (3)$$

Thereby, ε is the porosity and τ the tortuosity. The values are defined to be 0.5 and 4, respectively, according to the literature.^[188, 191] For the calculation of D_{eff} a diffusion coefficient

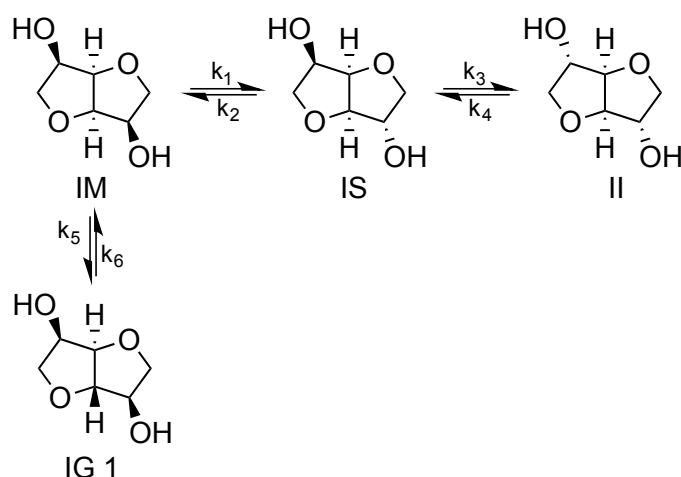
3 Results and Discussion

D was taken from literature for a comparable solute in water: $D_{D\text{-Mannitol}} = 0.5 \cdot 10^{-5} \text{ cm}^2 \text{ s}^{-1}$ at 15°C .^[192]

The calculated Weisz modulus is with $\psi = 7.1 \cdot 10^{-4}$ far below 1. Thus, a pore diffusion limitation can be ruled out.

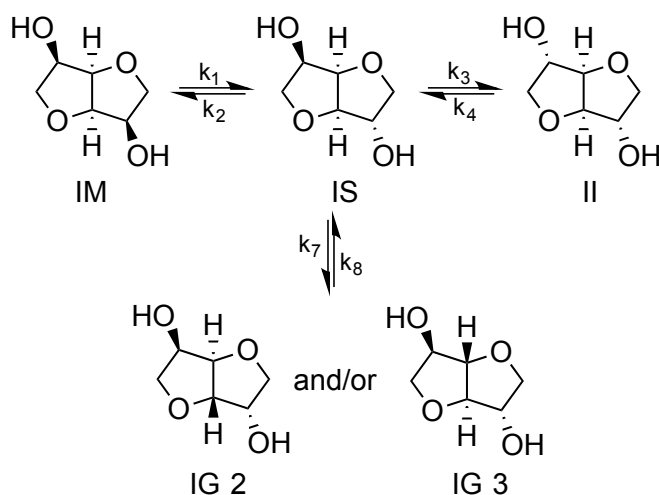
3.3.2 Details of the Reaction Network and Kinetic Model

In Scheme 22, a simplified reaction network for the isomerisation starting from isomannide is shown. For simplification the names of the isomers are abbreviated with IM for isomannide, IS for isosorbide, II for isoidide, and IG for isogalactide.



Scheme 22. Simplified reaction network for the isomerisation of isomannide (reaction network 1).

As discussed in chapter 3.2.2, there are different isogalactide isomers and depending on the substrate one or two of them can be formed, respectively (cf. Scheme 19). Therefore, starting from isomannide it is assumed that isogalactide, more precise isogalactide 1, is produced exclusively from isomannide. However, starting from isosorbide, the isogalactide isomers, more precise isogalactide 2 and 3, are solely produced from isosorbide (Scheme 23). All involved reactions are treated as equilibrium reactions. Further assumptions for the kinetic model are that no catalyst deactivation occurs during the reaction and that the reaction volume is constant. Additionally, side reactions (e.g. hydrodeoxygenation), which occur mainly with increasing reaction time, are neglected.



Scheme 23. Simplified reaction network for the isomerisation of isosorbide (reaction network 2).

As aforementioned the isomerisation proceeds most likely through a dehydrogenation/re-hydrogenation mechanism, although a direct C–H activation cannot be ruled out. However, the ketone intermediate was never observed (cf. chapter 2.1.1.3). Thus, both reaction steps are examined together and the corresponding rate constant, e.g. k_1 for the transformation of isomannide to isosorbide, includes the reaction constants for the dehydrogenation as well as re-hydrogenation. Additionally, because of the excess of molecular hydrogen and the fact that it is not consumed by the reaction, it is assumed that the reaction velocities are only dependent on the isohexide isomer concentrations.

Furthermore, in heterogeneously catalysed reactions, adsorption and desorption processes have to be considered since they can influence the reaction velocity. Therefore, besides the actual reaction on the catalyst surface, the adsorption of the substrate(s) and the desorption of the product(s) have to be taken into account. There are two main mechanisms often used to describe this behaviour: the Langmuir-Hinshelwood and the Eley-Rideal mechanisms.^[187] In the Langmuir-Hinshelwood mechanism, both reactants adsorb on the surface of the catalyst before they react and the product is desorbed. In the Eley-Rideal mechanism, only one reactant is adsorbed and it reacts with another substrate from the fluid phase before the product is desorbed. The basis for both kinetic mechanisms is the Langmuir isotherm describing the amount of occupied active sites θ of the catalyst.^[187] Since the rates for the adsorption and desorption are equal in the equilibrium the equation for the Langmuir isotherm is the following:

$$\theta = \frac{K_{ads,i}c_i}{1 + K_{ads,i}c_i} \quad (4)$$

Hereby $K_{ads,i}$ is the ratio of the adsorption and desorption rate constants for substrate i and c_i is its concentration.

In case of a reaction between two substrates (A and B) the reaction rate r described by a Langmuir-Hinshelwood mechanism is proportional to the amount of active sites occupied by A (θ_A) and by B (θ_B):

$$r = k\theta_A\theta_B = \frac{kK_{ads,A}c_A K_{ads,B}c_B}{(1 + K_{ads,A}c_A + K_{ads,B}c_B)^2} \quad (5)$$

For a Eley-Rideal mechanism where A is the substrate adsorbed to the catalyst and B the substrate in the fluid phase, the reaction rate is proportional to the amount of occupied sites by A (θ_A) and the concentration of substrate B (c_B):

$$r = k\theta_A c_B = \frac{kK_{ads,A}c_A c_B}{1 + K_{ads,A}c_A} \quad (6)$$

However, for the isomerisation of isohexides there is no adsorption data available. Thus, besides the rate constants also $K_{ads,i}$ needs to be modelled. Yet, considering the four isohexide isomer concentrations which can be measured and the eight rate constants needed for the equilibrium reactions, the system is already over-determined. Additionally, the more variables are given for the simulation, the higher the probability for a better fit. However, a higher quality of the fit not necessarily implies a more accurate description of the real system. Therefore, to obtain preliminary kinetic data in the present case the reactions were assumed to be pseudo first order. Thereby, the rate constants are lumped parameters. As already discussed they contain the rate constants for the dehydrogenation and rehydrogenation and additionally include the equilibrium constant of the adsorption. Thus, the reaction network 1 in Scheme 22 for the isomerisation of isomannide can be described by the following set of ordinary differential equations (ODEs).

$$\frac{dc_{IM}}{dt} = -k_1c_{IM} + k_2c_{IS} - k_5c_{IM} + k_6c_{IG} \quad (7)$$

$$\frac{dc_{IS}}{dt} = k_1c_{IM} - k_2c_{IS} - k_3c_{IS} + k_4c_{II} \quad (8)$$

$$\frac{dc_{II}}{dt} = k_3c_{IS} - k_4c_{II} \quad (9)$$

$$\frac{dc_{IG}}{dt} = k_5c_{IM} - k_6c_{IG} \quad (10)$$

The reaction network 2 for the isomerisation of isosorbide (Scheme 23) is described analogously by another set of ODEs.

$$\frac{dc_{IM}}{dt} = -k_1c_{IM} + k_2c_{IS} \quad (11)$$

$$\frac{dc_{IS}}{dt} = k_1c_{IM} - k_2c_{IS} - k_3c_{IS} + k_4c_{II} - k_7c_{IS} + k_8c_{IG} \quad (12)$$

$$\frac{dc_{II}}{dt} = k_3c_{IS} - k_4c_{II} \quad (13)$$

$$\frac{dc_{IG}}{dt} = k_7c_{IS} - k_8c_{IG} \quad (14)$$

3.3.3 Data Modelling and Determination of the Rate Constants

Concentration-time profiles of the isomerisation of isomannide and isosorbide were collected at 140, 150, and 160 °C. To increase the accuracy for each temperature, two experiments were performed and the mean value of the concentrations was used for the kinetic modelling. The time at which the desired reaction temperature was reached was set to 0 min. In appropriate intervals, samples were taken from the reaction mixture and analysed by HPLC. As mentioned above the HPLC has a rather large error, especially for the analysis of isogalactide (up to 40 % cf. Figure 41), because an approximated calibration factor is used. Due to this fact and the neglected side reactions the mass balance is not closed in most experiments. Nevertheless, by using the current data, preliminary rate constants and activation energies as well as pre-exponential factors can be obtained. These parameters give a good impression of the trends for the isomerisation reaction. The modelling of the data was performed with Python.^[193] A Nelder-Mead simplex algorithm,^[194] as implemented in the `scipy.optimize.fmin` script, was used for the minimisation of the least squares.

In Figure 44 the experimental data as well as the fit of the kinetic model for the isomannide isomerisation at 160 °C are displayed. As discussed in chapter 3.2.2, a certain amount of isogalactide is formed already during the heating period (approximately 20 min). The increase of the isomannide concentration in the beginning of the reaction indicates that the isogalactide is rapidly transformed back to the substrate. After a maximum is passed the concentration of isomannide decreases exponentially. The concentration of isosorbide increases directly from the beginning while the increase of the isoidide concentration occurs with a delay, indicating the consecutive nature of the reaction in which one hydroxy group is isomerised after the other. Thus, isomannide is converted to isosorbide first, which is then further converted to isoidide.

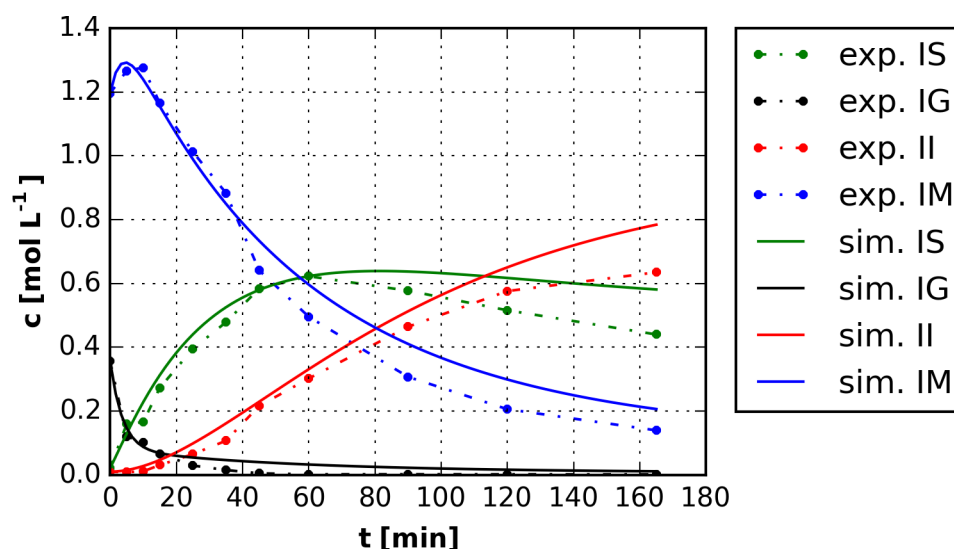


Figure 44. Concentration-time profile of the isomerisation of isomannide at 160 °C. Besides the experimental data (dots) the fit of the kinetic model (continuous lines) is displayed. Reaction conditions: 5 g isomannide, 1 mol-% Ru/C, 18 g H₂O, 25 bar H₂ pressure (at RT), 160 °C, and 500 rpm stirrer speed.

The quality of the fit can be displayed in parity plots. Thereby the values of the experimental data are plotted against the simulated values and the distance of the dots from the bisecting line expresses the deviation of the model from the experimental data. For example, in Figure 45 the parity plot of the kinetic model for the isomannide isomerisation at 160 °C is shown. It can be seen that the model overestimates especially lower concentrations. However, the deviation is rather small. Thus, in general the model describes the data well at 160 °C.

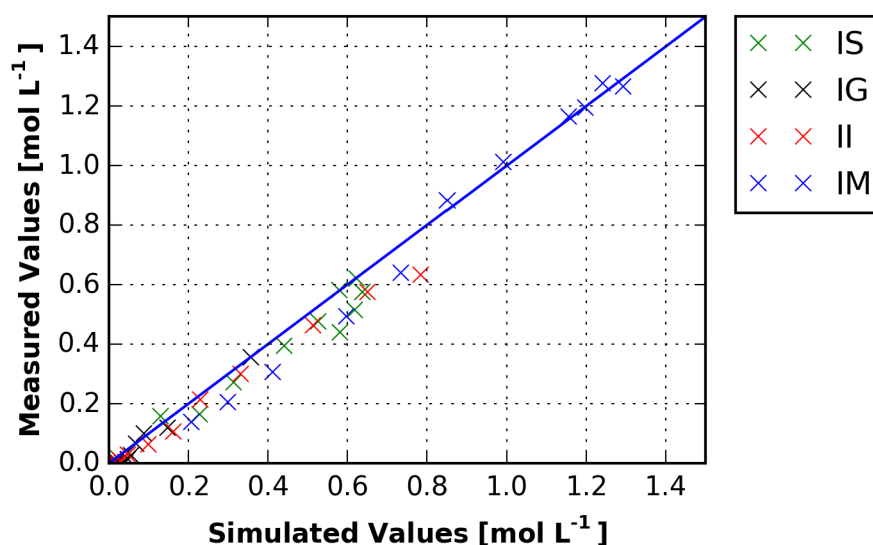


Figure 45. Parity plot of the kinetic model for the isomannide isomerisation data at 160 °C.

For simplification, the reactions from isomannide to isosorbide and from isosorbide to isoidide are called *main isomerisation reactions* since these are the reactions discussed in the literature. All obtained rate constants for the isomerisation of isomannide are summarised in Table 5. Comparing the rate constants for 160 °C, it can be seen that k_1 and k_3 , describing the forward reactions of the main isomerisation, are larger than k_2 and k_4 , describing the back reactions. This difference is more pronounced for the equilibrium between isomannide and isosorbide because k_1 is approximately 5 times larger than k_2 while k_3 is only 2 times larger than k_4 . For the equilibrium between isomannide and isogalactide 1 it is the other way around. The back reaction from isogalactide 1 to isomannide described by k_6 is approximately 19 times larger than k_5 , and in general this is the fastest reaction in the reaction network. These ratios of the rate constants of the forward and back reaction correspond to the equilibrium constant K of the equilibrium reaction (equation 15).

$$K = \frac{k_{forward}}{k_{back}} \quad (15)$$

All calculated equilibrium constants for the isomerisation of isomannide are summarised in Table 6. Based on this data the product distribution in the thermodynamic equilibrium can be calculated. As already mentioned, in the equilibrium a distribution of 5:40:55 for IM:IS:II can be observed experimentally (cf. chapter 2.1.1.3), which results in a ratio of 1:8:11 for IM:IS:II. The calculated ratio of the isohexides at 160 °C is 0.05:1:4.7:8.5 for IG 1:IM:IS:II. Thus, the amount of isogalactide is very low in the equilibrium. For the main isomerisation reactions the trend is described quite well, especially when considering the fact that the ratio mentioned in the literature is usually a normalised ratio not considering the mass loss. Herein, the rate constants and, thus, the equilibrium constants are gained on basis of the actual concentrations of the isohexide isomers in solution. Therefore, a certain variation is conceivable.

Figure 46 shows the experimental data and the fit of the kinetic model for the isomannide isomerisation at 150 °C. A trend similar to the data at 160 °C can be observed, although more isogalactide is present at the beginning of the reaction. This enhanced amount of isogalactide is another hint that it is preferably formed at lower temperatures while at higher temperatures the main isomerisation is favoured.

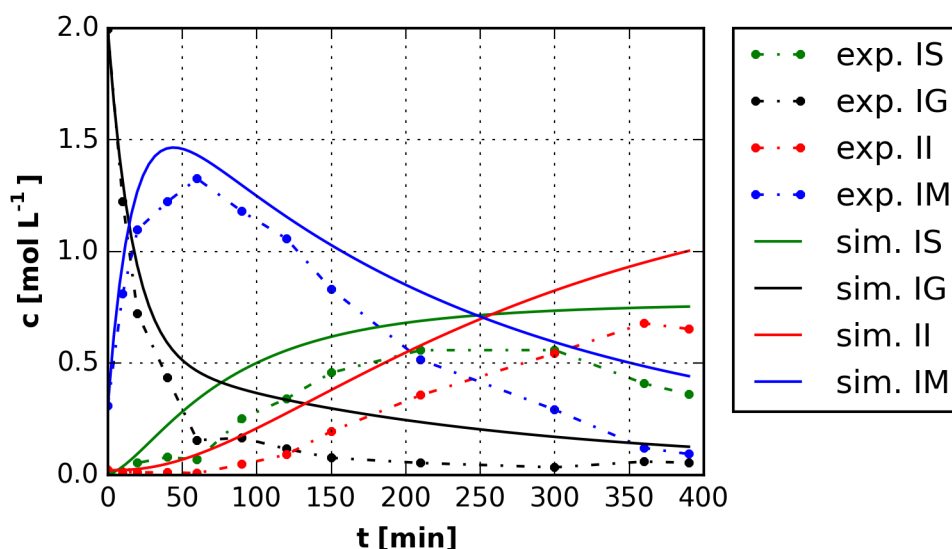


Figure 46. Concentration-time profile of the isomerisation of isomannide at 150 °C. Besides the experimental data (dots) the fit of the kinetic model (continuous lines) is displayed. Reaction conditions: 5 g isomannide, 1 mol-% Ru/C, 18 g H₂O, 25 bar H₂ pressure (at RT), 150 °C, and 500 rpm stirrer speed.

The concentration of isogalactide rapidly decreases while the concentration of isomannide steeply increases in the beginning. Additionally, the isosorbide concentration increases much slower. Thus, the isogalactide is mainly converted back to isomannide. The formation of isoidide is again delayed and started when isosorbide is available. This behaviour underlines once more the fact of the consecutive isomerisation of the hydroxy groups.

A comparison of the rate constants (Table 5) indicates that k_1 and k_3 are larger than k_2 and k_4 . Thus, the forward reactions are faster than the back reactions for the main isomerisation reactions. For the reaction of isomannide to isogalactide 1 it is once more vice versa: k_6 is larger than k_5 . Calculating the equilibrium constants at 150 °C (Table 6) a ratio of 0.25:1:6.4:11.5 of IG 1:IM:IS:II can be obtained, which is quite close to the experimental observed product distribution. In comparison to the rate constants determined at 160 °C, all values of all rate constants are lower at 150 °C. These lower values are expected because of a decreased reaction rate at lower temperatures. However, the errors on the rate constants at 150 °C are significantly higher, which is indicated by the considerably higher value of the least squares (cf. Table 5). At this temperature the model does not describe the data as well as for 160 °C, which can also be seen in the parity plot in Figure 47. The model overestimates the data. A reason for this is most likely the larger variation of the determined concentrations in between the two experiments at 150 °C in comparison to the 160 °C experiments.

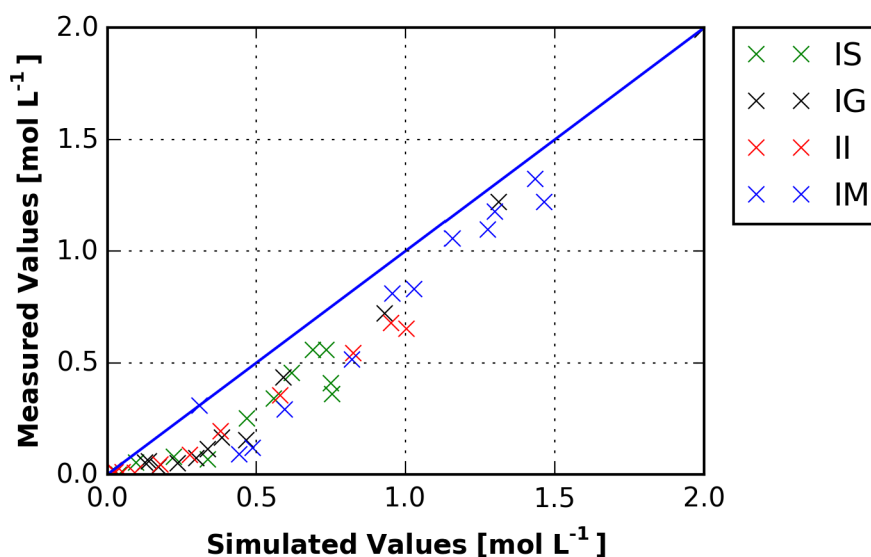


Figure 47. Parity plot of the kinetic model for the isomannide isomerisation data at 150 °C.

The experimental data and the fit of the kinetic model of the isomannide isomerisation at 140 °C is displayed in Figure 48. In general the behaviour is the same as described for the 150 °C data. Only the decrease of the isogalactide concentration is less steep than observed at 150 °C. The determined rate constants are once more larger for the forward reactions of the main isomerisation reactions and are the other way around for the reaction of isomannide to isogalactide 1. As expected, their values are smaller when compared to the rate constants determined at 150 and 160 °C because of the lower reaction rate at this lower temperature. Based on the equilibrium constants (Table 6) the ratio of IG 1:IM:IS:II is calculated to be 0.35:1:143:278, which is far off from the observed equilibrium. Also the value of the least squares is significantly high, indicating a considerable high error. The model again overestimates the data as can be seen in the parity plot (appendix Figure A 10).

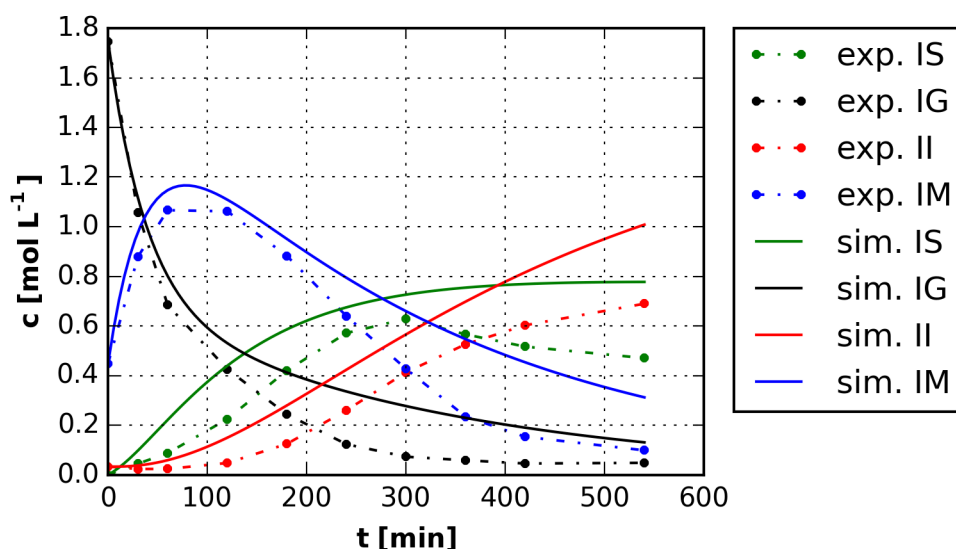


Figure 48. Concentration-time profile of the isomerisation of isomannide at 140 °C. Besides the experimental data (dots) the fit of the kinetic model (continuous lines) is displayed. Reaction conditions: 5 g isomannide, 1 mol-% Ru/C, 18 g H₂O, 25 bar H₂ pressure (at RT), 140 °C, and 500 rpm stirrer speed.

One reason for the poor fit could be the defective data. As mentioned already especially the concentrations of isogalactide have a rather large error. These values have an increased influence on the fits for lower reaction temperatures due to the larger amount of isogalactide in these reactions. Moreover, the Nelder-Mead simplex algorithm is prone to run into a local minimum instead of the desired global minimum. To eliminate this possibility, the modelling of the 140 °C data was additionally done with a differential evolution method for global optimisation problems:^[195] the `scipy.optimize.differential_evolution` function using Python.^[193] However, the obtained rate constants are identical to the one determined before, proving that the global minimum was obtained. Therefore, the poor fit is most likely attributed to the defective experimental data. Although the trends can be represented well, a more reliable data set has to be collected in the future in order to get a more precise description of the isomannide isomerisation. If the quality of the fit is still bad with more reliable data, another kinetic model has to be considered for the isomerisation at lower temperatures.

Table 5. Rate constants for the isomerisation of isomannide at 160, 150, and 140 °C.

	160 °C	150 °C	140 °C
k_1 [min ⁻¹]	$1.82 \cdot 10^{-2}$	$5.52 \cdot 10^{-3}$	$4.48 \cdot 10^{-3}$
k_2 [min ⁻¹]	$3.87 \cdot 10^{-3}$	$8.66 \cdot 10^{-4}$	$3.13 \cdot 10^{-5}$
k_3 [min ⁻¹]	$1.52 \cdot 10^{-2}$	$8.54 \cdot 10^{-3}$	$5.30 \cdot 10^{-3}$
k_4 [min ⁻¹]	$8.47 \cdot 10^{-3}$	$4.77 \cdot 10^{-3}$	$2.73 \cdot 10^{-3}$
k_5 [min ⁻¹]	$1.30 \cdot 10^{-2}$	$1.26 \cdot 10^{-2}$	$6.48 \cdot 10^{-3}$
k_6 [min ⁻¹]	0.25	$4.74 \cdot 10^{-2}$	$1.86 \cdot 10^{-2}$
Least Squares [mol ² L ⁻²]	0.13	1.96	1.11

Table 6. Equilibrium constants for the isomerisation of isomannide for 160, 150, and 140 °C. K_1 describes the equilibrium between IM and IS, K_2 the equilibrium between IS and II, and K_3 describes the equilibrium between IM and IG 1.

	160 °C	150 °C	140 °C
K_1	4.70	6.37	143
K_2	1.80	1.79	1.94
K_3	$5.09 \cdot 10^{-2}$	0.26	0.35

In addition to the experiments with isomannide as starting material concentration-time profiles for the isomerisation of isosorbide were collected at 160, 150, and 140 °C. The rate constants for the main isomerisation reaction should be the same since the same reactions are described. Yet, the rate constants for the equilibrium of isosorbide and isogalactide, in this case isogalactide 2 and 3, have to be determined. When the experimental data for 160 °C was modelled a good fit was obtained. However, the rate constants for the main isomerisation reaction were significantly lower than the ones determined with the data of the experiments at 160 °C of the isomannide isomerisation. Besides this unexpected finding, the modelling of the data collected at 150 and 140 °C led to negative rate constants. Especially k_7 was negative in all cases. However, negative rate constants are per definition not possible. Therefore, the data of the isosorbide isomerisation was modelled using the rate constants of the isomannide isomerisation data for the main isomerisation reactions since

they should be identical. Hence, only the rate constants for the formation of isogalactide (k_7 and k_8) were determined.

Figure 49 shows the experimental data as well as the fit of the kinetic model using the described approach for the 160 °C isosorbide isomerisation data. Interestingly, the determined values for k_7 and k_8 (Table 7) are almost identical to the ones obtained when all rate constants were modelled in the beginning. However, the quality of the fit decreased when using the previously determined rate constants for the main isomerisation reactions. Strikingly, k_7 , describing the formation of isogalactide, is very small and mostly adopts the order of magnitude, which was chosen as starting value. Additionally, it can also be set to zero without influencing the value of the least squares. This low value indicates that at reaction temperature the formation of isogalactide, in this case isogalactide 2/3, is not favoured. Thus, it is formed during the heating period. The course of the reaction displayed in Figure 49 shows that the concentration of isogalactide is decreasing fast in the beginning of the reaction. At the same time the concentration of isosorbide is rising, and after running through a maximum it decreases. This behaviour shows that isogalactide is mainly converted back to isosorbide.

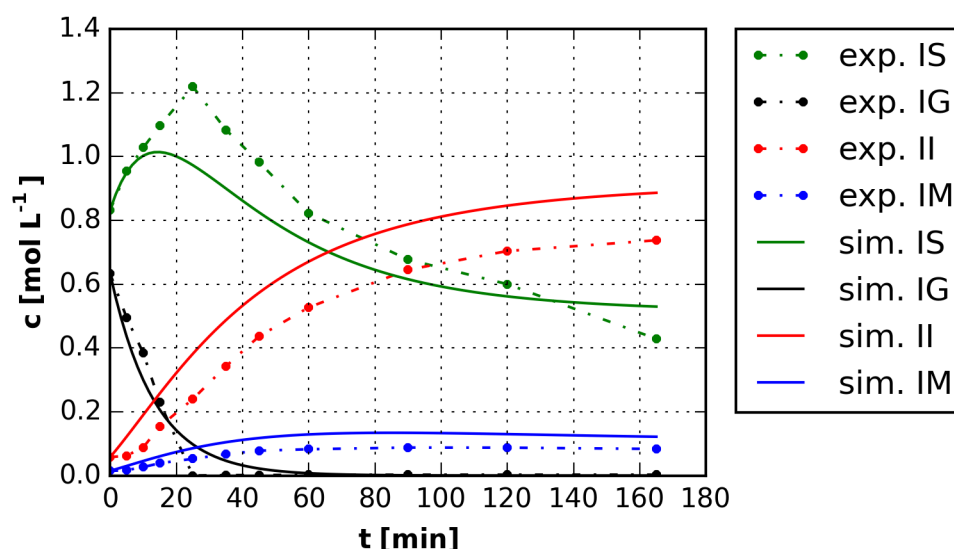


Figure 49. Concentration-time profile of the isomerisation of isosorbide at 160 °C. Besides the experimental data (dots) the fit of the kinetic model (continuous lines) is displayed. Reaction conditions: 5 g isosorbide, 1 mol-% Ru/C, 18 g H₂O, 25 bar H₂ pressure (at RT), 160 °C, and 500 rpm stirrer speed.

The parity plot (Figure 50) shows that there are deviations between the model and the experimental data. While the isomannide and isoidide data is overestimated, the data for isogalactide and isosorbide is underestimated, especially the higher concentrations.

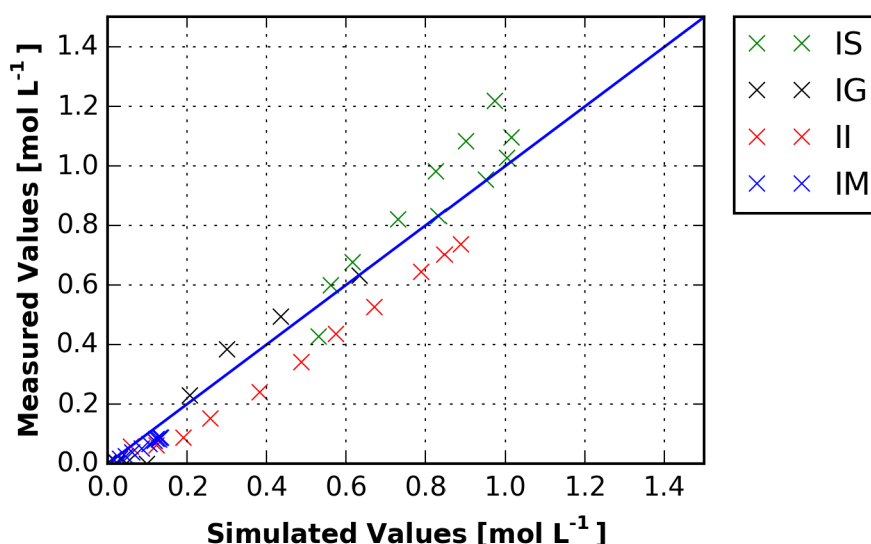


Figure 50. Parity plot of the kinetic model for the isosorbide isomerisation data at 160 °C.

The trend in the concentration-time profile of the isosorbide isomerisation at 150 °C is the same as for 160 °C (Figure 51). The concentration of isogalactide decreases exponentially in the beginning of the reaction and, simultaneously, the concentration of isosorbide increases. After a maximum is reached it decreases constantly. Figure 51 shows that the fit of the model is poor. The concentrations of isosorbide and isoidide are significantly overestimated, what is shown in more detail in the parity plot (appendix Figure A 11).

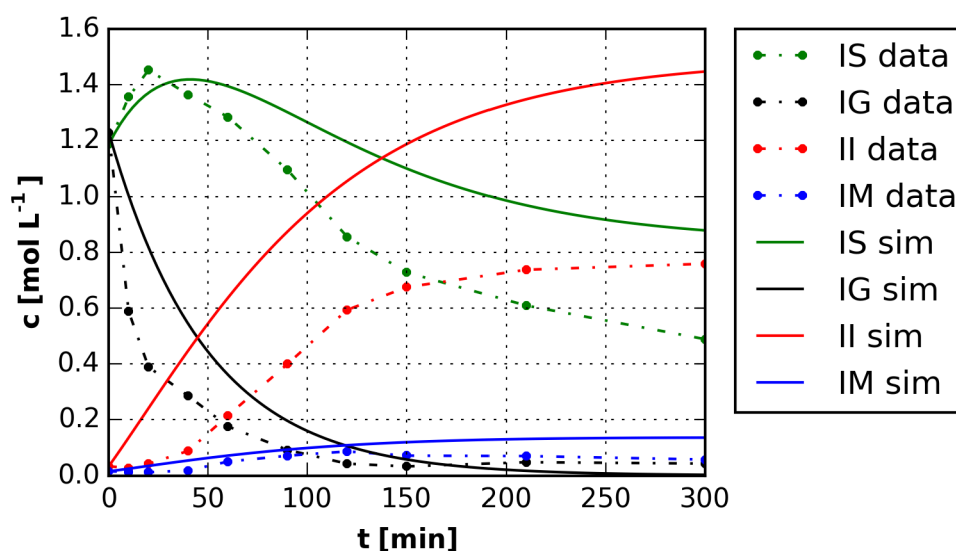


Figure 51. Concentration-time profile of the isomerisation of isosorbide at 150 °C. Besides the experimental data (dots) the fit of the kinetic model (continuous lines) is displayed. Reaction conditions: 5 g isosorbide, 1 mol-% Ru/C, 18 g H₂O, 25 bar H₂ pressure (at RT), 150 °C, and 500 rpm stirrer speed.

The concentration-time profile of the isomerisation of isosorbide at 140 °C (Figure 52) looks similar. Once more the experimental data is not described well by the model (cf. parity plot in appendix Figure A 12).

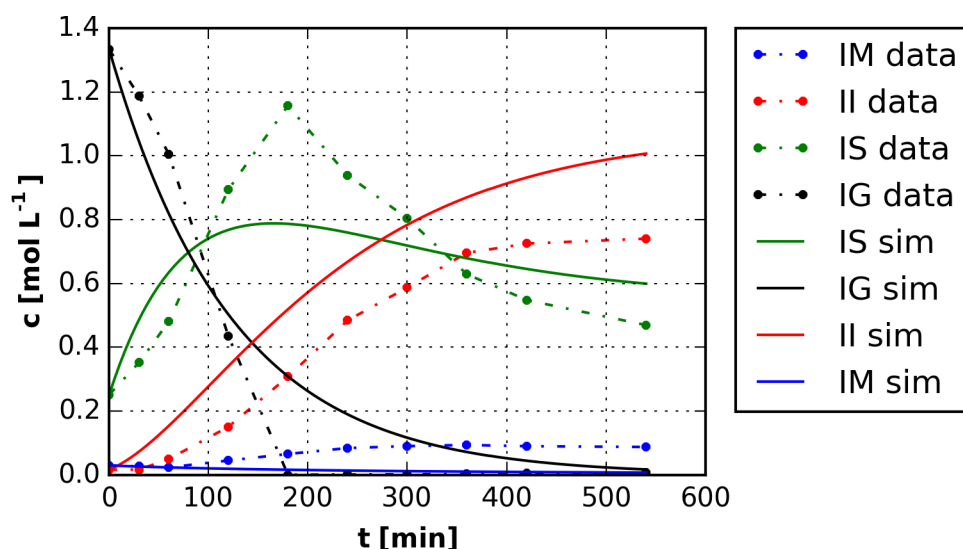


Figure 52. Concentration-time profile of the isomerisation of isosorbide at 140 °C. Besides the experimental data (dots) the fit of the kinetic model (continuous lines) is displayed. Reaction conditions: 5 g isosorbide, 1 mol-% Ru/C, 18 g H₂O, 25 bar H₂ pressure (at RT), 140 °C, and 500 rpm stirrer speed.

When comparing the rate constants (Table 7) at 150 and 140 °C, the behaviour of k_7 is similar to the 160 °C data. It adopts the order of magnitude chosen as starting point for the modelling and it can also be set to zero without influencing the value of the least squares. Thus, the formation of isogalactide under these reaction conditions seems unlikely. Therefore, it is most likely produced during the heating phase. In case of k_8 , describing the reaction from isogalactide 2/3 back to isosorbide, the rate constants are lower than for k_6 , describing the analogue reaction from isogalactide 1 to isomannide. However, it is still the fastest reaction in the network for the isosorbide isomerisation.

One reason for the poor fits, especially for the data obtained at 150 and 140 °C, is already discussed above: the use of an approximated calibration factor for isogalactide leading to an overestimation of the concentration by HPLC. Additionally, the peaks of isosorbide and isogalactide are not baseline-separated in the HPLC. This detail is more critical for the isosorbide isomerisation experiments than for the isomannide isomerisation experiments since in the latter most of the isogalactide is converted by the time the isosorbide concentration increases significantly. By starting with isosorbide in the beginning of the reaction, both compounds, isosorbide and isogalactide, are present in substantial amounts. Again the trends are represented well. However, for more reliable rate constants more accurate experimental data is needed. Therefore, an improvement of the analysis is required, in particular the separation of isogalactide and isosorbide. Furthermore, the determination of the calibration factor of isogalactide is essential. Therefore, a pure sample of the new isomer has to be prepared.

Table 7. Additional rate constants for the isomerisation of isosorbide at 160, 150, and 140 °C.

	160 °C	150 °C	140 °C
k_7 [min ⁻¹]	$1.40 \cdot 10^{-41}$	$1.41 \cdot 10^{-41}$	$1.08 \cdot 10^{-41}$
k_8 [min ⁻¹]	$7.48 \cdot 10^{-2}$	$2.04 \cdot 10^{-2}$	$8.13 \cdot 10^{-3}$
Least Squares [mol ² L ⁻²]	0.35	3.00	0.82

3.3.4 Determination of the Arrhenius Parameters

The Arrhenius parameters, activation energy and pre-exponential factor, can be obtained through the correlation stated in the Arrhenius equation (equation 1). From the Arrhenius plot ($\ln k$ versus $1/T$), the activation energy can be determined from the slope of the curve, which is $-E_A/R$. If the data is extrapolated to an infinite temperature, the pre-exponential factor can be identified. Thus, the y-axis intercept equals $\ln A$.

Figure 53 and Figure 54 show exemplarily the Arrhenius plots for the forward reactions of the main isomerisation reactions (k_1 and k_3). All other Arrhenius plots are found in the appendix (Figure A 13 to Figure A 18). The determined pre-exponential factors and activation energies are summarised in Table 8.

When comparing the activation energies for the main isomerisation reactions, the conversion of isosorbide to isoidide (78 kJ mol^{-1}) is more facile than the conversion of isomannide to isosorbide (103 kJ mol^{-1}) under the applied conditions. Furthermore, the activation energies for the back reactions (described by k_2 and k_4) are higher than for the forward reactions (described by k_1 and k_3). However, the difference in activation energy of the back reaction to the forwards reaction for the isomerisation of isosorbide to isoidide with 6 kJ mol^{-1} is much smaller than for the isomerisation of isomannide to isosorbide with 256 kJ mol^{-1} . This behaviour can also be seen in the equilibrium (5:40:55 for IM:IS:II). The fraction of isomannide is always the smallest while isoidide has the major share, although the difference in the amounts of isoidide and isosorbide is not very pronounced. For the conversion of isomannide to isogalactide 1, the activation energy for the forward reaction described by k_5 is much lower than the activation energy for the back reaction. This corresponds to the fact that isogalactide is formed mainly during the heating phase of the reaction, thus, at lower temperatures. Under reaction conditions, the activation energy necessary for the back reaction to isomannide can be overcome. The same trend is seen for the equilibrium between isosorbide and isogalactide 2/3. The activation energy for the formation of the latter is even lower than for isogalactide 1 starting from isomannide. However, as already discussed, k_7 , the rate constant describing this reaction, can theoretically also be zero without changing the value of the least squares. In this case, the activation energy would be zero as well and the reaction rate would be independent of the temperature change.

In general, the obtained Arrhenius parameters can be regarded as first estimation since the rate constants have rather big errors. However, they display the general trends, and the linear fits in the Arrhenius plot show good coefficients of determination with 0.74 and up to 0.99.

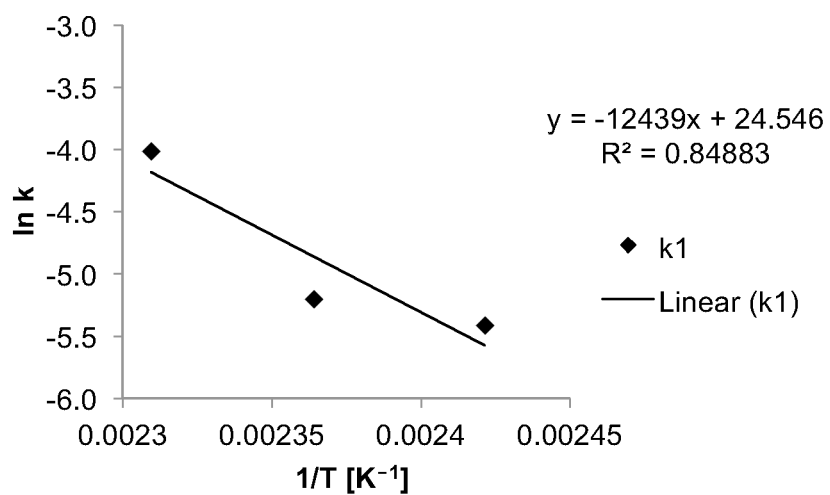


Figure 53. Arrhenius plot for the reaction described by k_1 (IM to IS).

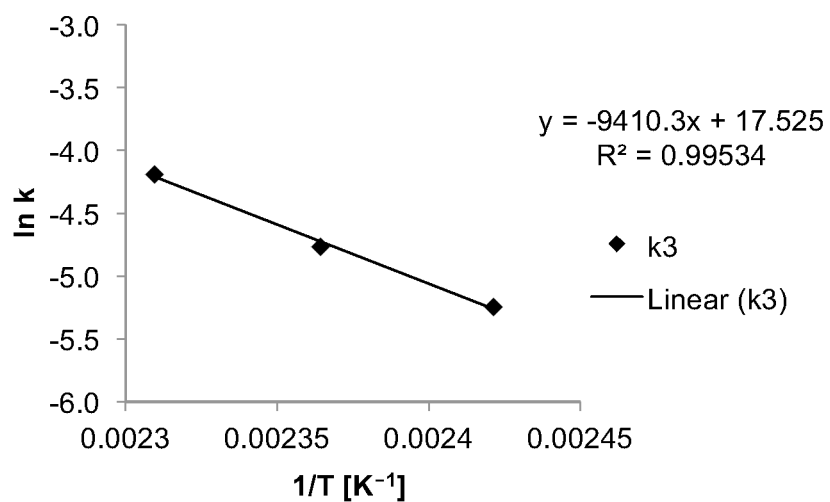


Figure 54. Arrhenius plot for the reaction described by k_3 (IS to II).

Table 8. Activation energies and pre-exponential factors obtained through the Arrhenius plots of the rate constants.

Rate Constant	E_A [kJ mol ⁻¹]	A [min ⁻¹]
k_1	103	$4.57 \cdot 10^{10}$
k_2	359	$1.10 \cdot 10^{41}$
k_3	78	$4.08 \cdot 10^{07}$
k_4	84	$1.17 \cdot 10^{08}$
k_5	52	$2.58 \cdot 10^{04}$
k_6	194	$5.71 \cdot 10^{22}$
k_7	20	$3.38 \cdot 10^{-39}$
k_8	165	$5.15 \cdot 10^{18}$

4 Conclusion

The present work addresses the catalytic transformations of isomannide and isosorbide comprising the catalytic amination and isomerisation. The main products isohexide amines or isoidide, respectively, are suitable monomers in the production of biogenic polymers.

Concerning the amination of isohexides, the first heterogeneously catalysed method was reported using a supported ruthenium on activated carbon catalyst (Ru/C) in aqueous ammonia solution. In the screening of different hydrogenation catalysts, only supported ruthenium catalysts were found to be active in this reaction. Additionally, it was demonstrated that small ruthenium nanoparticles (< 2 nm) are beneficial for the amination of isohexides. The commercial Ru/C catalyst used in most of the experiments showed a good stability. Despite the highly basic conditions, the leaching of the active ruthenium species was minor as verified by ICP-OES measurements. A deactivation of the catalyst was observed through product adsorption. However, this deactivation was reversible as revealed by recycling experiments. Strikingly, depending on the substrate, the product spectrum changed significantly. While starting from isosorbide mainly two amino alcohols (amino alcohols 1/2) were formed; isomannide as starting material led to two other amino alcohols (amino alcohols 3/4) as well as diamines. This fact indicates a preferential conversion of *endo*-configured hydroxy groups into amines. Moreover, the role of hydrogen and the possibility of a hydrogen autotransfer (HAT) mechanism, in which no external molecular hydrogen needs to be applied, were investigated. In the amination of isohexides catalysed by a solid ruthenium catalyst, molecular hydrogen was required in order to obtain reasonable activity. Therefore, the requirements for a HAT mechanism are not met. However, low hydrogen pressures and, thus, substoichiometric amounts of hydrogen, were sufficient. They are most likely necessary to activate the catalyst under reaction conditions and to saturate the surface with hydrogen. The latter is required to enhance the probability of contact between the sterically demanding isohexide imine intermediate and hydrogen to form the isohexide amine. Altogether, working in aqueous solution and with low hydrogen pressure as well as with a solid catalyst, which is easy to separate and recyclable, first steps towards a benign production process of isohexides amines were made.

In the isomerisation of isohexides the mechanism was investigated in detail. Therefore, deuterium labelling experiments at different temperatures with a Ru/C catalyst and isomannide as well as dimethyl isosorbide as substrates were performed. In the literature a dehydrogenation/re-hydrogenation mechanism is proposed. However, the results of the deuterium labelling experiments showed the existence of an alternative mechanism through direct C–H activation at higher temperatures (> 160 °C). Yet, at lower temperatures the dehydrogenation/re-hydrogenation mechanism seemed more likely. Moreover, in the context of kinetic investigations, concentration-time profiles were collected at 140, 150, and 160 °C. Surprisingly, in the beginning of the reaction course, a fourth compound could be observed.

Based on GC-MS measurements, it was assumed that this substance is another isohexide isomer called *isogalactide*, a compound not yet characterised in the literature. Unfortunately, this substance could only be obtained in small amounts and not yet be separated from its isomers. Therefore, the structure of this molecule could not be verified up to now. However, the only conceivable isomeric structure is an isohexide with *trans* configuration of the bridgehead hydrogen atoms. In fact, three different isomeric structures of isogalactide are possible. The formed structure depends on the starting material. Thus, two different reaction networks had to be considered in the kinetic modelling: one for isomannide and one for isosorbide. Rate constants and Arrhenius parameters were determined. However, the data obtained by means of HPLC was defective since the isogalactide and isosorbide peak was not baseline-separated and thus far no accurate calibration factor for isogalactide could be determined. Additionally, side reactions occurring mainly at longer reaction times were neglected, adding to a defective mass balance. Nevertheless, the determined kinetic data can be considered as preliminary result reflecting the correct trends of the reaction. For example, the rate constants for the forward reactions in the main isomerisation reaction are always larger than for the back reactions indicating fast reactions, and the equilibrium constants depict the equilibrium ratio of the isohexide isomers. Furthermore, the low activation energy calculated for the formation of isogalactide underlines the fact that this compound is mainly produced at lower temperatures, thus, during the heating process in the performed experiments. In conclusion, with the described procedures, new insights into the isohexide isomerisation reaction were gained generating a basis for a production process of isoidide starting from biogenic feedstock.

Since the alternative monomers reported in this work, the isohexide amines and isoidide, are very promising for the production of biomass-derived polymers, it is worthwhile to expand the research towards a larger scale production. Therefore, in the amination reaction the catalyst has to be optimised. Particularly the selectivity towards the diamines has to be enhanced. Comprehensive kinetic investigations and the adaption to a continuous system will facilitate the isohexide amine production. Concerning the isomerisation reaction, an improved analytical method is beneficial for further research and the application in a continuous system is desirable. For both investigated reactions, the separation of the products is important. Working in aqueous usually leads to energy-intensive separation processes. Thus, an alternative separation technique, liquid-phase adsorption, should be studied in further work.

5 Experimental

5.1 General Information

All commercially available chemicals were purchased from *abcr*, *Alfa Aesar*, *Chemsolute*, *Fluka*, *Gerling Holz + Co*, *Merck Millipore*, and *Sigma Aldrich* and used without further purification or treatment. Table 9 gives an overview of all used chemicals, their supplier, and their purity.

Table 9. Overview of the used chemicals.

Chemicals	Purity	Supplier
Aqueous Ammonia Solution (25 % NH ₃)	Reag. Ph. Eur.	Sigma Aldrich
Liquid Ammonia (anhydrous)	99.98 %	Gerling Holz + Co.
Chlorotrimethylsilane	99.0 %	Fluka (Sigma Aldrich)
Deuterium oxide	99.9 atom % D	Sigma Aldrich
Dimethyl isosorbide	98 %	Sigma Aldrich
Ethanol	99.5 %	Chemsolute
Isomannide	98 %	abcr
Isosorbide	98 %	Alfa Aesar
<i>N</i> -Methyl- <i>N</i> -(trimethylsilyl)trifluoro acetamide	Suitable for Silylation	Sigma Aldrich
Pyridine	Reag. Ph. Eur.	Merck Millipore
Ruthenium(III) chloride hydride (39-42 % Ru content)	99.9 % (Ru)	abcr

The commercial transition metal catalysts like Ru/C, Pd/C, and Pt/C were acquired from *abcr*, *Johnson Matthey*, and *Sigma Aldrich*. In order to prevent oxidation of the metal species, they have been stored under argon atmosphere. An overview about all used commercial catalyst, their supplier, as well as their metal content can be found in Table 10.

Table 10. Overview of all used commercial catalysts.

Catalyst	Additional Information	Metal Content	Supplier
Escat 4401	Ru/C; 50 % water wet paste	5 wt.-%	abcr (Product by Strem)
Pd/C		5 wt.-%	Johnson Matthey
Pd/C		5 wt.-%	Sigma Aldrich
Pt/C		5 wt.-%	Sigma Aldrich
Raney-Ni	Slurry; 50 % water	89 % Ni	abcr (Product by Strem)
Ru/C		5 wt.-%	abcr (Product by Strem)
Ru/C		5 wt.-%	Sigma Aldrich
Ruthenium Powder	Reduced	5 wt.-%	abcr (Product by Strem)

Conversion X and the yield Y were calculated using the following equations:

$$X = \frac{n_{i,0} - n_i}{n_{i,0}} \cdot 100\% \quad (14)$$

$$Y = \frac{n_j}{n_{i,0}} \cdot 100\% \quad (15)$$

Herein are $n_{i,0}$ the initial amount of substance of the substrate, n_i the residual amount of substance of the substrate, and n_j the amount of substance of the product.

5.2 Catalyst Preparation

For the preparation of Ru/C catalyst with 5 wt.-% loading of ruthenium, different activated carbon support materials from *Cabot* were applied in wet impregnation:

- Norit SX 1G
- Norit RX 3 Extra
- Norit ROX 0.8
- Norit A Supra EUR

Norit SX 1G and Norit A Supra EUR are powders while Norit RX 3 Extra and Norit ROX 0.8 are extrudates. Thus, the latter were pestled until a fine powder was obtained prior to impregnation.

In the standard synthetic procedure, 0.1235 g $\text{RuCl}_3 \cdot \text{H}_2\text{O}$ (38–42 % Ru content) were dissolved in 30 mL ethanol and 0.9500 g activated carbon were added. After stirring for 24 h the ethanol was removed. Subsequently the catalyst was dried at 120 °C for another 24 h. The reduction of the ruthenium species was performed in flowing hydrogen. If not stated otherwise, the heating ramp was set to 10 K min⁻¹ and the reduction temperature of 350 °C was held for 4 h. The catalyst was transferred into a storage container and stored under argon atmosphere.

5.3 Catalysis Procedures

5.3.1 Isohexide Amination

5.3.1.1 General Procedure

In a typical experiment, isomannide or isosorbide (1.00 g, 6.84 mmol), 2 mol-% of a 5 wt.-% Ru/C (0.277 g, 0.137 mmol Ru content), and 25 wt.-% aqueous ammonia (5 g) were placed in a 20 mL or 45 mL autoclave. After closing the autoclave it was pressurised with 10 bar hydrogen (at RT). The reaction mixture was stirred using a magnetic stirring bar at temperatures between 140-180 °C for 6-24 h. Subsequently, the autoclave was cooled down to room temperature using an ice bath. The autoclave was opened and the mixture was stirred for another hour to remove the residual ammonia before the solid catalyst was filtered off and a sample was analysed using GC. The GC-sample was derivatised prior to injection through silylation.

Two different sets of autoclaves were used. In the 20 mL autoclaves the temperature was monitored at the heating block while the 45 mL autoclaves were equipped with a thermocouple inside a capillary reaching into the autoclave. Thus, the temperature was monitored inside the 45 mL autoclave.

5.3.1.2 Experiments with Liquid Ammonia

Isomannide (1.00 g, 6.84 mmol), 2 mol-% of a 5 wt.-% Ru/C (0.277 g, 0.137 mmol Ru content), and water (5 g) were placed in a 45 mL autoclave. The autoclave was closed and weighed. Afterwards it was connected to a dosage pump (Carino 09 from *Fink Chem + Tec*) and the liquid ammonia was dosed into the autoclave. Then the autoclave was weighed once more to determine the amount of ammonia. Subsequently, 10 bar hydrogen pressure was applied (at RT) and the mixture was heated to 170 °C for 24 h.

5.3.1.3 Recycling Experiments of the Catalyst

A typical reaction as described above was performed only with doubled amounts (2 g isomannide, 0.5538 g 5 wt.-% Ru/C, and 10 g aqueous ammonia solution). For these experiments 45 mL autoclaves were used and the reaction temperature was 150°C. After each reaction the catalyst was filtered off and washed three times with water and once with ethanol. Subsequently the catalyst was dried at 120 °C in air. In every run the values of the substrate and solvent were adapted to the residual catalyst amount enabling the same ratio.

5.3.2 Isohexide Isomerisation and Mechanistic Investigations

For a typical isohexide isomerisation experiment in a 45 mL autoclave, isomannide or isosorbide (1.50 g, 10.3 mmol) were dissolved in water (5 g) and 1 mol-% of a 5 wt.% Ru/C (0.208 g, 0.103 mmol Ru content) were added. The closed autoclave was pressurised with 25 bar hydrogen (at RT). If not stated otherwise the reaction solution was stirred using a magnetic stirring bar for 3 h at 160 °C. Afterwards the autoclave was cooled to room temperature using an ice bath. Subsequently the solid catalyst was filtered off and a sample was analysed using HPLC.

5.3.2.1 Deuterium Labelling Experiments

In a 45 mL autoclave, isomannide (1.50 g, 10.3 mmol) or dimethyl isosorbide (1.788 g, 10.3 mmol) were dissolved in D₂O (5 g) and 1 mol-% of a 5 wt.% Ru/C (0.208 g, 0.103 mmol Ru content) were added. The closed autoclave was pressurised with 25 bar hydrogen (at RT). The reaction mixture was stirred using a magnetic stirring bar for 3 h at temperatures between 80-160 °C. Afterwards the autoclave was cooled to room temperature using an ice bath. Subsequently the solid catalyst was filtered off and a sample was analysed using HPLC and NMR.

5.3.2.2 Isomerisation of Dimethyl Isosorbide

Dimethyl isosorbide (1.788 g, 10.3 mmol), D₂O (5 g), and 1 mol-% of a 5 wt.% Ru/C (0.208 g, 0.103 mmol Ru content) were placed into a 45 mL autoclave. After pressurising the closed autoclave with 25 bar (at RT), the reaction solution was stirred using a magnetic stirring bar for 3 h at 160 °C. Subsequently the autoclave was cooled to room temperature using an ice bath. After the solid catalyst was filtered off a sample was analysed using HPLC and GC-MS.

5.3.3 Isohexide Isomerisation Kinetic Experiments

For the experiments to obtain the concentration-time profiles for the kinetic investigations, a 50 mL autoclave with overhead stirrer and equipped with a capillary for taking samples was used. Isomannide or isosorbide (5.40 g, 37.0 mmol) were dissolved in water (18 g) and 1 mol-% of a 5 wt.% Ru/C (0.747 g, 0.370 mmol Ru content) were added. The autoclave was pressurised with 25 bar hydrogen (at RT). The reaction mixture was stirred and heated to the desired reaction temperature (140, 150 or 160 °C). Once the temperature was reached the time was defined as 0 min and the first sample was taken. All other samples were taken in appropriate time intervals depending on the temperature. Afterwards the cooling process was facilitated with an ice bath. All samples were analysed by HPLC.

5.3.4 Isohexide Adsorption Experiment

For the adsorption experiments an aqueous solution containing isosorbide and isomannide in equimolar ratio was used and as adsorbent Norit A Supra EUR (Cabot) was applied. The concentration of the solution ranged from $0.025 \text{ mmol g}_{\text{solution}}^{-1}$ to $0.331 \text{ mmol g}_{\text{solution}}^{-1}$. The experiments were performed in batch mode using a water shaking bath with reciprocating agitation and temperature control under equilibrium conditions. In each adsorption experiment, 2 g solution and 0.04 g adsorbent were placed in a 5 mL capped glass vial and the mixture was kept at 20°C . The adsorbed amount of substance (at the equilibrium) q_e was calculated using the following equation:

$$q_e = \frac{(c_{i,0} - c_{i,e})m_{\text{solution}}}{m_{\text{adsorbent}}} \quad (16)$$

Herein $c_{i,0}$ and $c_{i,e}$ are the initial and equilibrium concentrations of the adsorbate i , respectively. m_{solution} is the mass of the solution and $m_{\text{adsorbent}}$ is the mass of the dry adsorbent. The analysis was done by HPLC.

5.4 Kinetic Modelling

The modelling of the kinetic data was performed with Python.^[193] A Nelder-Mead simplex algorithm^[194] was used for the minimisation of the least squares as implemented in the `scipy.optimize.fmin` script of the SciPy library. To check whether the obtained minimum is the global minimum, in some cases the modelling was done with a differential evolution method for global optimisation problems implemented in the `scipy.optimize.differential_evolution` script of the SciPy library.^[195]

5.5 Analytics

5.5.1 Gas Chromatography

The product mixtures of the amination reactions were analysed by means of gas chromatography after derivatisation and using *n*-dodecane as the standard. The GC method was established in cooperation with the analytical staff of the Central Department Research, Development and Services of the company *Südzucker AG*.

The derivatisation procedure is the following. The sample (20 mg) and the analytical standard (7 mg) were dissolved in pyridine (0.5 mL). Subsequently chlorotrimethylsilane (10 µL) and *N*-methyl-*N*-(trimethylsilyl) trifluoroacetamide (560 µL) were added. Afterwards the mixture was heated to 80 °C for one hour.

The correction factors for the derivatised compounds (trimethylsilyl (TMS) derivatives) are summarised in Table 11.

Table 11. Correction factors for the GC analysis.

Isoidide	Isosorbide	Isomannide	Amino Alcohols 1-4 ^[a]	Diamines 1-3 ^[a]
1.03	1.07	1.11	1.40	1.40

^[a]The correction factors of the amine compounds were obtained in a mixture.

In Table 12 the details of the GC method are summarised and Table 13 displays the retention times of all TMS-derivatised compounds.

Table 12. GC conditions for the analysis of the amination reaction solutions.

GC Conditions	
Device	Focus GC (<i>Thermo Scientific</i>)
Column	Rtx-1 Pona, 50 m
Inner Diameter	0.25 mm
Film Thickness	0.5 µm
Carrier Gas	Hydrogen (1.2 mL min ⁻¹)
Split Flow	40 mL min ⁻¹
Detector	FID (250 °C)
Temperature Programme	80 °C, 5 min iso, 8 °C min ⁻¹ to 250 °C, 30 min

Table 13. Retention times of all compounds in an amination reaction mixture in the GC analysis and functional group assignments.

Compound	Retention Time [min]	Assignment of Functional Groups [2/5]
Isoidide	19.75	<i>exo/exo</i>
Isosorbide	20.04	<i>exo/endo</i>
Isomannide	20.29	<i>endo/endo</i>
Amino Alcohol 1	20.88	
Amino Alcohol 2	20.98	
Amino Alcohol 3	21.08	
Amino Alcohol 4	21.12	
Diamine 1	21.97	<i>exo/exo</i> ^[a]
Diamine 2	22.08	
Diamine 3	22.13	

^[a] Assignment based on comparison with the retention time of the synthesised compound. Synthesis according to THIYAGARAJAN *et. al.*^[153]

5.5.2 Gas Chromatography – Mass Spectrometry

5.5.2.1 GC-MS of the Isohexide Amination Reaction Products

The gas chromatography – mass spectrometry (GC-MS) analysis of the TMS-derivatised isohexides and their amine derivatives was conducted at the Central Department Research, Development and Services of the company *Südzucker AG*. The ionisation method was chemical ionisation (CI). The details of the GC and MS conditions are summarised in Table 14 and Table 15, respectively.

Table 14. GC conditions in the GC-MS analysis of the TMS-derivatised isohexide amine derivatives.

GC Conditions	
Device	GC6890 (<i>Agilent</i>)
Column	Fused Silica VF5, 60 m
Inner Diameter	0.25 mm
Film Thickness	0.25 μm
Carrier Gas	Helium (1 mL min^{-1})
Split	1:25
Temperature Programme	80 $^{\circ}\text{C}$, 1 min iso, 5 $^{\circ}\text{C min}^{-1}$ to 300 $^{\circ}\text{C}$

Table 15. MS conditions of the GC-MS analysis of the TMS-derivatised isohexide amine derivatives.

MS Conditions	
Device	GCmate-2 (<i>Jeol</i>)
Ionisation Method	CI
Ionisation Energy	200 eV
Resolution	1000
Voltage	500-600 V
Attenuator	16
CI-Gas	Ammonia

5.5.2.2 GC-MS of the Dimethyl Isosorbide Isomerisation Reaction Products

The product mixture of the dimethyl isosorbide (DMI) isomerisation reaction was analysed by means of GC-MS using electron ionisation (EI). The conditions for the GC as well as MS can be found in Table 16 and Table 17, respectively.

Table 16. GC conditions in the GC-MS analysis of the DMI derivatives.

GC Conditions	
Device	Trace 1310 (<i>Thermo Scientific</i>)
Column	Rxi-1-MS, 60 m
Inner Diameter	0.25 mm
Film Thickness	0.50 μm
Carrier Gas	Helium (1.2 mL min^{-1})
Split Flow	50 mL min^{-1}
Temperature Programme	$50 \text{ }^{\circ}\text{C}$, 5 min iso, $8 \text{ }^{\circ}\text{C min}^{-1}$ to $280 \text{ }^{\circ}\text{C}$

Table 17. MS conditions in the GC-MS analysis of the DMI derivatives.

MS Conditions	
Device	ISQ Single Quadrupole MS (<i>Thermo Scientific</i>)
Ionisation Method	EI
Ionisation Energy	70 eV

5.5.2.3 GC-MS of the Isohexide Isomers

The GC-MS analysis of the TMS-derivatised isohexides was conducted at the Central Department Research, Development and Services of the company *Südzucker AG*. The ionisation method was chemical ionisation (CI). The details of the GC and MS conditions released by the company are summarised in Table 18 and Table 19, respectively.

Table 18. GC conditions in the GC-MS analysis of the TMS-derivatised isohexide isomers.

GC Conditions	
Device	GC7890 (<i>Agilent</i>)
Column	Fused Silica Rxi5SIL MS, 40 m
Inner Diameter	0.18 mm
Film Thickness	0.18 μm
Injector	Split/Splitless-Injector
Injected Volume	1 μL
Temperature Programme	80 °C, 1 min iso, 5 °C min ⁻¹ to 300 °C

Table 19. MS conditions in the GC-MS analysis of the TMS-derivatised isohexide isomers.

MS Conditions	
Device	QTOF 7200 (<i>Agilent</i>)
Ionisation Method	CI
CI-Gas	Ammonia

5.5.3 High-Pressure Liquid Chromatography

The product mixtures of the isohexides isomerisation reactions were analysed by high-pressure liquid chromatography (HPLC). Table 20 shows the details of the HPLC method.

Table 20. HPLC conditions for the analysis of the isomerisation reaction solutions.

HPLC Conditions	
Device	LC MS 2020 (<i>Shimadzu</i>)
Column	Aminex HPX-87P (<i>Bio-Rad</i>)
Column Pressure	22 bar
Eluent	Water
Flow	0.5 mL min ⁻¹
Detector	RI
Oven Temperature	80 °C

Table 21 gives an overview of the retention times and calibration factors of the measured compounds.

Table 21. Retention times and calibration factors for all compounds of the isomerisation reaction in HPLC analysis.

Compound	Retention Time [min]	Calibration Factor
Isoidide	14.70	54063.5
Isosorbide	18.52	57882.4
Isomannide	22.55	58951.1
4 th Isomer (Isogalactide)	19.50	-

5.5.4 Nuclear Magnetic Resonance Spectroscopy

Nuclear Magnetic Resonance (NMR) spectroscopy was conducted using the device Avance III 400 from the company *Bruker*, a spectrometer with an operating frequency of 400.2 MHz for ¹H-NMR measurements. The proton signal of the deuterated solvent was adequate as internal standard in ¹H-NMR spectra. For the used solvent, deuterium oxide, the residual proton signal is at a chemical shift of 4.79 ppm. All NMR measurements were conducted at room temperature.

5.5.5 Catalyst Characterisation

5.5.5.1 Nitrogen Physisorption

Nitrogen physisorption isotherms were measured at $-196\text{ }^{\circ}\text{C}$ using a Quadrasorb SI from *Quantachrome Instruments*. Prior to the measurements, the samples were pre-treated at $120\text{ }^{\circ}\text{C}$ for at least 18 h under vacuum. For the determination of the specific surface area the method according to Brunauer, Emmett, and Teller (BET)^[166] was used in the relative pressure region of 0.05-0.3.

5.5.5.2 Inductive Coupled Plasma Optical Emission Spectroscopy

For the inductive coupled plasma optical emission spectroscopy (ICP-OES) the device ICP Spectroflame D from the company *Spectro* was used. The procedure for investigating the solid ruthenium catalysts is the following:

The catalyst (30 mg) is solubilised by melting and digesting it with KNO_3 (0.12 g) and KOH (1 g). Afterwards it is diluted in hydrochloric acid.

5.5.5.3 Powder X-Ray Diffraction

Powder X-Ray Diffraction (XRD) chromatograms were collected using a *Siemens* D5000 diffractometer with $\text{Cu } k_{\alpha}$ rays in the area of $2\theta = 3\text{--}90\text{ }^{\circ}$.

5.5.5.4 Thermogravimetry and Differential Scanning Calometry

The apparatus for thermogravimetry (TG) and differential scanning calometry (DSC) was a *Netzsch* STA 409. The analyses were carried out in air and with a heating rate of 5 K min^{-1} .

5.5.5.5 Carbon Monoxide Chemisorption

The carbon monoxide chemisorption was performed in pulse mode using a TPD/R/O 1100 device by the company *CE Instruments*. In the pre-treatment step the sample was purged with nitrogen ($30\text{ cm}^3\text{ min}^{-1}$). Afterwards the temperature was risen with 10 K min^{-1} to $250\text{ }^{\circ}\text{C}$ and held for 10 min. Subsequently the sample was reduced at $250\text{ }^{\circ}\text{C}$ using 10 % hydrogen in argon ($30\text{ cm}^3\text{ min}^{-1}$) for 150 min. Then the sample was cooled under nitrogen flow ($30\text{ cm}^3\text{ min}^{-1}$). Prior to the injections of the carbon monoxide pulses (5 % CO in Ar), the sample was purged with argon. The data evaluation was done with the included programme.

5.5.5.6 Transmission Electron Microscopy

The transmission electron microscopy (TEM) measurements were performed at Gent University using a JEM-2200FS high resolution, aberration corrected transmission electron microscope from the company *JEOL* in a scanning transmission electron microscopy (STEM) mode.

6 References

- [1] P. Gallezot, *ChemSusChem* **2008**, 1, 734-737.
- [2] F. Seitz, in *Catalysis for the Conversion of Biomass and Its Derivatives* (Eds.: M. Behrens, A. K. Datye), Max Planck Research Library for the History and Development of Knowledge, Berlin, **2013**.
- [3] B. Kamm, M. Kamm, P. R. Gruber, S. Kromus, in *Biorefineries – Industrial Processes and Products, Vol. 1* (Eds.: B. Kamm, M. Kamm, P. R. Gruber), Wiley-VCH, Weinheim, **2006**.
- [4] R. Rinaldi, F. Schüth, *ChemSusChem* **2009**, 2, 1096-1107.
- [5] B. Dean, T. Dodge, F. Valle, G. Chotani, in *Biorefineries – Industrial Processes and Products, Vol. 1* (Eds.: B. Kamm, M. Kamm, P. R. Gruber), Wiley-VCH, Weinheim, **2006**.
- [6] D. J. Hayes, S. Fitzpatrick, M. H. B. Hayes, J. R. H. Ross, in *Biorefineries – Industrial Processes and Products, Vol. 1* (Eds.: B. Kamm, M. Kamm, P. R. Gruber), Wiley-VCH, Weinheim, **2006**.
- [7] GFBiochemicals, <http://www.gfbiochemicals.com/company/>, 11.03.2016.
- [8] M. J. Climent, A. Corma, S. Iborra, *Green Chem.* **2011**, 13, 520-540.
- [9] G. W. Huber, S. Iborra, A. Corma, *Chem. Rev.* **2006**, 106, 4044-4098.
- [10] W. Leitner, in *Die Zukunft der Energie* (Eds.: P. Gruss, F. Schüth), C.H.Beck, München, **2008**.
- [11] F. M. A. Geilen, T. vom Stein, B. Engendahl, S. Winterle, M. A. Liauw, J. Klankermayer, W. Leitner, *Angew. Chem. Int. Ed.* **2011**, 50, 6831-6834.
- [12] M. G. Al-Shaal, A. Dzierbinski, R. Palkovits, *Green Chem.* **2014**, 16, 1358-1364.
- [13] IFEU (Institut für Energie- und Umweltforschung Heidelberg), *Biomasse - Rohstoff für die chemische Industrie*, **2007**.
- [14] R. Rinaldi, F. Schuth, *Energy Environ. Sci.* **2009**, 2, 610-626.
- [15] R.-J. van Putten, J. C. van der Waal, E. de Jong, C. B. Rasrendra, H. J. Heeres, J. G. de Vries, *Chem. Rev.* **2013**, 113, 1499-1597.
- [16] F. D. Pileidis, M. M. Titirici, *ChemSusChem* **2016**.
- [17] M. Rose, R. Palkovits, *ChemSusChem* **2012**, 5, 167-176.
- [18] H. I. Russek, *Am. J. Cardiol.* **1968**, 21, 44-54.
- [19] I. Delidovich, P. J. C. Hausoul, L. Deng, R. Pfützenreuter, M. Rose, R. Palkovits, *Chem. Rev.* **2016**, 116, 1540-1599.
- [20] F. Fenouillot, A. Rousseau, G. Colomines, R. Saint-Loup, J. P. Pascault, *Prog. Polym. Sci.* **2010**, 35, 578-622.
- [21] S. Imm, S. Bähn, M. Zhang, L. Neubert, H. Neumann, F. Klasovsky, J. Pfeffer, T. Haas, M. Beller, *Angew. Chem. Int. Ed.* **2011**, 50, 7599-7603.
- [22] D. Pinggen, O. Diebolt, D. Vogt, *ChemCatChem* **2013**, 5, 2905-2912.
- [23] L. F. Wiggins, *J. Chem. Soc.* **1945**, 4-7.
- [24] R. Montgomery, L. F. Wiggins, *J. Chem. Soc.* **1946**, 390-393.
- [25] A. C. Cope, T. Y. Shen, *J. Am. Chem. Soc.* **1956**, 78, 3177-3182.
- [26] G. Flèche, M. Huchette, *Starch/Stärke* **1986**, 38, 26-30.

-
- [27] H. G. Fletcher, R. M. Goepp, *J. Am. Chem. Soc.* **1946**, 68, 939-941.
- [28] J. S. Brimacombe, A. B. Foster, M. Stacey, D. H. Whiffen, *Tetrahedron* **1958**, 4, 351-360.
- [29] H. G. Fletcher, R. M. Goepp, *J. Am. Chem. Soc.* **1945**, 67, 1042-1043.
- [30] M. Rose, K. Thenert, R. Pfützenreuter, R. Palkovits, *Catal. Sci. Technol.* **2013**, 3, 938-941.
- [31] R. Pfützenreuter, M. Helmin, S. Palkovits, R. Palkovits, M. Rose, *Catal. Today* **2014**, 234, 113-118.
- [32] L. W. Wright, J. D. Brandner, *J. Org. Chem.* **1964**, 29, 2979-2982.
- [33] S. Van de Vyver, J. Geboers, P. A. Jacobs, B. F. Sels, *ChemCatChem* **2011**, 3, 82-94.
- [34] Y.-H. P. Zhang, L. R. Lynd, *Biotechnol. Bioeng.* **2004**, 88, 797-824.
- [35] H. Lüers, *Angew. Chem.* **1932**, 45, 369-376.
- [36] F. Bergius, *J. Soc. Chem. Ind.* **1933**, 52, 1045-1052.
- [37] L. Hu, L. Lin, Z. Wu, S. Zhou, S. Liu, *Appl. Catal., B* **2015**, 174-175, 225-243.
- [38] Transparency Market Research, *Global Sorbitol Market - Isosorbide, Propylene Glycol, Glycerol & Other Downstream Opportunities, Applications (Toothpaste, Vitamin C, Sweetener etc.), Size, Share, Growth, Trends and Forcast 2012-2018*, **2012**.
- [39] J. T. Power, *US2280975 A*, **1942**.
- [40] J. Zhang, J.-b. Li, S.-B. Wu, Y. Liu, *Ind. Eng. Chem. Res.* **2013**, 52, 11799-11815.
- [41] P. Gallezot, P. J. Cerino, B. Blanc, G. Flèche, P. Fuertes, *J. Catal.* **1994**, 146, 93-102.
- [42] B. Kusserow, S. Schimpf, P. Claus, *Adv. Synth. Catal.* **2003**, 345, 289-299.
- [43] S. Schimpf, C. Louis, P. Claus, *Appl. Catal., A* **2007**, 318, 45-53.
- [44] J. Zhang, S. Wu, Y. Liu, B. Li, *Catal. Commun.* **2013**, 35, 23-26.
- [45] B. W. Hoffer, E. Crezee, P. R. M. Mooijman, A. D. van Langeveld, F. Kapteijn, J. A. Moulijn, *Catal. Today* **2003**, 79-80, 35-41.
- [46] P. Gallezot, N. Nicolaus, G. Flèche, P. Fuertes, A. Perrard, *J. Catal.* **1998**, 180, 51-55.
- [47] H. Kobayashi, H. Yokoyama, B. Feng, A. Fukuoka, *Green Chem.* **2015**, 17, 2732-2735.
- [48] J. Xia, D. Yu, Y. Hu, B. Zou, P. Sun, H. Li, H. Huang, *Catal. Commun.* **2011**, 12, 544-547.
- [49] I. Ahmed, N. A. Khan, D. K. Mishra, J. S. Lee, J.-S. Hwang, S. H. Jung, *Chem. Eng. Sci.* **2013**, 93, 91-95.
- [50] A. Kamimura, K. Murata, Y. Tanaka, T. Okagawa, H. Matsumoto, K. Kaiso, M. Yoshimoto, *ChemSusChem* **2014**, 7, 3257-3259.
- [51] F. Aricò, P. Tundo, A. Maranzana, G. Tonachini, *ChemSusChem* **2012**, 5, 1578-1586.
- [52] W. C. Brinegar, M. Wohlers, M. A. Hubbard, E. G. Zey, G. Kvakovszky, T. H. Shockley, R. Roesky, U. Dingerdissen, W. Kind, **2003**.
- [53] K. M. Moore, A. J. Sanborn, P. Bloom, *US7439352B2*, **2008**.
- [54] J. Shi, Y. Shan, Y. Tian, Y. Wan, Y. Zheng, Y. Feng, *RSC Adv.* **2016**, 6, 13514-13521.
-

-
- [55] N. A. Khan, D. K. Mishra, I. Ahmed, J. W. Yoon, J.-S. Hwang, S. H. Jung, *Appl. Catal., A* **2013**, *452*, 34-38.
- [56] Z.-C. Tang, D.-H. Yu, P. Sun, H. Li, H. Huang, *Bull. Korean Chem. Soc.* **2010**, *31*, 3679-3683.
- [57] F. Aricò, S. Evaristo, P. Tundo, *Green Chem.* **2015**, *17*, 1176-1185.
- [58] A. Yamaguchi, N. Hiyoshi, O. Sato, M. Shirai, *Green Chem.* **2011**, *13*, 873-881.
- [59] R. Palkovits, K. Tajvidi, J. Procelewska, R. Rinaldi, A. Ruppert, *Green Chem.* **2010**, *12*, 972-978.
- [60] R. M. de Almeida, J. Li, C. Nederlof, P. O'Connor, M. Makkee, J. A. Moulijn, *ChemSusChem* **2010**, *3*, 325-328.
- [61] R. Palkovits, K. Tajvidi, A. M. Ruppert, J. Procelewska, *Chem. Commun.* **2011**, *47*, 576-578.
- [62] B. Op de Beeck, J. Geboers, S. Van de Vyver, J. Van Lishout, J. Snelders, W. J. J. Huijgen, C. M. Courtin, P. A. Jacobs, B. F. Sels, *ChemSusChem* **2013**, *6*, 199-208.
- [63] P. Sun, X. Long, H. He, C. Xia, F. Li, *ChemSusChem* **2013**, *6*, 2190-2197.
- [64] G. Liang, C. Wu, L. He, J. Ming, H. Cheng, L. Zhuo, F. Zhao, *Green Chem.* **2011**, *13*, 839-842.
- [65] H. W. Wisselink, R. A. Weusthuis, G. Eggink, J. Hugenholtz, G. J. Grobbs, *Int. Dairy J.* **2002**, *12*, 151-161.
- [66] S. H. Song, C. Vieille, *Appl. Microbiol. Biotechnol.* **2009**, *84*, 55-62.
- [67] L. M. Hanover, J. S. White, *Am. J. Clin. Nutr.* **1993**, *58*, 724S-732S.
- [68] C. Moreau, R. Durand, A. Roux, D. Tichit, *Appl. Catal., A* **2000**, *193*, 257-264.
- [69] Y. Román-Leshkov, M. Moliner, J. A. Labinger, M. E. Davis, *Angew. Chem. Int. Ed.* **2010**, *49*, 8954-8957.
- [70] J. Dijkmans, D. Gabriëls, M. Dusselier, F. de Clippel, P. Vanelderen, K. Houthoofd, A. Malfliet, Y. Pontikes, B. F. Sels, *Green Chem.* **2013**, *15*, 2777-2785.
- [71] L. Weisgerber, S. Palkovits, R. Palkovits, *Chem. Ing. Tech.* **2013**, *85*, 512-515.
- [72] I. Delidovich, R. Palkovits, *Catal. Sci. Technol.* **2014**, *4*, 4322-4329.
- [73] J. Le Nôtre, J. van Haveren, D. S. van Es, *ChemSusChem* **2013**, *6*, 693-700.
- [74] J. D. Brandner, L. W. Wright, *US3023223A*, **1962**.
- [75] E. Hagberg, K. Martin, J. Van Ee, J. Le Nôtre, D. S. Van Es, J. Van Haveren, **2013**.
- [76] J. Müller, H. Ulrich, *DE488602 (C)*, **1927**.
- [77] J. C. KRANTZ, C. J. CARR, S. E. FORMAN, F. W. ELLIS, *J. Pharmacol. Exp. Ther.* **1939**, *67*, 191-200.
- [78] U. Thadani, H.-L. Fung, A. C. Darke, J. O. Parker, M. J. Cruise, *Am. J. Cardiol.* **1982**, *49*, 411-419.
- [79] L. A. Luzzi, J. K. H. Ma, *US4228162A*, **1980**.
- [80] H. Zia, J. H. Ma, J. O'Donnell, L. Luzzi, *Pharm. Res.* **1991**, *8*, 502-504.
- [81] M. Durand, A. Mouret, V. Molinier, T. Féron, J.-M. Aubry, *Fuel* **2010**, *89*, 2729-2734.
- [82] M. Durand, Y. Zhu, V. Molinier, T. Féron, J.-M. Aubry, *J. Surfact. Deterg.* **2009**, *12*, 371-378.
-

-
- [83] A. Lavergne, Y. Zhu, A. Pizzino, V. Molinier, J.-M. Aubry, *J. Colloid Interface Sci.* **2011**, *360*, 645-653.
- [84] A. Behler, C. Breffa, H. C. Rath, T. Löhl, *US8546446B2*, **2013**.
- [85] C. Breffa, W. Poly, A. Behler, T. Löhl, *US8420588B2*, **2013**.
- [86] B. Deflort, S. Joly, T. Lacome, P. Gateau, F. Paille, *US6527816B2*, **2003**.
- [87] R. M. de Almeida, C. R. K. Rabello, *US20090538451A1*, **2010**.
- [88] A. Hirao, H. Mochizuki, S. Nakahama, N. Yamazaki, *J. Org. Chem.* **1979**, *44*, 1720-1722.
- [89] M. Kadraoui, T. Maunoury, Z. Derriche, S. Guilleme, C. Saluzzo, *Eur. J. Org. Chem.* **2015**, *2015*, 441-457.
- [90] A. Loupy, D. Monteux, *Tetrahedron Lett.* **1996**, *37*, 7023-7026.
- [91] A. Loupy, D. A. Monteux, *Tetrahedron* **2002**, *58*, 1541-1549.
- [92] J. Bakos, B. Heil, L. Markó, *J. Organomet. Chem.* **1983**, *253*, 249-252.
- [93] G. De Coster, K. Vandyck, E. Van der Eycken, J. Van der Eycken, M. Elseviers, H. Röper, *Tetrahedron: Asymmetry* **2002**, *13*, 1673-1679.
- [94] K.-D. Huynh, H. Ibrahim, E. Kolodziej, M. Toffano, G. Vo-Thanh, *New J. Chem.* **2011**, *35*, 2622-2631.
- [95] H. Ibrahim, C. Bournaud, R. Guillot, M. Toffano, G. Vo-Thanh, *Tetrahedron Lett.* **2012**, *53*, 4900-4902.
- [96] S. Kumar, U. Ramachandran, *Tetrahedron* **2005**, *61*, 4141-4148.
- [97] L.-Y. Chen, S. Guilleme, C. Saluzzo, *Arkivoc* **2013**, *3*, 227-244.
- [98] O. Nguyen Van Buu, A. Aupoix, N. D. T. Hong, G. Vo-Thanh, *New J. Chem.* **2009**, *33*, 2060-2072.
- [99] O. Nguyen Van Buu, A. Aupoix, G. Vo-Thanh, *Tetrahedron* **2009**, *65*, 2260-2265.
- [100] S. Shin, J. W. Seo, J. K. Cho, S. Kim, J. Cha, M. S. Gong, *Green Chem.* **2012**, *14*, 1163-1167.
- [101] J. Thiem, H. Lüders, *Starch/Stärke* **1984**, *36*, 170-176.
- [102] J. Thiem, H. Lüders, *Polym. Bull.* **1984**, *11*, 365-369.
- [103] J. Thiem, H. Lüders, *Macromol. Chem.* **1986**, *187*, 2775-2785.
- [104] D. Braun, M. Bergmann, *J. prakt. Chem.* **1992**, *334*, 298-310.
- [105] H. R. Kricheldorf, *J. Macromol. Sci., Rev. Macromol. Chem. Phys.* **1997**, *37*, 599-631.
- [106] J. Thiem, F. Bachmann, *Macromol. Chem.* **1991**, *192*, 2163-2182.
- [107] J. L. J. van Velthoven, L. Gootjes, B. A. J. Noordover, J. Meuldijk, *Eur. Polym. J.* **2015**, *66*, 57-66.
- [108] J. Wu, P. Eduard, S. Thiagarajan, L. Jasinska-Walc, A. Rozanski, C. F. Guerra, B. A. J. Noordover, J. van Haveren, D. S. van Es, C. E. Koning, *Macromolecules* **2012**, *45*, 5069-5080.
- [109] R. Storbeck, M. Ballauff, *J. Appl. Polym. Sci.* **1996**, *59*, 1199-1202.
- [110] J. C. Bersot, N. Jacquelin, R. Saint-Loup, P. Fuertes, A. Rousseau, J. P. Pascault, R. Spitz, F. Fenouillot, V. Monteil, *Macromol. Chem. Phys.* **2011**, *212*, 2114-2120.
- [111] H. R. Kricheldorf, S. M. Weidner, *Macromol. Chem. Phys.* **2013**, *214*, 726-733.
-

-
- [112] D. Juais, A. F. Naves, C. Li, R. A. Gross, L. H. Catalani, *Macromolecules* **2010**, *43*, 10315-10319.
- [113] A. F. Naves, H. T. C. Fernandes, A. P. S. Immich, L. H. Catalani, *J. Polym. Sci., Part A: Polym. Chem.* **2013**, *51*, 3881-3891.
- [114] E. C. Varkey, K. Sreekumar, *J. Mater. Sci.* **2010**, *45*, 1912-1920.
- [115] R. Marín, A. Alla, A. Martínez de Ilarduya, S. Muñoz-Guerra, *J. Appl. Polym. Sci.* **2012**, *123*, 986-994.
- [116] H.-s. Park, M.-S. Gong, J. Knowles, *J. Mater. Sci.: Mater. Med.* **2013**, *24*, 281-294.
- [117] M. Charlon, B. Heinrich, Y. Matter, E. Couzigné, B. Donnio, L. Avérous, *Eur. Polym. J.* **2014**, *61*, 197-205.
- [118] H.-J. Kim, M.-S. Kang, J. C. Knowles, M.-S. Gong, *J. Biomater. Appl.* **2014**, *29*, 454-464.
- [119] M. D. Zenner, Y. Xia, J. S. Chen, M. R. Kessler, *ChemSusChem* **2013**, *6*, 1182-1185.
- [120] L. Jasinska, M. Villani, J. Wu, D. van Es, E. Klop, S. Rastogi, C. E. Koning, *Macromolecules* **2011**, *44*, 3458-3466.
- [121] L. Jasinska-Walc, D. Dudenko, A. Rozanski, S. Thiyagarajan, P. Sowinski, D. van Es, J. Shu, M. R. Hansen, C. E. Koning, *Macromolecules* **2012**, *45*, 5653-5666.
- [122] L. Jasinska-Walc, M. Villani, D. Dudenko, O. van Asselen, E. Klop, S. Rastogi, M. R. Hansen, C. E. Koning, *Macromolecules* **2012**, *45*, 2796-2808.
- [123] B. S. Rajput, S. R. Gaikwad, S. K. Menon, S. H. Chikkali, *Green Chem.* **2014**, *16*, 3810-3818.
- [124] J. J. Gallagher, M. A. Hillmyer, T. M. Reineke, *ACS Sustainable Chem. Eng.* **2015**, *3*, 662-667.
- [125] S. A. Lawrence, *Amines: Synthesis, Properties and Application*, Cambridge University Press, Cambridge, **2004**.
- [126] M. Fischer, *Kunststoffe* **2004**, *10*, 90-95.
- [127] J. I. van der Vlugt, *Chem. Soc. Rev.* **2010**, *39*, 2302-2322.
- [128] O. Mitsunobu, M. Wada, T. Sano, *J. Am. Chem. Soc.* **1972**, *94*, 679-680.
- [129] S. Bähn, S. Imm, L. Neubert, M. Zhang, H. Neumann, M. Beller, *ChemCatChem* **2011**, *3*, 1853-1864.
- [130] K. S. Hayes, *Appl. Catal., A* **2001**, *221*, 187-195.
- [131] M. Pera-Titus, F. Shi, *ChemSusChem* **2014**, *7*, 720-722.
- [132] C. Gunanathan, D. Milstein, *Angew. Chem. Int. Ed.* **2008**, *47*, 8661-8664.
- [133] S. Imm, S. Bähn, L. Neubert, H. Neumann, M. Beller, *Angew. Chem. Int. Ed.* **2010**, *49*, 8126-8129.
- [134] D. Pingen, C. Müller, D. Vogt, *Angew. Chem. Int. Ed.* **2010**, *49*, 8130-8133.
- [135] K. Das, R. Shibuya, Y. Nakahara, N. Germain, T. Ohshima, K. Mashima, *Angew. Chem.* **2012**, *124*, 154-158.
- [136] X. Cui, X. Dai, Y. Deng, F. Shi, *Chem. Eur. J.* **2013**, *19*, 3665-3675.
- [137] K.-i. Shimizu, K. Kon, W. Onodera, H. Yamazaki, J. N. Kondo, *ACS Catal.* **2013**, *3*, 112-117.
- [138] M. H. S. A. Hamid, P. A. Slatford, J. M. J. Williams, *Adv. Synth. Catal.* **2007**, *349*, 1555-1575.
-

-
- [139] K.-i. Shimizu, *Catal. Sci. Technol.* **2015**, 10.1039/C4CY01170H.
- [140] E. J. Derrah, M. Hanauer, P. N. Plessow, M. Schelwies, M. K. da Silva, T. Schaub, *Organometallics* **2015**, 34, 1872-1881.
- [141] F. Klasovsky, J. C. Pfeffer, T. Tacke, T. Haas, M. Beller, A. Koeckritz, J. Deutsch, A. Martin, S. Imm, *US2013/0245276A1*, **2013**.
- [142] R. Kawahara, K.-i. Fujita, R. Yamaguchi, *J. Am. Chem. Soc.* **2010**, 132, 15108-15111.
- [143] H. Ohta, Y. Yuyama, Y. Uozumi, Y. M. A. Yamada, *Org. Lett.* **2011**, 13, 3892-3895.
- [144] F. G. Mutti, T. Knaus, N. S. Scrutton, M. Breuer, N. J. Turner, *Science* **2015**, 349, 1525-1529.
- [145] F. F. Chen, Y. Y. Liu, G. W. Zheng, J. H. Xu, *ChemCatChem* **2015**, 7, 3838-3841.
- [146] S. Klatte, V. F. Wendisch, *Biorg. Med. Chem.* **2014**, 22, 5578-5585.
- [147] K.-i. Shimizu, S. Kanno, K. Kon, S. M. A. Hakim Siddiki, H. Tanaka, Y. Sakata, *Catal. Today* **2014**, 232, 134-138.
- [148] T. Takanashi, Y. Nakagawa, K. Tomishige, *Chem. Lett.* **2014**, 43, 822-824.
- [149] R. Montgomery, L. F. Wiggins, *J. Chem. Soc.* **1946**, 393-396.
- [150] J. Kuszmann, G. Medgyes, *Carbohydr. Res.* **1980**, 85, 259-269.
- [151] T. G. Archibald, K. Baum, *Synth. Commun.* **1989**, 19, 1493-1498.
- [152] S. Thiyagarajan, L. Gootjes, W. Vogelzang, J. Wu, J. van Haveren, D. S. van Es, *Tetrahedron* **2011**, 67, 383-389.
- [153] S. Thiyagarajan, L. Gootjes, W. Vogelzang, J. van Haveren, M. Lutz, D. S. van Es, *ChemSusChem* **2011**, 4, 1823-1829.
- [154] G. Streukens, C. Lettmann, S. Schneider, *US2013/0116451A1*, **2013**.
- [155] U. Dingerdissen, J. Pfeffer, T. Tacke, T. Haas, H. Schmidt, M. Volland, M. Rimbach, C. Lettmann, R. Sheldon, M. Janssen, *US8378127B2*, **2013**.
- [156] J. Gross, K. Tauber, M. Fuchs, N. G. Schmidt, A. Rajagopalan, K. Faber, W. M. F. Fabian, J. Pfeffer, T. Haas, W. Kroutil, *Green Chem.* **2014**, 16, 2117-2121.
- [157] F. Klasovsky, J. C. Pfeffer, T. Tacke, T. Haas, A. Martin, J. Deutsch, A. Koeckritz, *US2013/0165672A1*, **2013**.
- [158] M. Schelwies, M. Brinks, T. Schaub, J. P. Melder, R. Paciello, M. Merger, *US2014/0024833A1*, **2014**.
- [159] A. Lerchner, S. Achatz, C. Rausch, T. Haas, A. Skerra, *ChemCatChem* **2013**, 5, 3374-3383.
- [160] R. Pfützenreuter, M. Rose, *ChemCatChem* **2016**, 8, 251-255.
- [161] W. R. H. Wright, R. Palkovits, *ChemSusChem* **2012**, 5, 1657-1667.
- [162] P. Mäki-Arvela, I. L. Simakova, T. Salmi, D. Y. Murzin, *Chem. Rev.* **2014**, 114, 1909-1971.
- [163] C. Michel, P. Gallezot, *ACS Catal.* **2015**, 5, 4130-4132.
- [164] M. Besson, P. Gallezot, C. Pinel, *Chem. Rev.* **2013**, 114, 1827-1870.
- [165] C. Weidenthaler, *Nanoscale* **2011**, 3, 792-810.
- [166] S. Lowell, J. E. Shields, M. A. Thomas, M. Thommes, *Characterization of Porous Solids and Powders: Surface Area, Pore Size and Density*, Springer Science+Business Media, New York, **2004**.
-

-
- [167] C. Detoni, C. H. Gierlich, M. Rose, R. Palkovits, *ACS Sustainable Chem. Eng.* **2014**, *2*, 2407-2415.
- [168] K. Schute, Y. Louven, C. Detoni, M. Rose, *Chem. Ing. Tech.* **2016**, *88*, 355-362.
- [169] M. W. Schmidt, K. K. Baldrige, J. A. Boatz, S. T. Elbert, M. S. Gordon, J. H. Jensen, S. Koseki, N. Matsunaga, K. A. Nguyen, S. Su, T. L. Windus, M. Dupuis, J. A. Montgomery, *J. Comput. Chem.* **1993**, *14*, 1347-1363.
- [170] C. Lee, W. Yang, R. G. Parr, *Phys. Rev. B* **1988**, *37*, 785.
- [171] A. D. Becke, *J. Chem. Phys.* **1993**, *98*, 5648-5652.
- [172] R. Ditchfield, W. J. Hehre, J. A. Pople, *J. Chem. Phys.* **1971**, *54*, 724-728.
- [173] W. J. Hehre, R. Ditchfield, J. A. Pople, *J. Chem. Phys.* **1972**, *56*, 2257-2261.
- [174] H. Sajiki, T. Kurita, H. Esaki, F. Aoki, T. Maegawa, K. Hirota, *Org. Lett.* **2004**, *6*, 3521-3523.
- [175] T. Kurita, F. Aoki, T. Mizumoto, T. Maejima, H. Esaki, T. Maegawa, Y. Monguchi, H. Sajiki, *Chem. Eur. J.* **2008**, *14*, 3371-3379.
- [176] Y. Sawama, Y. Monguchi, H. Sajiki, *Synlett* **2012**, *23*, 959-972.
- [177] H. Esaki, F. Aoki, M. Umemura, M. Kato, T. Maegawa, Y. Monguchi, H. Sajiki, *Chem. Eur. J.* **2007**, *13*, 4052-4063.
- [178] T. Maegawa, Y. Fujiwara, Y. Inagaki, H. Esaki, Y. Monguchi, H. Sajiki, *Angew. Chem. Int. Ed.* **2008**, *47*, 5394-5397.
- [179] Y. Fujiwara, H. Iwata, Y. Sawama, Y. Monguchi, H. Sajiki, *Chem. Commun.* **2010**, *46*, 4977-4979.
- [180] T. Maegawa, Y. Fujiwara, Y. Inagaki, Y. Monguchi, H. Sajiki, *Adv. Synth. Catal.* **2008**, *350*, 2215-2218.
- [181] Y. Sawama, Y. Yabe, H. Iwata, Y. Fujiwara, Y. Monguchi, H. Sajiki, *Chem. Eur. J.* **2012**, *18*, 16436-16442.
- [182] J. Haber, in *Handbook of Heterogeneous Catalysis*, 2 ed. (Eds.: G. Ertl, H. Knözinger, F. Schüth, J. Weitkamp), Wiley-VCH, Weinheim, **2008**.
- [183] G. Fleche, P. Fuertes, R. Tamion, H. Wyart, *US7122661B2*, **2006**.
- [184] L. Mentink, J. Bernaerts, *US2008/0191164A1*, **2008**.
- [185] P. Fuertes, H. Wyart, *US8609872B2*, **2013**.
- [186] M. Hesse, H. Meier, B. Zeeh, *Spektroskopische Methoden in der organischen Chemie*, 7 ed., Thieme, Stuttgart, New York, **2005**.
- [187] P. W. Atkins, J. de Paula, *Physikalische Chemie*, 4 ed., Wiley-VCH, Weinheim, **2006**.
- [188] L. Negahdar, J. U. Oltmanns, S. Palkovits, R. Palkovits, *Appl. Catal., B* **2014**, *147*, 677-683.
- [189] M. Baerns, A. Behr, A. Brehm, J. Gmehling, H. Hofmann, U. Onken, A. Renken, *Technische Chemie*, Wiley-VCH, Weinheim, **2006**.
- [190] G. H. Vogel, *Lehrbuch Chemische Technologie*, Wiley-VCH, Weinheim, **2004**.
- [191] L. Negahdar, *Kinetic investigation of the hydrolytic hydrogenation of oligosaccharides to sorbitol*, Dissertation, RWTH Aachen, **2014**.
- [192] Taylor & Francis Group, *Handbook of Chemistry and Physics*, **2014**.
- [193] <https://www.python.org>,
- [194] J. A. Nelder, R. Mead, *Comput. J.* **1965**, *7*, 308-313.
-

- [195] R. Storn, K. Price, *J. Global Optim.* **1997**, *11*, 341-359.

7 Abbreviations and Formula Symbols

7.1 List of Abbreviations

AMI	Acetylated methacrylic isosorbide
APT	Attached proton test
aq.	aqueous
BET	Brunauer, Emmet, Teller
CI	Chemical ionisation
DABCO	1,4-diazabicyclo[2.2.2]octane
DBTDL	Dibutyltin dilaurate
DBU	1,8-diazabicyclo[5.4.0]undec-7-ene
DEAD	Diethyl azodicarboxylate
DF	Dark field
DFT	Density functional theory
DMC	Dimethyl carbonate
DMI	Dimethyl isosorbide
DSC	Differential scanning calorimetry
EI	Electron ionisation
eq.	equivalent
FID	Flame ionisation detector
GC	Gas chromatography
HAT	Hydrogen autotransfer
5-HMF	5-Hydroxymethylfurfural
HPA	Heteropoly acid
HPLC	High-performance liquid chromatography
ICP-OES	Inductively coupled plasma atomic emission spectroscopy
IG	Isogalactide
II	Isoidide
IM	Isomannide
IS	Isosorbide

NMR	Nuclear magnetic resonance
NOESY	Nuclear Overhauser effect spectroscopy
NP	Nanoparticles
MS	Mass spectrometry
nBA	<i>n</i> -butyl acrylate
ODE	Ordinary differential equation
OPEX	Operating expense
PET	Poly(ethylene terephthalate)
PEIT	Poly(ethylene-co-isosorbide terephthalate)
PIT	Poly(isosorbide terephthalate)
ppm	Parts per million
RAFT	Reverse addition-fragmentation chain transfer
RI	Refractive index
rpm	Rounds per minutes
RT	Room temperature
STEM	Scanning transmission electron microscopy
TEM	Transmission electron microscopy
TEMPO	(2,2,6,6-Tetramethylpiperidin-1-yl)oxyl
TGA	Thermogravimetric analysis
TMS	Trimethylsilyl
XRD	X-ray diffraction

7.2 List of Formula Symbols

A	Pre-exponential factor
c_i	Concentration of the compound i
c_s	Concentration of the substrate on the catalyst surface
D	Diffusion coefficient
D_{eff}	Effective diffusion coefficient
E_A	Activation energy
k	Rate constants
$K_{ads,i}$	Ratio of the adsorption and desorption rate constants of substrate i
K	Equilibrium constant
L_{Ch}	Characteristic length
m	Mass
n_i	Amount of substance of the substrate i
n_j	Amount of substance of the product j
p	Pressure
q_e	Adsorbed amount of substance at the equilibrium
r	Reaction rate
r_{eff}	Effective reaction rate
R	Ideal gas constant
t	Time
T	Temperature
X	Conversion
Y	Yield
ε	Porosity
θ_i	Amount of occupied sites by compound i
τ	Tortuosity
ψ	Weisz modulus

8 Curriculum Vitae

Personal Data

Name: Rebecca Veronika Engel
Maiden Name: Pfützenreuter
Date of Birth: 23 July, 1988
Place of Birth: Leinefelde, Germany

Academic Career

08/2014 – 11/2014 Research stay at the Institute of Inorganic Nanochemistry and Catalysis (Prof. Dr. Pascal Dietzel) at Bergen University, Norway
10/2012 – 06/2016 Doctoral studies at the chair for Heterogeneous Catalysis and Chemical Technology at RWTH Aachen University (Prof. Dr. Regina Palkovits)
Topic: „Heterogeneously Catalysed Amination and Isomerisation of Isohexides“
03/2012 – 09/2012 Master thesis at the chair of Nanostructured Catalysts at RWTH Aachen University (Prof. Dr. Regina Palkovits)
Topic: „Process Development for the Continuous Etherification of Sugar Alcohols“
10/2010 – 09/2012 Chemistry studies at RWTH Aachen University (M.Sc.)
10/2007 – 07/2010 Chemistry studies at RWTH Aachen University (B.Sc.)

Awards and Scholarships

2013 DECHEMA-Student Award 2013 (for efficient academic studies with excellent results)
2015 Conference Visit Scholarship for participation at NAM24 in Pittsburgh/PA, USA by ACalNet, a thematic network of the DAAD

Publications and Patents

Aqueous Phase Amination of Biogenic Isohexides using Ru/C as Solid Catalyst,

R. Pfützenreuter, M. Rose*

ChemCatChem, **2016**, 8, 251-255.

Alternative monomers based on lignocellulose and their use for polymer production,

I. Delidovich, P. J. C. Hausoul, L. Deng, R. Pfützenreuter, M. Rose, R. Palkovits*

Chem. Rev., **2016**, 116, 1540-1599.

Deoxygenation and cracking of free fatty acids over acidic catalysts by single step conversion for the production of diesel fuel and fuel blends.,

K. Hengst, M. Arend, R. Pfützenreuter, W. F. Hölderich*

Appl. Catal. B – Environ. **2015**, 174-175, 383-394.

Process for the Synthesis of Primary Isohexide Amines,
R. Palkovits, R. Pfützenreuter, A. Haji Begli, C. Kröner, M. Rose
Patent **2014**, PCT/EP2014/065556.

Reaction Network Analysis and Continuous Production of Isosorbide tert-Butyl Ethers,
R. Pfützenreuter, M. Helmin, S. Palkovits, R. Palkovits, M. Rose*
Catal. Today **2014**, 234, 113-118.

Heterogeneously catalysed production of isosorbide tert-butyl ethers,
M. Rose,* K. Thenert, R. Pfützenreuter, R. Palkovits*
Catal. Sci. Tech. **2013**, 3, 938-941.

Conference Contributions

- | | |
|---------------|--|
| Presentations | <p><i>Heterogeneously catalyzed aqueous phase amination and isomerisation of isohexides</i>
R. Pfützenreuter, M. Rose
Green & Sustainable Chemistry Conference, Berlin, Germany, 2016.</p> <p><i>Tailored Isohexide Monomers by Catalytic Isomerisation & Amination</i>
R. Pfützenreuter, M. Rose
23rd Meeting of the Bio-Environmental Polymer Society, Karlsruhe, Germany, 2015.</p> <p><i>Heterogeneously Catalyzed Amination and Isomerization of Isohexides</i>
R. Pfützenreuter, M. Rose
NAM24, Pittsburgh, PA, USA, 2015.</p> <p><i>Biogenic isosorbide tert-butyl ethers (ITBE) – Continuous production and reaction kinetics</i>
R. Pfützenreuter, M. Rose, R. Palkovits
Biorefinery for Food & Fuel & Materials, Wageningen, Netherlands, 2013.</p> |
| Posters | <p><i>The isomerisation of isohexides: Investigation of the reaction mechanism by isotope labelling and kinetic modelling</i>
R. Pfützenreuter, M. Rose
49. Jahrestreffen Deutscher Katalytiker, Weimar, Germany, 2016.</p> <p><i>Heterogeneously catalysed isomerisation and amination of biogenic isohexides</i>
R. Pfützenreuter, A. Fink, R. Palkovits, M. Rose
Neujahrssymposium, Aachen, Germany, 2015.</p> |

Process development for the production of biogenic ethers

R. Pfützenreuter, M. Rose, R. Palkovits

Jahrestreffen Reaktionstechnik, Würzburg, Germany, 2014.

Investigating the heterogeneously catalyzed isomerization and amination of isosorbide using the “borrowing hydrogen” method

R. Pfützenreuter, R. Palkovits M. Rose

47. Jahrestreffen Deutscher Katalytiker, Weimar, Germany, 2014.

Isosorbide tert-butyl ethers (ITBE) - Reaction kinetics and continuous production

R. Pfützenreuter, M. Rose, R. Palkovits

XIV. Netherlands' Catalysis and Chemistry Conference,
Noordwijkerhout, Netherlands, 2013.

Biogenic isosorbide tert-butyl ethers (ITBE) - Reaction kinetics and continuous production

R. Pfützenreuter, M. Rose, R. Palkovits

2nd International Symposium on Chemistry for Energy Conversion
and Storage, Berlin, Germany, 2013.

Isosorbide etherification for the production of biogenic fuel additives and high boiling solvents

R. Pfützenreuter, K. Thenert, M. Rose, R. Palkovits

Cat4Bio Conference, Thessaloniki, Greece, 2012.

9 Appendix

Table A 1. Overview over the catalysts' specific surface area, metal loading, resulting yields, and normalised yields per amount of metal loading.

Catalyst	Aldrich	SX 1G	ROX 0.8	RX3 Extra	A Supra EUR
S_{BET} (m² g⁻¹)	696	714	835	1108	1675
Y_{Total} (%)	38	51	46	51	48
Metal Loading (wt.-%)*	4.1	4.6	4.4	5.1	5.3
Y_{Total}/Metal Loading (%/wt.-%)	9.3	11.1	10.5	10.0	9.1

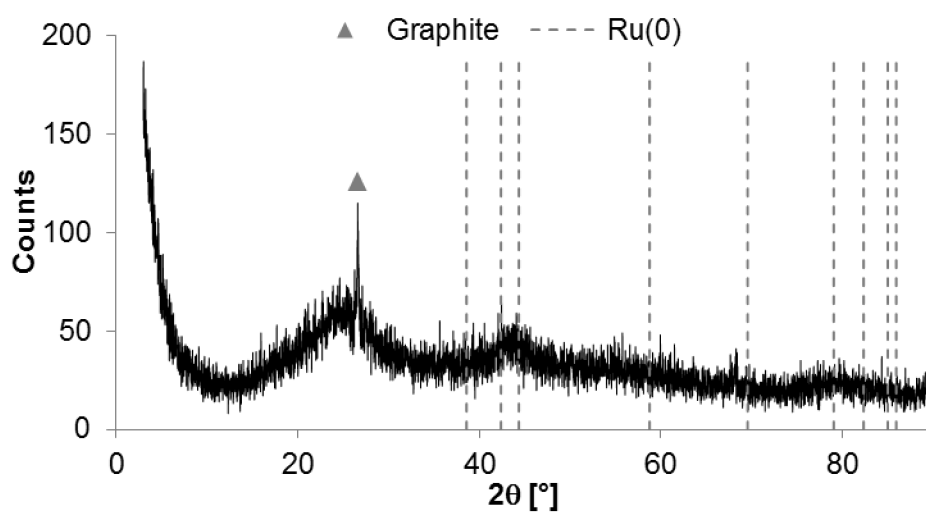


Figure A 1. XRD diffraction pattern of the commercial 5 wt.-% Ru/C catalyst.

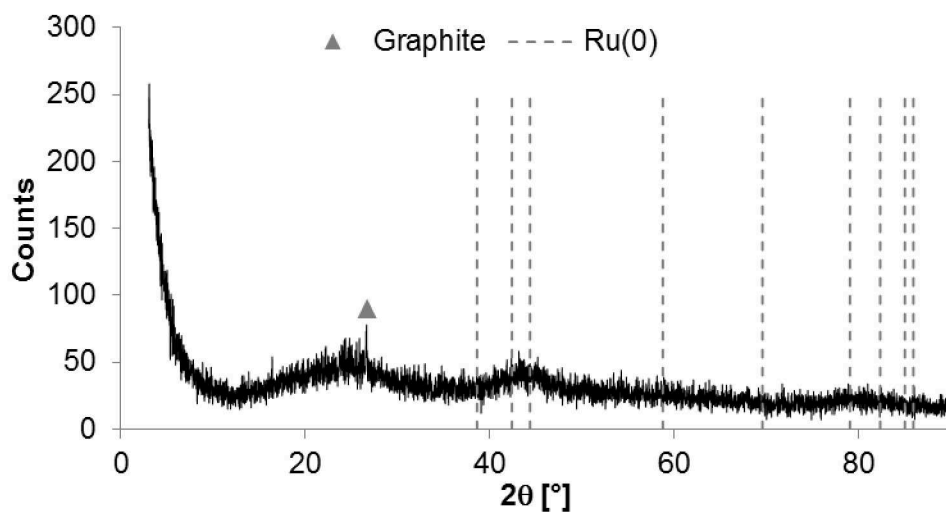


Figure A 2. XRD diffraction pattern of the 5 wt.-% Ru/C catalyst with A Supra EUR as support material, 10 K min^{-1} heating rate, and 350°C reduction temperature.

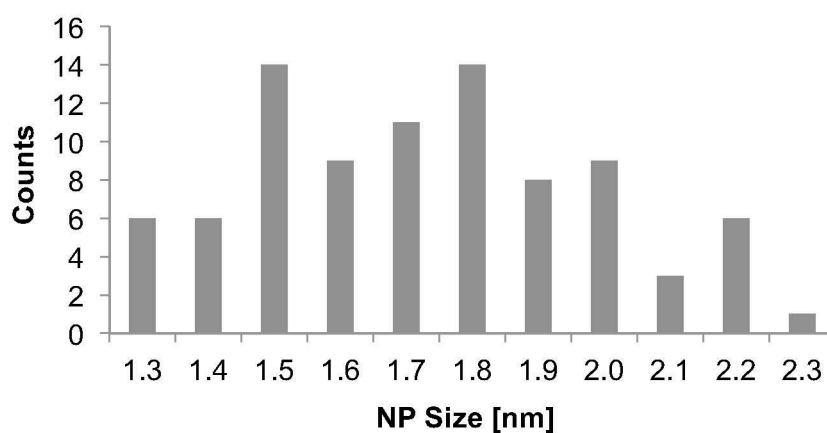
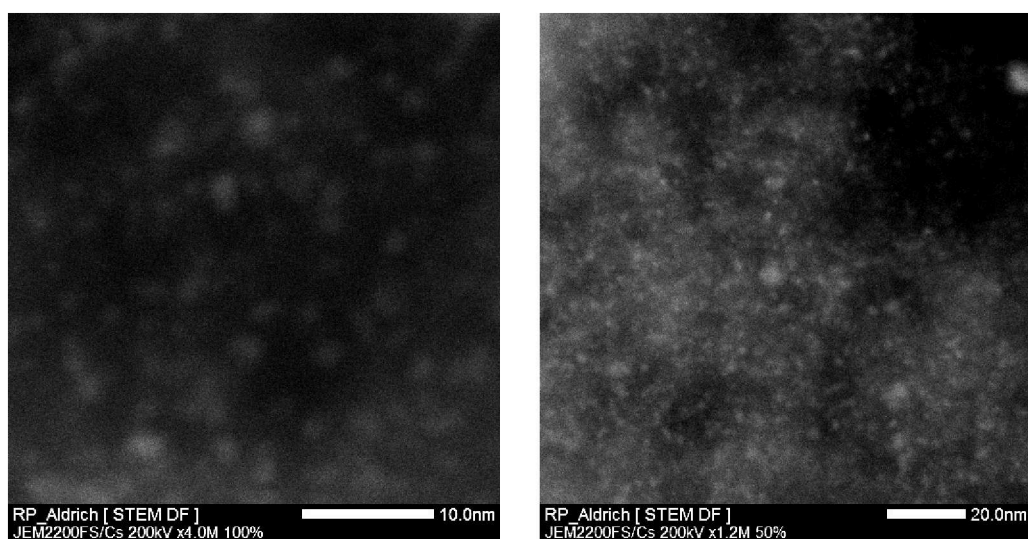


Figure A 3. STEM DF pictures and the Ru NP size distribution of the commercial Ru/C catalyst.

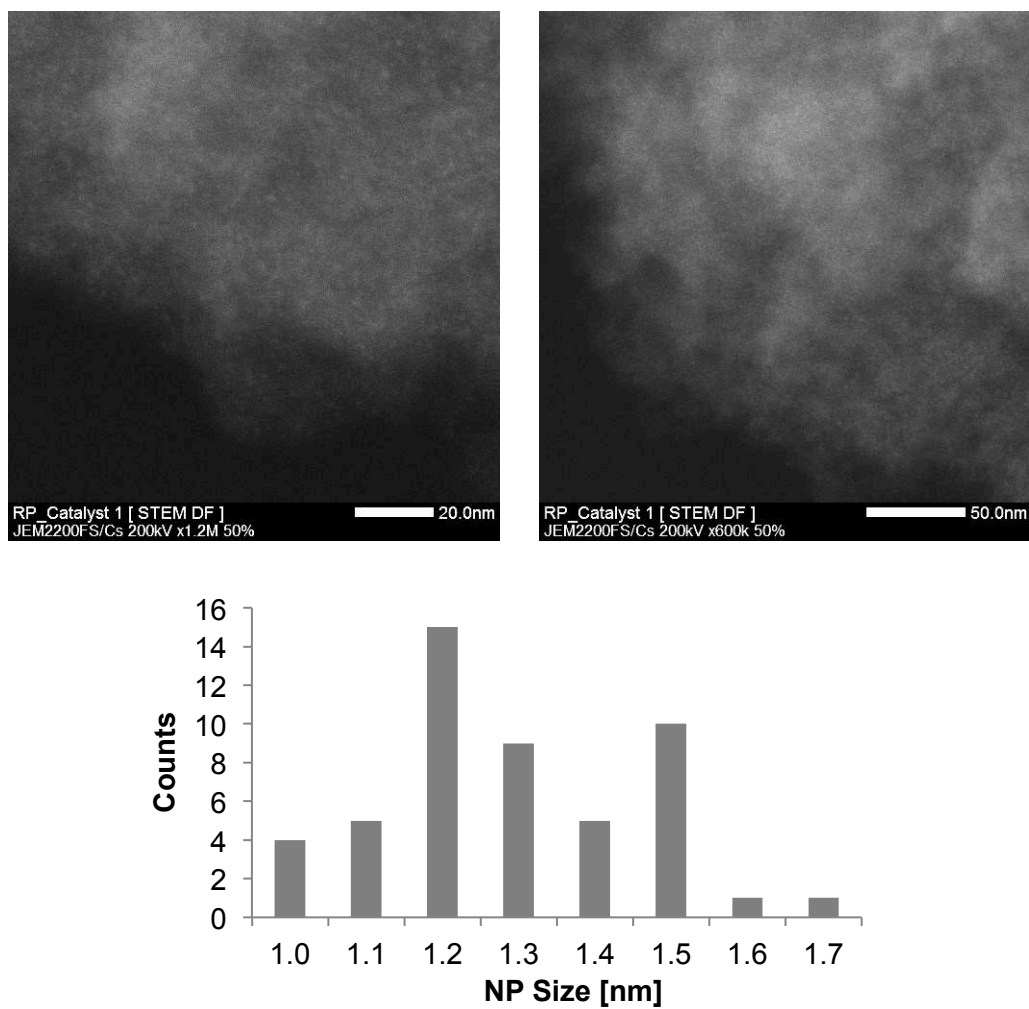


Figure A 4. STEM DF pictures and Ru NP size distribution of catalyst 1 (A Supra EUR, 10 K min⁻¹ heating rate, and 300 °C reduction temperature).

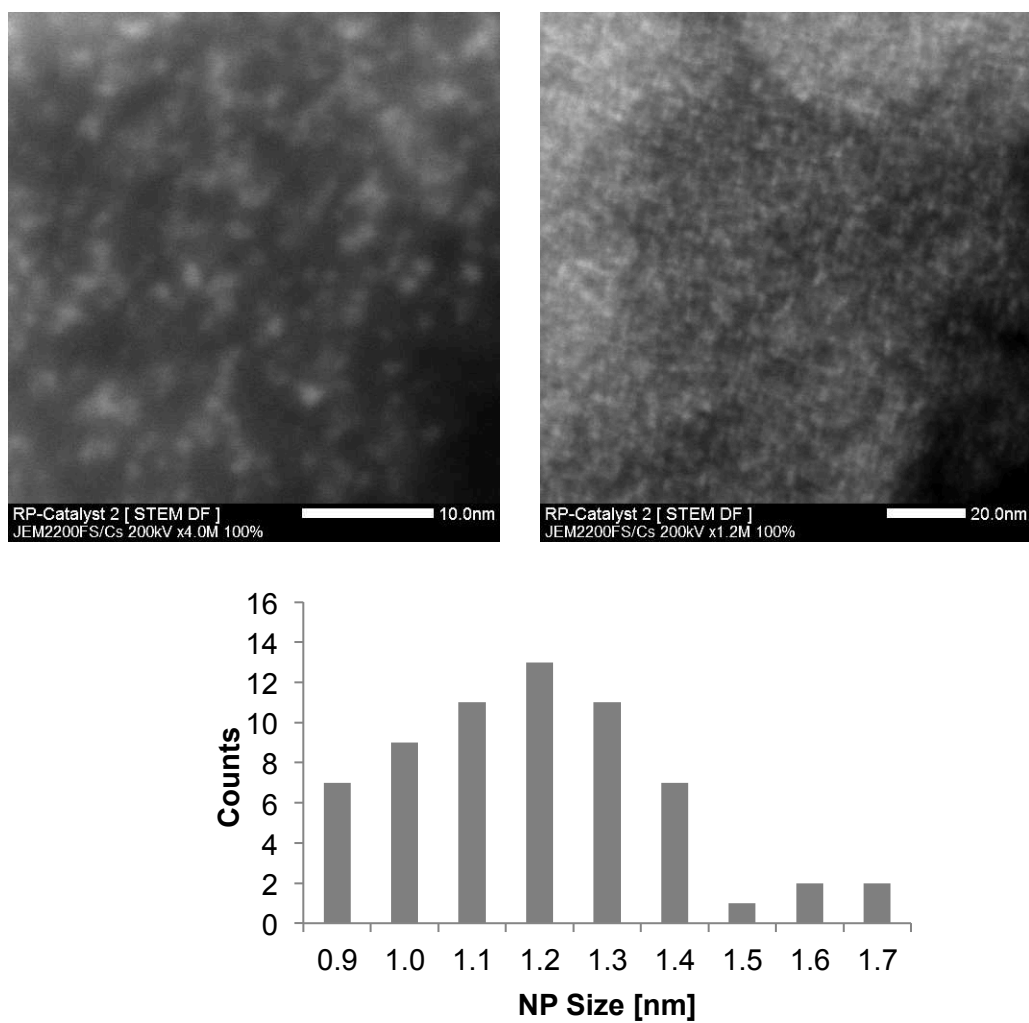


Figure A 5. STEM DF pictures and Ru NP size distribution of catalyst 2 (A Supra EUR, 10 K min⁻¹ heating rate, and 350 °C reduction temperature).

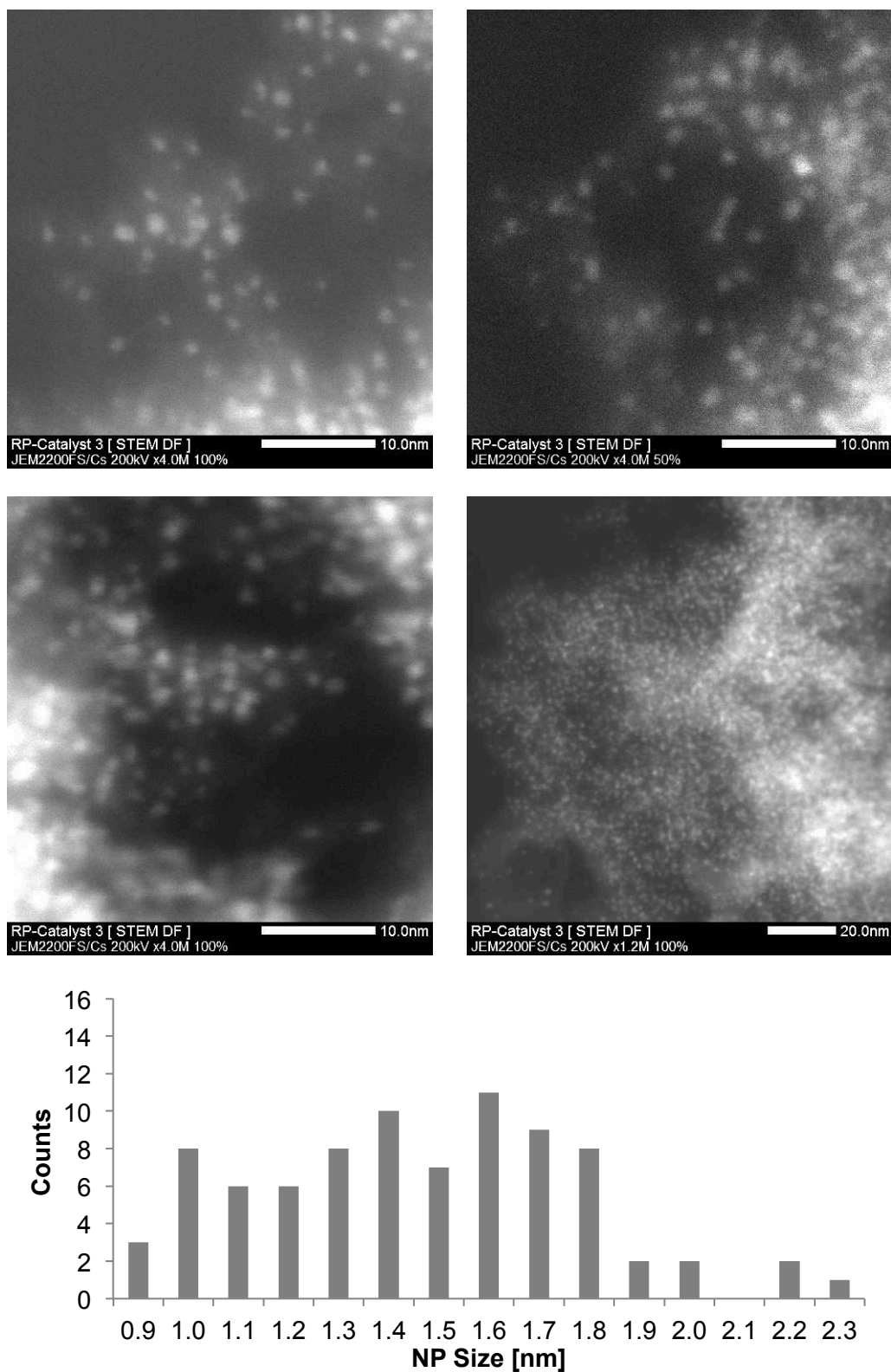


Figure A 6. STEM DF pictures and Ru NP size distribution of catalyst 3 (A Supra EUR, 10 K min⁻¹ heating rate, and 400 °C reduction temperature).

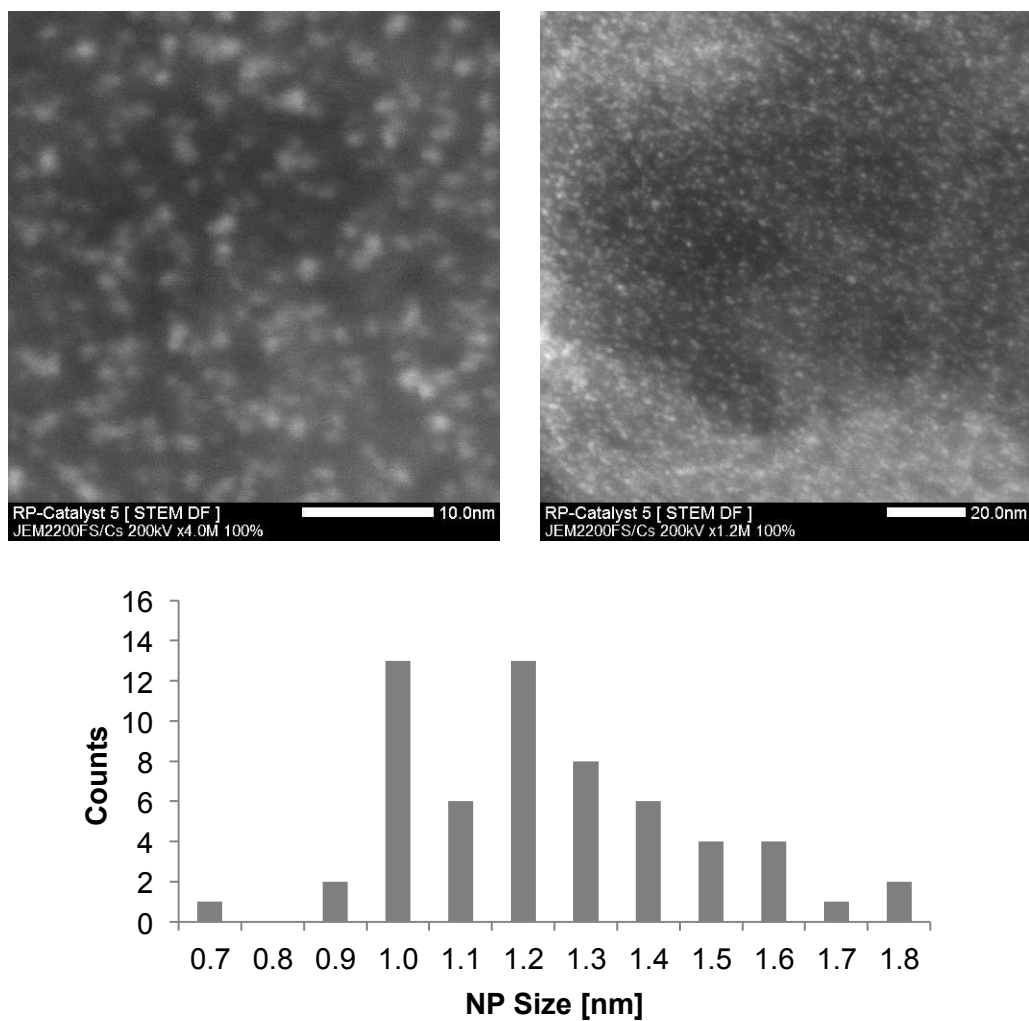


Figure A 7. STEM DF pictures and Ru NP size distribution of catalyst 5 (A Supra EUR, 5 K min⁻¹ heating rate, and 350 °C reduction temperature).

Table A 2. Yields of the isohexide isomers at reaction temperature and after the isomerisation at RT.

Substrate / Temperature		Y (II) [%]	Y (IS) [%]	Y (IM) [%]	ΣY [%]
IS / 160 °C (120 min)	at reaction temp.	46.8	38.6	5.4	90.8
	at RT	50.2	23.9	5.2	79.3
IS / 160 °C (165 min)	at reaction temp.	47.2	32.7	5.8	85.7
	at RT	46.7	21.4	5.7	73.8
IS / 150 °C (300 min)	at reaction temp.	51.6	33.8	4.1	89.5
	at RT	53.7	23.3	2.5	79.5
IS / 140 °C (540 min)	at reaction temp.	50.2	31.8	5.9	87.9
	at RT	48.0	22.2	5.8	76.0
IS / 140 °C (540 min)	at reaction temp.	47.2	30.0	5.6	82.8
	at RT	33.8	15.6	4.3	53.7
IM / 160 °C (165 min)	at reaction temp.	43.8	30.4	9.7	83.9
	at RT	42.1	19.2	6.1	67.4
IM / 150 °C (300 min)	at reaction temp.	30.5	40.8	25.4	96.7
	at RT	52.0	26.5	4.3	82.8
IM / 150 °C (390 min)	at reaction temp.	42.3	23.4	6.0	71.7
	at RT	47.4	25.0	5.2	77.6
IM / 140 °C (540 min)	at reaction temp.	44.8	31.3	6.6	82.7
	at RT	48.0	22.4	2.7	73.1
IM / 140 °C (540 min)	at reaction temp.	44.5	29.6	6.2	80.3
	at RT	48.3	23.5	3.7	75.5

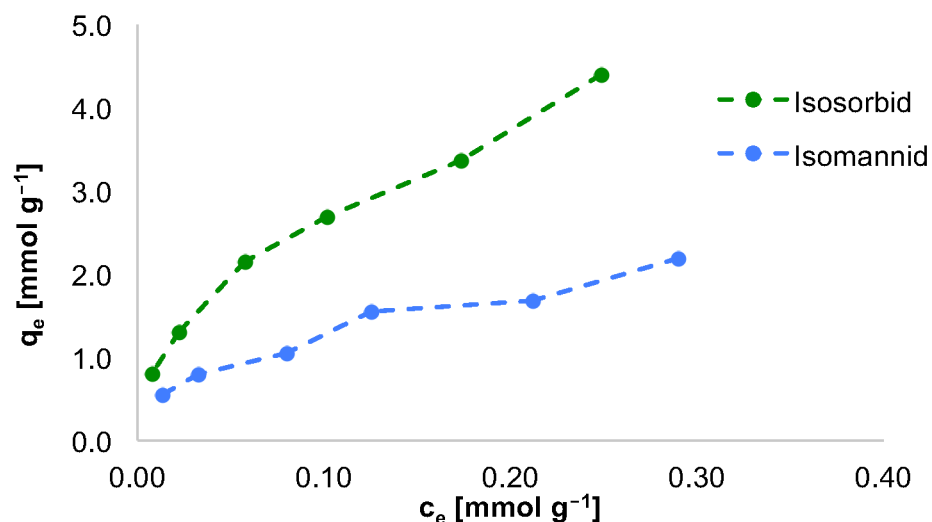


Figure A 8. Liquid phase adsorption data of an equimolar solution of isosorbide and isomannide in water using activated carbon (A Supra EUR) as adsorbent at 20 °C.

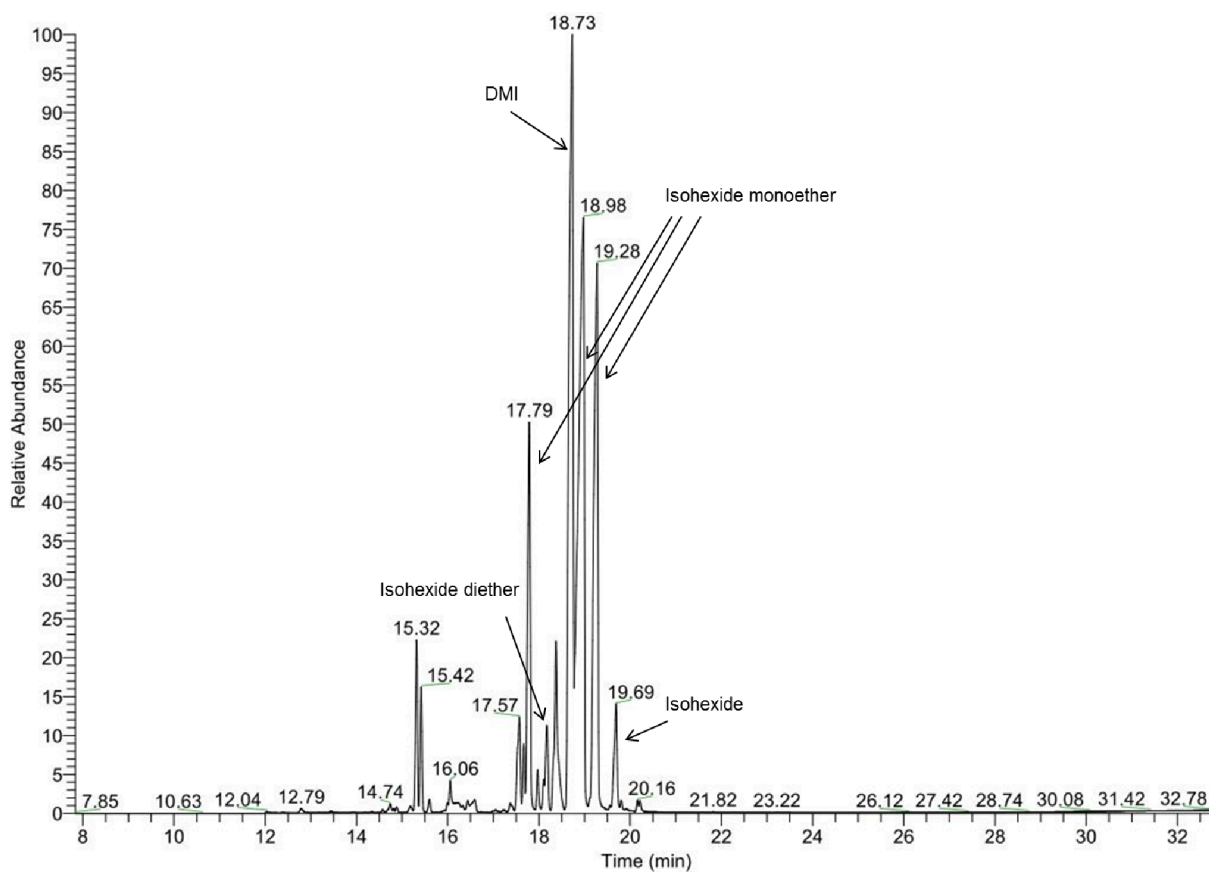


Figure A 9. Chromatogram of the GC-MS measurement of the product solution of the isomerisation of DMI.

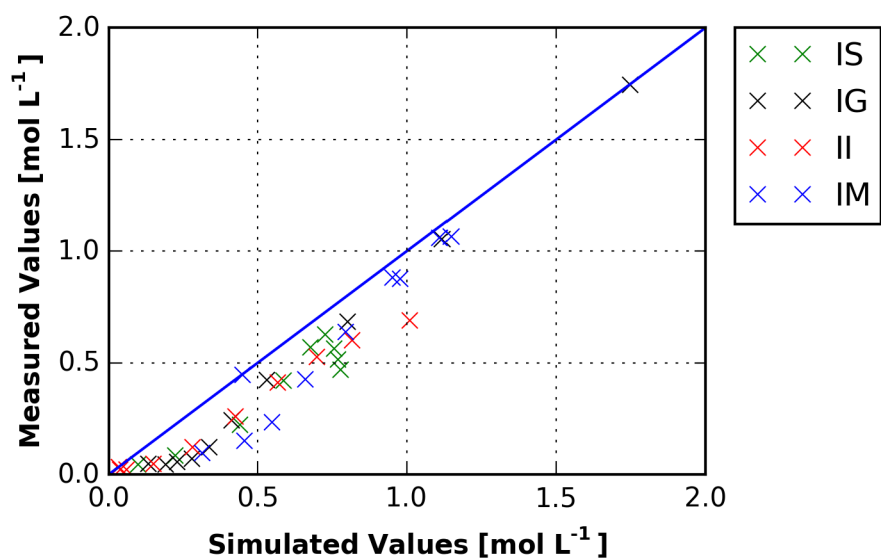


Figure A 10. Parity plot of the kinetic model for the isomannide isomerisation data at 140 °C.

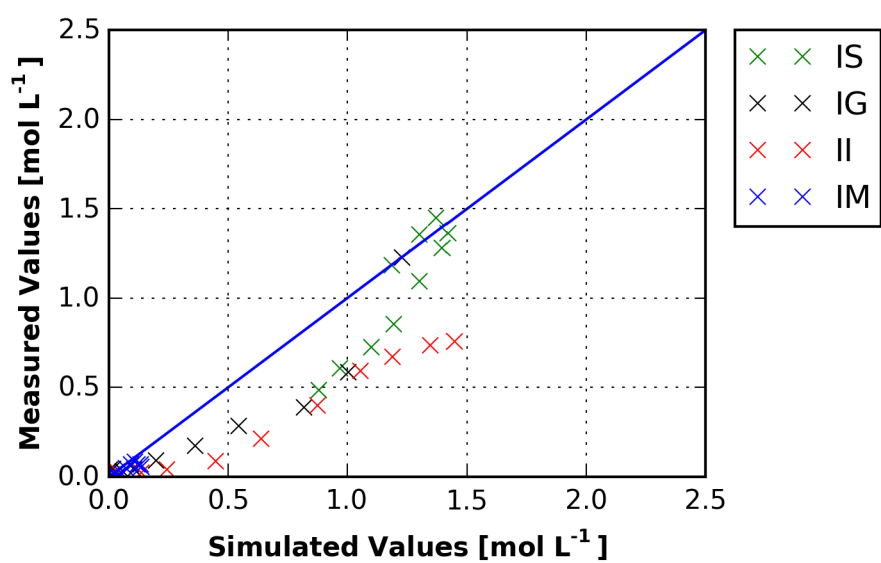


Figure A 11. Parity plot of the kinetic model for the isosorbide isomerisation data at 150 °C.

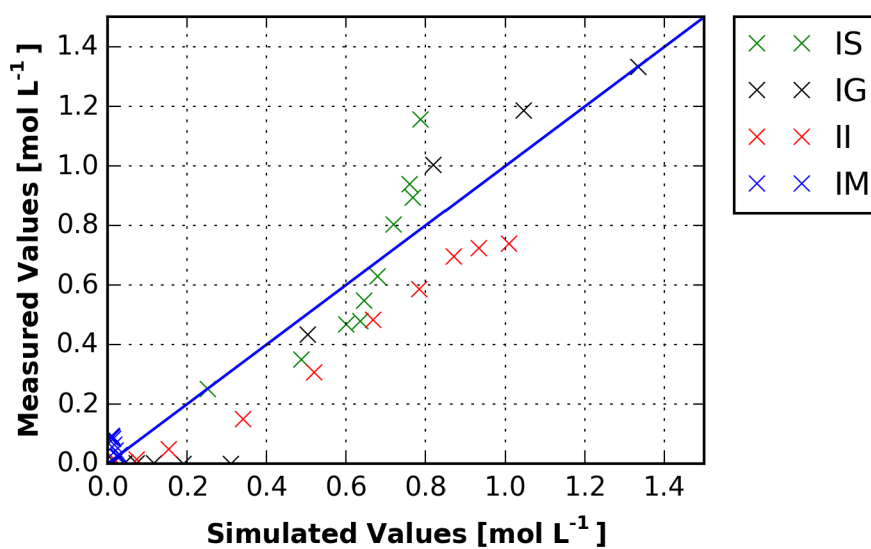


Figure A 12. Parity plot of the kinetic model for the isosorbide isomerisation data at 140 °C.

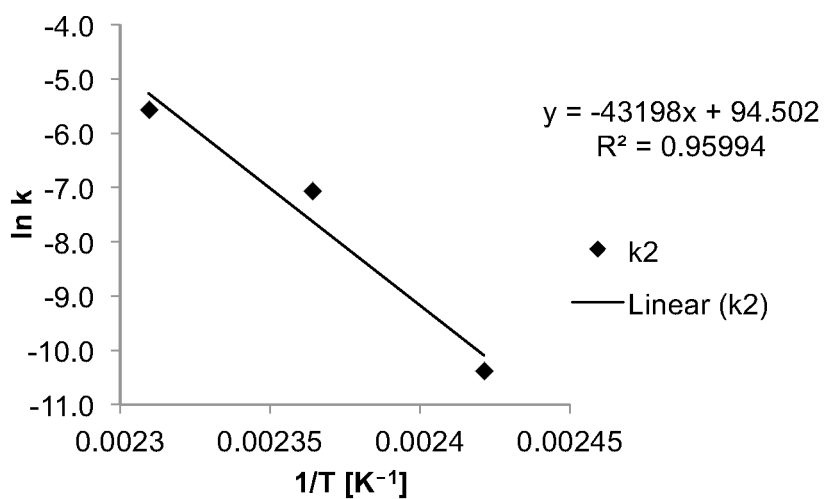
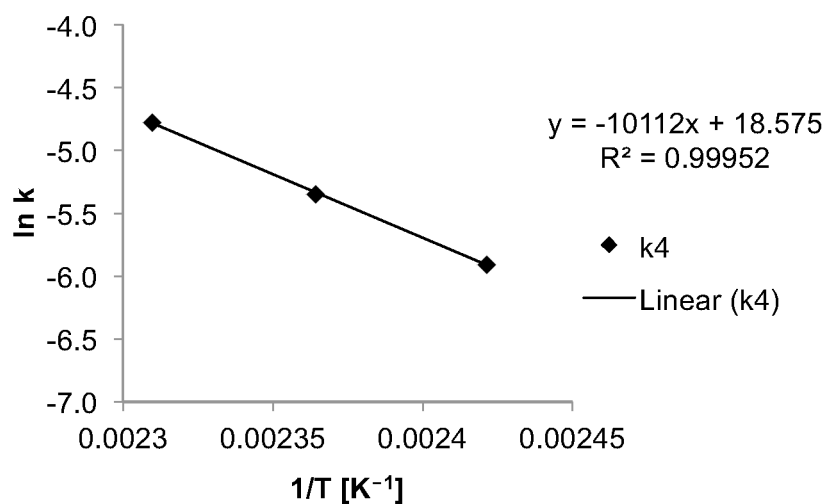
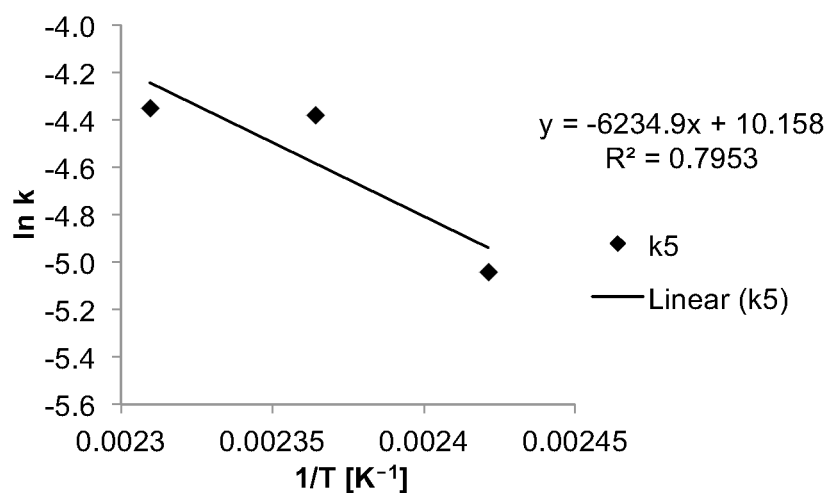
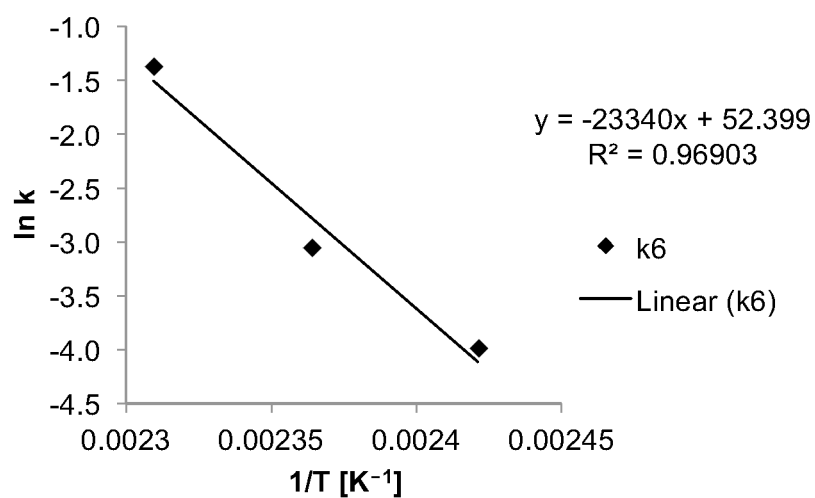


Figure A 13. Arrhenius plot for the reaction described by k_2 (I2 to IM).

Figure A 14. Arrhenius plot for the reaction described by k_4 (II to IS).Figure A 15. Arrhenius plot for the reaction described by k_5 (IM to IG 1).Figure A 16. Arrhenius plot for the reaction described by k_6 (IG 1 to IM).

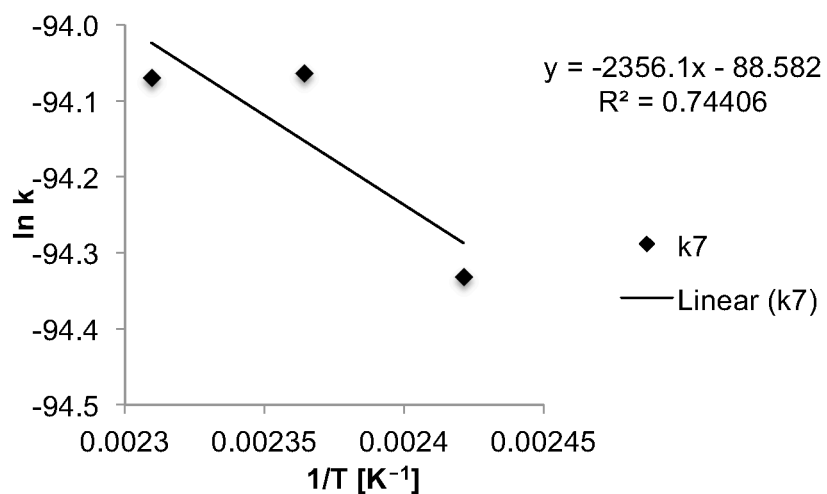


Figure A 17. Arrhenius plot for the reaction described by k_7 (IS to IG 2/3).

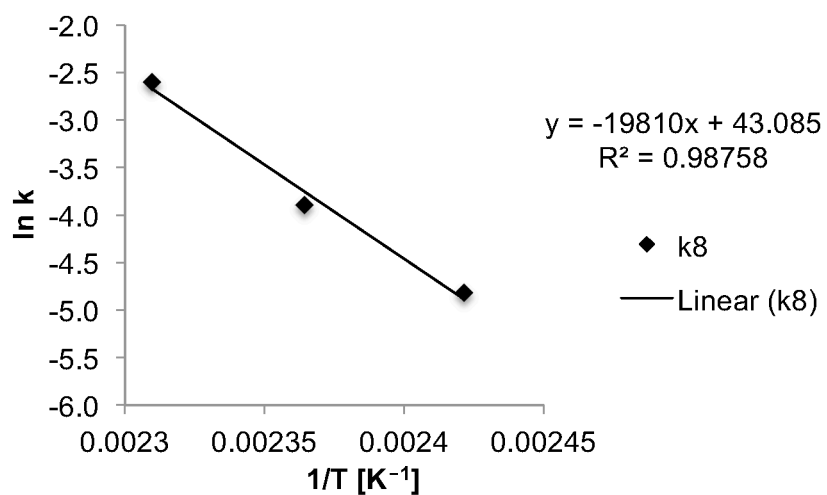


Figure A 18. Arrhenius plot for the reaction described by k_8 (IG 2/3 to IS).